

Clustering buildings with ATEs systems to improve Amsterdam's Fifth Generation Heating and Cooling Network

A sustainable heating and cooling solution for a densely
populated urban area

by

Thom van den Akerboom

Student number: 4596374
Master: Complex Systems Engineering and Management
Faculty: Technology, Policy and Management
Thesis committee: Dr. ir. P. Heijnen TU Delft
Prof. dr. M. E. Warnier TU Delft
Dr. M. K. Dang TU Delft & AMS Institute
Msc. P. Voskuilen AMS Institute



Preface

This report not only marks the conclusion of my Complex systems engineering and management master's degree, but also the end of my 7 year journey of studying at the TU Delft. With this work, I hope to have contributed to a better understanding of aquifer thermal energy storage, as well as to the potential future implementation of it in combination with a district heating network in Amsterdam. I'm grateful to have had the opportunity to explore the implementation of a district heating network in Amsterdam. District heating networks and the application of graph theory had captured my interest greatly, particularly because I had previously explored them during my bachelor's final project.

This report could never have been made without all the help and support I received during the past year. I would like to thank Maeva Dang and Paul Voskuilen from AMS for introducing and explaining the topic, providing all the necessary data and helping me understand it, and encouraging me to fully explore the case and broaden the scope of my project. On the other hand, I would like to thank Martijn Warnier and Petra Heijnen for their valuable contributions to my research and maintaining a realistic scope. I would like to extend my special thanks to Petra Heijnen, whose support was crucial during my project. She broke down the project in smaller steps when I was unable to see the wood for the trees. Lastly, I would like to thank all my friends and family for the constant support that I received during the last couple of months. First, my parents, who always supported me during the process and listened to me talk about my project, even though they didn't always understand what it was about. Secondly, to Kevin, with whom I spent many hours studying together in Delft. And finally, to Tessa, who has consistently supported me and always provided a welcome distraction from the project on wednesdays and weekends.

Thom van den Akerboom

Delft, August, 2024

Executive summary

The Netherlands aims to phase out gas by 2050, but this is challenging as 92% of houses are currently heated with gas. Alternatives are more feasible for new neighborhoods, but for old city centers like Amsterdam, it is more complex due to poorly insulated buildings and densely built areas. The demand for cooling is also higher in cities because heat is retained more than in rural areas. Solutions like hydrogen and green gas are unfeasible for such a large area due to limited availability.

A potential solution is a fifth-generation district heating and cooling (5GDHC) network, an energy system that provides both heating and cooling to buildings using external energy. This is possible due to a low temperature heat carrier in combination with bidirectional operation. Heating and cooling can be exchanged between buildings within the network, reducing the need for external energy. A 5GDHC network for a large city requires clustering of the buildings to create smaller networks, which can later be connected. Clustering allows for a bottom-up approach, reducing both the investment risks and the overload risk. A benefit of 5GDHC is the possibility to use aquifer thermal energy storage (ATES), where thermal energy is stored underground.

However, research on 5GDHC, particularly on large-scale implementation, is scarce. Dividing buildings into clusters is crucial for large-scale implementation, since it reduces the investment and overload risk, but the best methods are unknown. Additionally, the possibility of implementing ATES is not considered in research during the clustering process. This research investigates a method to cluster buildings and integrate ATES systems within these clusters. The goal is to create compact clusters to minimize the use of space in the already crowded subsurface. The clusters must also have a high demand fulfillment, meaning the heating and cooling demands must be fulfilled as much as possible within the cluster, either through energy exchange between buildings or through the use of storage. A higher demand fulfillment reduces the need for external energy.

The developed method clusters buildings based on their geographical location using both k-means and equal size k-means to ensure compactness. Each cluster's total heating demand is then assessed to determine the storage needed, as the heating demand is higher than the cooling demand. After this, ATES systems are implemented in the clusters, which can only be placed in available open space. This is done for both the k-means and equal size k-means results. These ATES systems are positioned as centrally as possible within the cluster, maintaining a minimum distance between ATES systems to prevent them from affecting each other, which would decrease the efficiency. This process continues until all demand is met or no free space remains.

The model results indicate that implementing ATES systems can increase the demand fulfillment from 1.4% to 58.6% for the entire center of Amsterdam. This is on the condition that the buildings are insulated to a level fit for low temperature heating. The demand fulfillment differs per cluster; some clusters achieve 100% fulfillment, particularly in the eastern and northwestern parts of the center, while others have lower fulfillment rates, with a minimum of 16.7%. The results show that very compact areas struggle more to meet heating demand. k-means outperforms equal size k-means in both compactness and demand fulfillment, making it the recommended method. The findings suggest that a 5GDHC network with ATES implementation has significant potential, with the most potential for clusters in the east and northwest.

The identified method is robust, adaptable to various geographical regions, and particularly effective in densely populated urban areas with limited space and high heat demand. One limitation pertains to the data used, which does not facilitate exchange between buildings due to identical weather-based demand profiles for all buildings. This data also underestimates the potential cooling demand expected during implementation. Furthermore, the study did not assess the availability of adequate regeneration when installing ATES systems. Regeneration is required to replenish the energy extracted from the ATES, in order to maintain the thermal balance. Without this process, ATES efficiency will decrease and the aquifer will degrade. Local sources are needed for regeneration, but their presence was not included in the research. Additionally, subsurface constraints, including existing underground systems and restricted areas, were not considered in determining suitable open spaces for ATES placement.

Looking forward, opportunities for further research include exploring alternative design configurations for ATES systems, with doublets or different sized monowells. For the AMS institute future research could include using more comprehensive and future-oriented data, incorporating current subsurface limitations and assessing regeneration requirements for ATES systems.

In conclusion, this research contributes to the fields of aquifer thermal energy storage and fifth generation district heating and cooling. It not only fills critical gaps in existing literature but also provides a practical methodology for optimizing urban energy systems. This approach holds promise for supporting initiatives like the 'High-hanging fruit' project by the AMS Institute, assisting sustainable urban heating solutions in Amsterdam and beyond.

Contents

Preface	1
Executive summary	2
List of abbreviations	7
List of Figures	8
List of Symbols	10
List of Tables	12
1 Introduction	13
1.1. Problem introduction	13
1.2. Thesis outline	16
2 Literature review	17
2.1. Literature review	17
2.1.1. History	17
2.1.2. Fifth generation heating and cooling network characteristics	19
2.1.2.1. Low temperature	19
2.1.2.2. Bidirectional Heating and cooling	19
2.1.2.3. Clustering	20
2.1.3. Aquifer thermal energy storage	21
2.2. Knowledge gap	22
2.3. Research Approach	23
2.4. Link to COSEM	23
2.5. Scientific contribution	24
2.6. Practical contribution	24
3 Overview design choices	25
3.1. Fifth generation heating and cooling	25
3.1.1. Temperature	26
3.1.2. Required electricity	27
3.1.3. Temperature fluctuations	27
3.1.4. Insulation	28
3.1.5. Pipe configurations	28
3.1.5.1. Two-pipe system	28
3.1.5.2. Three-pipe system	29
3.1.5.3. Four-pipe system	30
3.1.5.4. Pipe configuration conclusion	31
3.2. Aquifer thermal energy storage	31
3.2.1. Exclusion of BTES as an Alternative	31
3.2.2. Regeneration	32
3.2.3. Monowell or doublet	32

3.2.3.1. Design with doublets only-----	34
3.2.3.2. Design with equal well screen monowells only-----	35
3.2.4. Thermal capacity-----	35
3.2.5. Planning-----	36
3.2.6. Restrictions-----	37
3.3 Summary design choices-----	37
4 Actor analysis-----	39
4.1. Key actors-----	39
4.1.1. Heat and cooling users-----	39
4.1.2. Energy suppliers-----	39
4.1.3. Housing corporations-----	40
4.1.4. Operators electricity grid-----	40
4.1.5. Municipality of Amsterdam-----	40
4.2. Main objectives-----	41
5 Methodology-----	43
5.1. Key performance indicators-----	43
5.1.2. Demand fulfillment-----	43
5.1.2. Cluster compactness-----	45
5.1.3. Balance across clusters-----	45
5.2. Order of the methodology-----	46
5.3. Clustering-----	46
5.3.1.K-means-----	47
5.3.2. DBSCAN-----	48
5.3.3. Single linkage clustering-----	48
5.3.4. K-minimum spanning tree-----	49
5.3.5. Clustering method selection-----	50
5.4. Method Selection and Explanation-----	51
5.4.1. Clustering of the buildings-----	52
5.4.2. Determining the required storage capacity for the clusters-----	54
5.4.3. Implementing ATES installations-----	57
5.4.4. Evaluating KPI performance-----	63
6 Model input-----	66
6.1. Data-----	66
6.1.1. Heating and cooling demand per building-----	66
6.1.1.1. Energy profiles-----	67
6.1.1.2. Building information-----	70
6.1.2. Potential ATES locations-----	71
6.2. Input-----	72
6.2.1. ATES configuration-----	72

6.2.2. Remaining input values-----	74
7 Results-----	77
7.1. Model outcomes-----	77
7.2. K-means sensitivity analysis-----	81
7.3. Number of clusters sensitivity analysis-----	83
7.4 Davies-Bouldin index-----	85
8 Discussion-----	87
8.1. Scientific and practical contribution-----	87
8.2 Advantages-----	88
8.3. Limitations-----	89
8.3.1. Demand data-----	89
8.3.2. Regeneration-----	90
8.3.3. Subsurface limitations-----	90
9 Conclusion-----	91
9.1. The outcome-----	91
9.2 Future research-----	93
References-----	94
A Assumptions-----	102
B Demand profiles-----	104
C Supporting figures results-----	106

List of abbreviations

5GDHC	Fifth Generation District Heating and Cooling Network
AMS	Amsterdam Institute for Advanced Metropolitan Solutions
ATES	Aquifer Thermal Energy Storage
BTES	Borehole Thermal Energy Storage
CO ₂	Carbon Dioxide
DBSCAN	Density-Based Spatial Clustering of Applications with Noise
DFC	Demand Fulfillment Coefficient
DOC	Demand Overlap Coefficient
HT	High Temperature
KPI	Key Performance Indicator
LT	Low Temperature
MinPts	Minimum Points
MT	Medium Temperature
R _{th}	Thermal Radius
ULT	Ultra-Low Temperature
WCSS	Within-Cluster Sum of Squares

List of Figures

2.1	A representation of a future sustainable energy system (Boesten, 2019)	18
2.2	The cold and warm pipe of a two pipe system (KoWaNet, 2021)	20
2.3	The extraction of energy out of the wells done by a heat exchanger (Steinebach, 2013)	21
3.1	The concept of the Mijwater project in Heerlen (Boesten, 2019)	26
3.2	The concept of a decentralized 2 pipe system (Blom et al., 2024)	29
3.3	The concept of a centralized 4 pipe system (Blom et al., 2024)	30
3.4	The placement of the wells in a doublet and monowell configuration (Bloemendal & Olsthoorn, 2018)	33
3.5	Simplified representation of the volume of an ATES well	36
5.1	The overlapping in demands which determines the DOC (Wirtz et al., 2020b)	44
5.2	Example calculation of the DOC	44
5.3	An example of implementing the k-means algorithm (Arya, 2022)	48
5.4	The performance of DBSCAN on various point sets (Andrewngai, 2020)	48
5.5	An example result of the single linkage algorithm (Dozmorov, 2016)	49
5.6	The results of the k-minimum spanning tree algorithm with varying numbers of clusters	50
5.7	The result of applying k-means (Right) on the small example area (Left)	52
5.8	An example of applying the equal-size k-means algorithm	53
5.9	The results of k-means (left) and equal-sized k-means (right) to the example area	54
5.10	A representation of the method	54
5.11	The process to determine suitable ATES locations	60
5.12	A polygon with the randomly placed points	62
5.13	The chosen nodes from the free space for k-means (left) and equal size k-means (right) of the small example area	63

5.14	The DFC for the different clusters of k-means (left) and equal size k-means (right) after ATES implementation	65
6.1	The monthly heating demand for all archetypes in kWh/m ²	68
6.2	The monthly cooling demand for all archetypes in kWh/m ²	68
6.3	The heating and cooling demand for archetype 1 in kWh/m ²	69
6.4	The locations of all buildings from the dataset of the center of Amsterdam	70
6.5	The available free space from the dataset of the center of Amsterdam	71
6.6	A table of ATES-well properties of Amsterdam (Bloemendal, 2018)	72
7.1	The buildings in the center of Amsterdam divided into 60 clusters by k-means	78
7.2	A visualization of the DFC values across the 60 clusters in the center of Amsterdam	80
7.3	The Davies-Bouldin index for different number of clusters	85
B.1	The monthly heating demand for all archetypes in kWh/m ²	104
B.2	The monthly cooling demand for all archetypes in kWh/m ²	105
B.3	The legend for both the heating and cooling demand profiles	105
C.1	The locations of placed ATES systems in the center of Amsterdam	106
C.2	The compactness per cluster for k-means with the shared scale	107
C.3	The compactness per cluster for equal size k-means with the shared scale	108
C.4	The compactness per cluster for k-means with the individual scale	109
C.5	The compactness per cluster for equal size k-means with the individual scale	109

List of Symbols

Symbol	Definition	Unit
c_{aq}	Volumetric heat capacity of the aquifer	[J/m ³ /K]
$CD_{h,j}$	The cooling demand for hour h of building j , where $h \in \{1,2,\dots,G\}$ and $j \in \{1,2,\dots,J\}$	[kWh]
CS_j	The cooling surplus of building j , where $j \in \{1,2,\dots,J\}$	[kWh/year]
c_w	Volumetric heat capacity of water	[J/m ³ /K]
$DFCC_k$	The Demand Fulfillment Coefficient for cooling of cluster k , where $k \in \{1,2,\dots,K\}$	[-]
$DFCH_k$	The Demand Fulfillment Coefficient for heating of cluster k , where $k \in \{1,2,\dots,K\}$	[-]
DO_k	The demand overlap between the heating and cooling demand for cluster k , where $k \in \{1,2,\dots,K\}$	[kWh/year]
η	The total efficiency of transporting energy from the wells to the buildings	[-]
G	The total amount of hours in a year	[-]
$HD_{h,j}$	The heating demand for hour h of building j , where $h \in \{1,2,\dots,G\}$ and $j \in \{1,2,\dots,J\}$	[kWh]
HS_j	The heating surplus of building j , where $j \in \{1,2,\dots,J\}$	[kWh/year]
L	Well screen length	[m]
μ_k	The location of the cluster center of cluster k , where $k \in \{1,2,\dots,K\}$	[m]
n_k	The number of monowells placed in cluster k , where $n \in \{1,2,\dots,N\}$ and $k \in \{1,2,\dots,K\}$	[-]
N	The maximum number of ATEs systems that can be placed in the area	[-]
NRC_k	Required capacity after the implementation of n monowells in cluster k , where $n \in \{1,2,\dots,N\}$ and $k \in \{1,2,\dots,K\}$	[kWh/year]
RC_k	The required capacity of cluster k , where $k \in \{1,2,\dots,K\}$	[kWh/year]
R_{th}	Thermal radius of the ATEs system	[m]
SC_{ates}	Storage capacity of one ATEs well	[kWh/year]
ΔT	Temperature difference between the warm and the cold well	[K]
TC_k	The total capacity of storage in cluster k , where $k \in \{1,2,\dots,K\}$	[kWh/year]
TCD_j	The total cooling demand of building j , where $j \in \{1,2,\dots,J\}$	[kWh/year]
$TCCD_k$	The total cooling demand of cluster k , where $k \in \{1,2,\dots,K\}$	[kWh/year]
$TCHD_k$	The total heating demand of cluster k , where $k \in \{1,2,\dots,K\}$	[kWh/year]
TCS_k	The total cooling surplus of cluster k , where $k \in \{1,2,\dots,K\}$	[kWh/year]

Symbol	Definition	Unit
THD_j	The total heating demand of building j , where $j \in \{1,2,\dots,J\}$	[kWh/year]
THS_k	The total heating surplus of cluster k , where $k \in \{1,2,\dots,K\}$	[kWh/year]
V_{in}	Groundwater storage volume per ATEs well	[m ³]
W_k	The within cluster variation of cluster k , where $k \in \{1,2,\dots,K\}$	[m ²]
WCSS	The within cluster sum of squares	[m ²]
x_j	The location of building j , where $j \in \{1,2,\dots,J\}$	[m]
Z	Conversion factor	[J/kWh]

List of Tables

3.1	Temperature levels of different categories of district heating networks	26
4.1	The system objectives of the key actors	41
5.1	The properties of the compactness values for the 6 clusters in the example area, divided by 10^6	64
5.2	The properties of the DFC values for the 6 clusters in the example area before and after ATES implementation	65
6.1	The L/R_{th} ratio determined based on different configurations	73
6.2	An overview of all input values	76
7.1	The properties of the DFC values for the different clusters in the center of Amsterdam before ATES implementation	78
7.2	The properties of the DFC values for the different clusters in the center of Amsterdam after ATES implementation	79
7.3	The properties of the compactness for the different clusters in the center of Amsterdam, divided by 10^6	81
7.4	The properties of the compactness for the k-means sensitivity analysis, divided by 10^6	82
7.5	The properties of the DFC values for the k-means sensitivity analysis	82
7.6	The properties of the compactness for the number of clusters sensitivity analysis, divided by 10^6	83
7.7	The properties of the DFC values for the number of clusters sensitivity analysis	84

Introduction

1.1. Problem introduction

In 2015, 196 Parties signed the Paris Agreement at the UN Climate Change Conference (COP21) in Paris (UNFCCC, 2015). The goal of this agreement is to hold “the increase in the global average temperature to well below 2°C above pre-industrial levels” and pursue efforts “to limit the temperature increase to 1.5°C above pre-industrial levels.”, by drastically decreasing greenhouse gas emissions. To reach this, the countries must be CO₂-neutral in their emissions by 2050. The Dutch Government has decided to stop using natural gas by 2050 (Planbureau voor de leefomgeving, 2023). This decision supports the goal of reducing CO₂ emissions, as burning natural gas releases significant amounts of CO₂ into the atmosphere. Another reason for the government to stop using natural gas, is the safety concerns associated with gas drilling in Groningen. This gas drilling has been directly linked to earthquakes in the area (Liefing, 2022). Out of the 62 earthquakes in the Groningen area in 2023, 50 were determined to be induced by gas drilling (KNMI, 2024). However, 92% of all the houses in the Netherlands were connected to natural gas in 2019, mostly for heating (Centraal Bureau voor de Statistiek, 2021). While the Dutch government aims to be gas-free by 2050, some municipalities are setting even more ambitious climate goals. Such as the municipality of Amsterdam, which aims to reduce CO₂ emissions by 60 percent by 2030 compared to 1990 levels and be completely natural gas-free by 2040 (Gemeente Amsterdam, 2024). Since all buildings need to be gas-free by 2040, an alternative method for the heating of buildings must be found.

A possible solution is to replace natural gas with a more sustainable gas like green hydrogen or green gas. Hydrogen is a gas generated by electrolysis. This process requires a significant amount of electricity; if this electricity is sourced from renewable energy, such as wind or solar power, the gas is referred to as green hydrogen. However, hydrogen has not yet been used for heating large areas and has only been tested in pilot projects to gather experience. Due to the limited availability of green hydrogen, it is currently not feasible to use it for heating extensive regions like the center of Amsterdam (Nationaal Programma Lokale Warmtetransitie, 2020).

Green gas is gas produced from biomass and upgraded to be of the same quality as natural gas. Since it matches the quality of natural gas, it can be utilized within the existing gas infrastructure. Green gas has a similar problem as green hydrogen, where it is only available to a limited extent and will only be used in areas if alternatives are either technically impractical or far more expensive (Nationaal Programma Lokale Warmtetransitie, 2021).

The municipality of Amsterdam, like all other municipalities, is allowed to draw up their own plan for an alternative heating strategy to reach the goal set by the government. These plans are more obvious for new-build neighborhoods, while old neighborhoods and historical city centers are more difficult due to poorly insulated buildings. This leads to increased heating demand in older areas during temperature drops, which mostly happen during the winter.. Moreover, historical city centers are recognized as 'heat islands', where temperatures rise more rapidly compared to surrounding areas (Patz et al., 2005). This higher temperature amplifies the intensity of heatwaves, which increases the demand for cooling, which mostly happens during the summer. Amsterdam experiences this effect, where the city center is warmer because the heat is trapped in stones, roads and buildings (AMS, n.d.). This demand for cooling is expected to triple by 2050 without action (IEA, 2018). By then, the absolute cooling demand in the EU is projected to be approximately one-sixth of the absolute heating demand (Sanner et al., 2011).

The increase in cooling demand and the uncertainty for the future surrounding hydrogen and green gas emphasize the opportunity for a heating and cooling system. A solution could be a fifth-generation district heating and cooling (5GDHC) network, which is an energy system created to provide heating and cooling to buildings. A 5GDHC network has a low temperature heat carrier and has bidirectional operation, meaning it can provide both heating and cooling to the connected buildings (Volkova et al., 2022). It's crucial for the buildings to be well insulated to effectively utilize the heating and cooling received, (NLPW, 2022). Providing this heating and cooling requires external energy, ideally supplied by renewable energy sources or waste heat from industrial processes. The need for external energy is minimized by the exchange of heating and cooling between buildings of a 5GDHC network and the use of thermal energy storage (KoWaNet, 2021). Through the exchange of heating and cooling between buildings, the buildings effectively become 'heat exchangers': Buildings that have a demand for heat, supply 'cold' back to the grid. This cold can then be used for buildings which have a cooling demand, like supermarkets and data centers. The greater the coverage of heating demand by cooling demand, and vice versa, the less external energy is required. The incorporation of thermal energy storage allows for the excess of heat from the summer to be stored to use for heating in the winter, while the excess of cold water in the winter can be stored to use for cooling in the summer. Such seasonal thermal energy storage can be crucial to allow for compensating mismatches between the demands for heating and cooling (Buffa et al., 2019).

A form of thermal energy storage is aquifer thermal energy storage (ATES). ATES is a technology that can be used to store and retrieve energy in aquifers underground. This energy can be in the form of cold or heat. These systems can significantly reduce greenhouse gas emissions from space heating and cooling (Stemmler et al., 2024), and are a part of low energy geothermal energy, which shows the single largest potential to provide renewable heat in the Netherlands (Hoogenvorst, 2017).

Limited 5GDHC networks have been constructed and the scale of the implementation has been small. A 5GDHC network for a large city requires clustering of the buildings to create smaller networks, which can later be connected. Clustering allows for a bottom-up approach, reducing both the investment risks and the overload risk (NLPW, 2022). If the entire network is not constructed all at once but developed by cluster, there is less need for a large upfront capital investment, which reduces financial risk. Once a cluster is completed, it can start generating revenue immediately, even if the other clusters are still under development. This immediate return might support the investments for other clusters and is not possible if the entire network is built in one go. The overload risk refers to the possibility that the demand for heating and cooling falls short of the quantities projected in advance (Expertise Centrum Warmte, n.d.).

If demand is lower than expected during the implementation of the clusters, there is the possibility to postpone or not proceed with the development of additional clusters if they are no longer seen as profitable. This approach means that the financial risk is smaller compared to constructing the entire network at once, where this isn't possible.

Amsterdam is a densely populated city, given the density of 4,880 people per square kilometer (Kadastralekaart.com, n.d.). The city of Amsterdam is still growing, with the pressure on space rising. However, Installing ATES requires open space on the surface, for the placement of the installation. Furthermore, there is limited space remaining in the subsurface. The subsurface currently contains cables for data and telecom, drainage systems and pipes for drinking water, gas and wastewater (Gemeente Amsterdam, 2019). This implies that ATES installations must efficiently utilize the limited space, and the clusters within the 5GDHC network need to be compact to reduce the total required pipe length in the network. Compact clusters mean that the buildings within each cluster are close to one another. When buildings are situated closer together, the length of pipe required to connect them all is reduced.

1.2. Thesis outline

Chapter 2 conducts a review of the existing literature on the topics to determine areas where current research is lacking. This determines the knowledge gap, which will be used to formulate the research question. Chapter 3 provides an overview of the proposed new system and the potential design choices for both the ATES installations and the 5GDHC network and Chapter 4 gives the system's objective as perceived by the actors. The goal of chapter 5 is to review the potential clustering methods and to develop a suitable approach to address the research questions. How the model functions will be showcased using a small example. Chapter 6 outlines the required data, input and assumptions used for the method. Chapter 7 provides the results of applying the developed method to the center of Amsterdam. The performance of the method will be analyzed and discussed. Finally, Chapter 8 contains the discussion, while chapter 9 contains the conclusion, to summarize the finding and their implications.

2

Literature review

This chapter contains the literature review, which was conducted to delve deeper into the subject. This provides insight into the state of knowledge on the subject by reviewing and synthesizing different sources. The literature review examines the history of district heating, the fifth generation district heating and cooling networks with its characteristics and the ATES. The knowledge gap is then identified after which the research questions can be formulated. These questions lead to a research approach and the planned scientific and practical contribution of this research.

2.1. Literature review

2.1.1. History

The first generation of district heating systems was created in the 1880s. These systems used steam to transport the heat, which caused significant heat losses and severe accidents from steam explosions (Lund et al., 2014). The second generation was introduced in the 1930s and used pressurized hot water, with supply temperatures typically above 100 °C, as the heat carrier. The driving force for the second generation was the potential use of Combined heat and power to reduce the fuel consumption (Lund et al., 2014). The third generation utilized supply temperatures typically under 100 °C and implemented components that were prefabricated and more lean (Lund et al., 2014). The fourth generation has a higher efficiency, reduced capital costs and utilizes a lower temperature of 50 up to 70 °C (Meesenburg et al., 2020). The higher temperatures of the third generation were a barrier for the implementation of a renewable and recycled heat supply (Averfalk & Werner, 2020). As a result, the fourth generation was introduced to implement heat from renewable sources and to reuse lower temperature waste heat (Mazhar et al., 2018). The main difference between the fourth and fifth generation heating networks is the location where the heat is upgraded to the required temperature.

In the fourth generation, heat is upgraded at a central location, while in the fifth generation, the heat is upgraded decentrally at the location of each user (KoWaNet, 2021). The fifth generation aims to exploit the synergy of combined heating and cooling. Since more end users will consume and add heat to and from the network, the overall heat demand decreases. However, the fifth generation should be seen as a sequential development as opposed to a parallel development, since the difference with the fourth generation is so minor (Lund et al., 2021). Lund et al. (2014) stated some properties that all future district heating systems, so both fourth and fifth generation, should have, to fulfill their role in sustainable energy systems:

1. The capability to provide low-temperature heat to both existing and new buildings.
2. The capability to effectively distribute heat in networks with low grid loss
3. The capability to reuse low-temperature heat and integrate renewable sources like solar and geothermal energy.
4. The capability to be an integrated part of smart energy systems, including 4th Generation District Cooling systems.
5. The capability to have a robust business model, particularly in the transition to renewable energy sources.

A representation of such a system on a district level can be seen in figure 2.1.

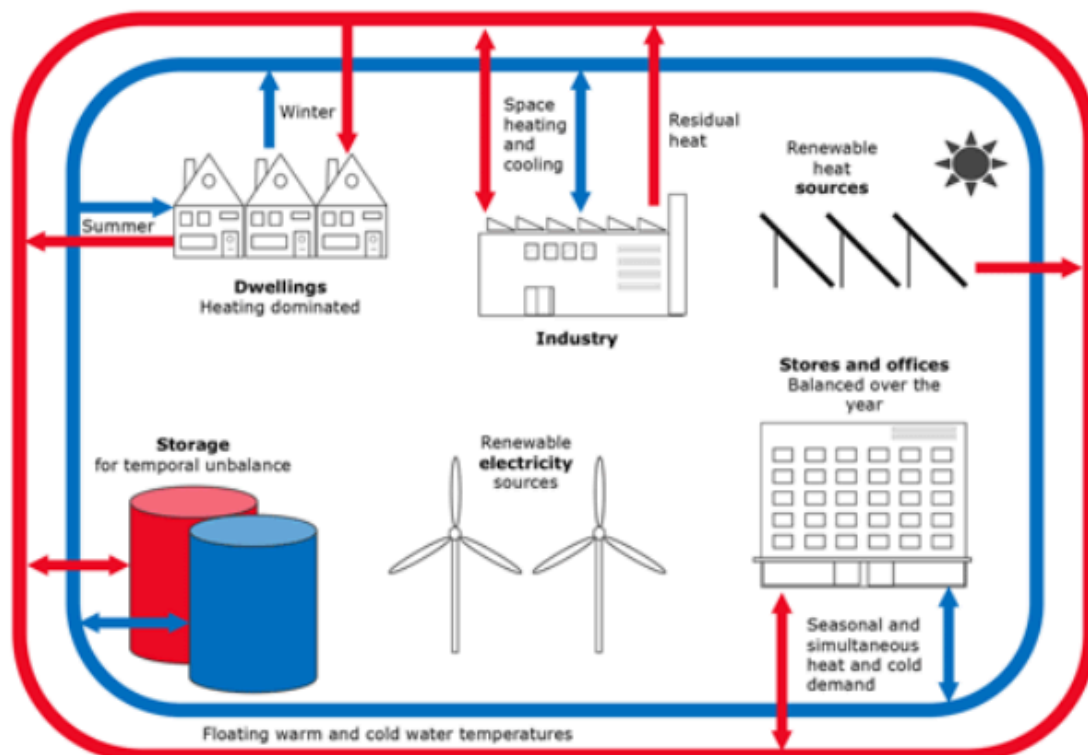


Figure 2.1: A representation of a future sustainable energy system (Boesten, 2019)

2.1.2. Fifth generation heating and cooling network characteristics

The fifth generation heating and cooling (5GDHC) network is characterized by a few features. The network uses low temperature to carry the heat to the users. Additionally, The system is capable of providing both heating and cooling, since the temperature is raised or lowered by heat pumps before it reaches the user. This accommodates bi-directional exchange of heat and cold, which can be assisted by seasonal storage (Boesten et al., 2019).

2.1.2.1. Low temperature

The 5GDHC network has a low supply temperature covering a range of 5 °C to 30 °C, where the warm pipe has a temperature that is approximately 5 °C to 10 °C higher than the cold pipe (Wirtz et al., 2020a). There are various benefits to the network's low supply temperature. The low temperature allows excess heat to be recovered without the requirement of heat pumps. Furthermore, the temperature of the excess heat is near equal to that of the heat demand, negating the need for extra transmission pipelines (Buffa et al., 2019). Additionally, there is the possibility to utilize energy conversion techniques with high efficiencies, like heat pumps and condensing boilers (Kiani et al., 2004). Lastly, the lower temperature results in less heat losses, due to a lower average temperature differential between the water in the pipes and the surrounding environment (Averfalk & Werner, 2020). However, for this to be effective, all the houses must be insulated to a certain extent.

2.1.2.2. Bidirectional Heating and cooling

The heating and cooling can occur concurrently, since the network is bidirectional. Users can make use of the cooling at the same time as other users make use of the heating. The system generally has two pipe systems; one with cold and one with warm water (figure 2.2). In the case of heating demand, the system uses the warm water which is heated by the heat pumps to a certain usable temperature. The water is then discharged to the cold water system after usage. The system works in the opposite direction with a cooling demand (Bünning et al., 2018). Less energy is wasted in this way, since users with opposite demand are supplied by the same system, where thermal energy is exchanged between the users (Gjoka et al., 2023). The demand for heat and cold should ideally be of equivalent size, to reach a better heat balance of the energy flows, which minimizes the requirement of external energy. However, the peaks of these demands do not coincide; heating demand is highest in winter, while cooling demand peaks in summer. Therefore, even if the demands are of

equivalent size, some form of thermal energy storage is still necessary. If the heat and cold demand are of equivalent size, the heat and cold demands can be offset against each other, although the intervention of a heat pump is often still necessary since the heat isn't always at the right temperature after use. While most building types have a higher demand for heating than for cooling, some types of buildings require constant cooling, resulting in a higher overall cooling demand. Such buildings are supermarkets, hotels, hospitals, university facilities and data centers. Other structures can also be used like indoor car parks and subway ventilation shafts (Dobbelsteen, 2020). 5GDHC allows for local matching of these demands, which reduces the need for external energy.

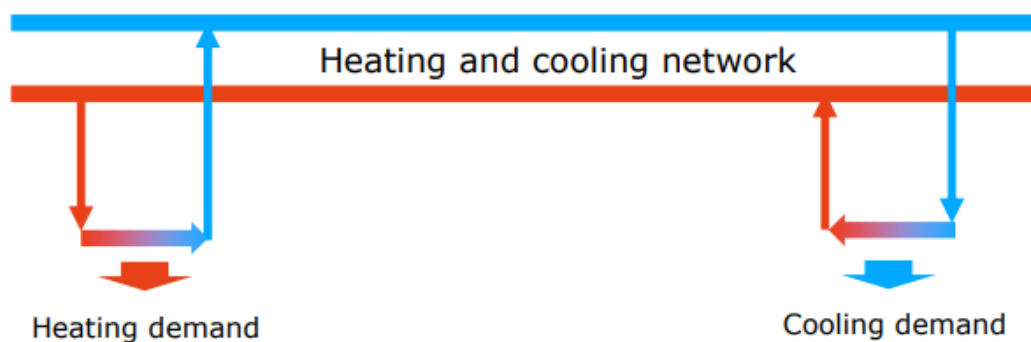


Figure 2.2: The cold and warm pipe of a two pipe system (KoWaNet, 2021)

2.1.2.3. Clustering

The current 5GDHC networks are built on a small scale, not exceeding 10 kilometers in network length (Buffa et al., 2019). Large networks are less feasible due to the characteristics of the heat carrier. Water experiences substantial thermal and pressure losses, which increase with distance from the source. Consequently, the thermal energy is ideally consumed close to the generation location to maintain the system efficiency (Haiwen et al., 2010). To address these issues, buildings are clustered. Clustering allows for a bottom-up approach where the network is constructed incrementally in small segments rather than all at once. Clustering entails the grouping of buildings based on relevant factors. This is mostly done based on the geographical location, but can also be done based on energy demand and supply. Each cluster functions as a smaller network where heat and cold can be exchanged between buildings (Verhoeven et al., 2014). Possible ways to create these clusters is to apply clustering algorithms and heuristics.

2.1.3. Aquifer thermal energy storage

ATES works by exchanging heat with the underground. This is either done by running water through a pipe system or by directly injecting and withdrawing the groundwater through groundwater wells (W. Sommer, 2015). These systems mostly operate on a seasonal basis, where they mostly deliver heating in the winter and mostly cooling in the summer. The system has two groundwater wells, where cool groundwater is extracted during the summer from the cold well. This water is reinjected after usage in the warm well. The direction is flipped in the winter, where warm groundwater is extracted from the warm well and injected into the cold well after usage (Dickinson et al., 2009). While seasonal changes typically alter the direction, variations could occur on an hourly or daily basis as well (M. Bloemendal, personal communication, 3 May 2024).

The extraction of energy from the water out of the wells is done by a heat exchanger (figure 2.3). The heat exchanger transfers heat between the water in the ATES and in the network. Such seasonal thermal energy storage can be crucial to allow for compensating mismatches between the demands for heating and cooling (Buffa et al., 2019).

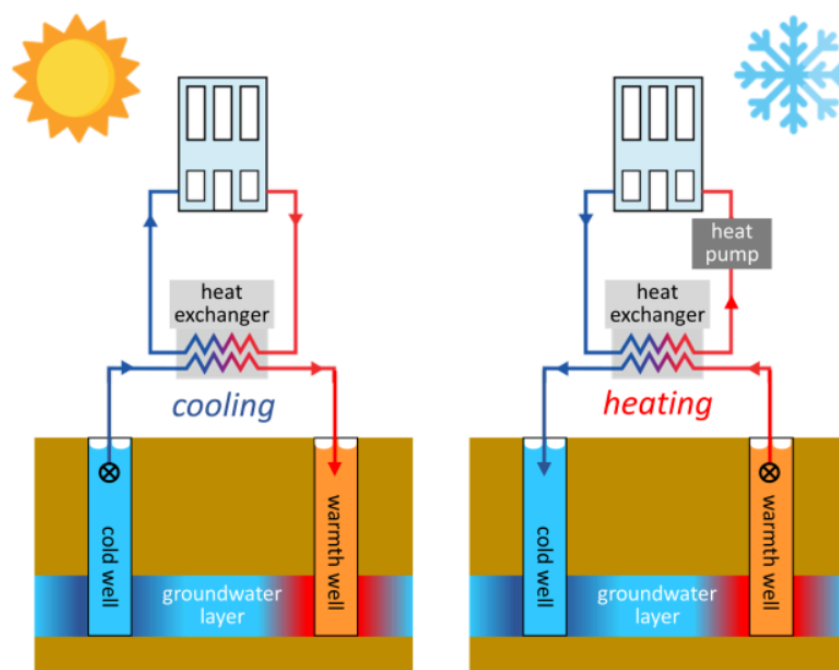


Figure 2.3: The extraction of energy out of the wells done by a heat exchanger (Steinebach, 2013)

ATES is especially well-suited for storing vast amounts of thermal energy and has evolved into an affordable technology for the heating and cooling of buildings (Sanner et al., 2003). ATES systems do have heat losses, since the heat dissipates towards the surroundings and due to advection with regional groundwater flow (Bakr et al., 2013). Systems that are too close to each other also suffer from these effects and harm each other's efficiency, due to thermal interference. This thermal interference is a major challenge to implement ATES systems with the highest performance and most efficient use of the subsurface (Sommer et al., 2015). Finding the optimal locations for these systems is thus crucial.

2.2. Knowledge gap

The literature review provided an overview of the 5GDHC network, while it also gave insight into the current state of ATES systems. 5GDHC networks have great potential to provide sustainable heating. However, 5GDHC is still a newer technology, where research into large scale implementation is scarce. Dividing buildings into clusters is crucial for this implementation, but the best methods for it are unknown. ATES systems could benefit the 5GDHC networks, but they aren't taken into account during the clustering methods yet. Based on the identified knowledge gap and its application to the center of Amsterdam, the following research question emerged:

How can buildings in a dense city center be clustered for a fifth generation district heating and cooling network (5GDHC) and integrated with Aquifer Thermal Energy Storage (ATES) to optimize the demand fulfillment, given the limited space?

several sub-questions have been drawn up to answer the main research question:

1. *What are the priorities of stakeholders and what design choices can be made when implementing a fifth generation district heating and cooling with ATES?*
2. *How can a method be developed to cluster buildings and integrate ATES in these clusters, adhering to the priorities of the stakeholders?*
3. *What are the impacts of clustering the buildings and integrating ATES on the demand fulfillment and compactness in the fifth generation distinct heating and cooling network in the center of Amsterdam?*

2.3. Research Approach

This research will build on the work of Sarah van Burk, who developed a methodology to identify clusters in a 5GDHC network, to assist the large-scale implementation (van Burk, 2023). She used the single linkage clustering algorithm and Geometric Graph theory to cluster the buildings based on their locations and energy profiles. In addition to clustering the buildings, this research will also add ATES installations in order to improve the heat balance. The research of Sarah van Burk is used as inspiration and not directly implemented in this work.

The aim of this research is to ascertain the most effective design of a 5GDHC network in the center of Amsterdam, aligning with the preferences of the actors as determined through an actor analysis. A system overview of 5GDHC networks and ATES installations is conducted to explore various design options and ultimately choose the most suitable design for these systems. Subsequently, A methodology to cluster buildings and integrate ATES installations is developed. The required data for the method is determined, and selected based on the previously chosen design. This allows for the method to be applied to the center of Amsterdam. The performance of the method on the center of Amsterdam will be evaluated, leading to the discussion and conclusion of the research findings.

2.4. Link to COSEM

This is a relevant topic for a thesis of the Complex Systems Engineering and Management master, since a district heating network constitutes a complex socio-technical system. While the technical design is very important, to determine the most efficient way to distribute the heat to the users. However, the socio-technical system where the network will be a part of must be taken into account. The socio-technical system is influenced by different social factors like policy, economics and environment and has different actors, who have different needs and requirements for this new system. The success of the district heating network relies on the cooperation and acceptance of the different actors.

2.5. Scientific contribution

This research aims to contribute to the scientific fields of aquifer thermal energy storage and fifth generation district heating and cooling. For 5GDHC networks, the primary contribution will be the examination of a larger area than previously studied. This research will also focus on an area with a high density of buildings, addressing a factor that has been less explored in earlier studies. Additionally, the integration of ATES installations into the design method for the 5GDHC network will be a novel aspect of this research. The development of a new method through this research will potentially be used for future studies in different locations, facilitate the planning of 5GDHC networks with integrated ATES, or inspire the development of new methodologies.

2.6. Practical contribution

This research is intended to assist the Amsterdam Institute for Advanced Metropolitan Solutions (AMS) in their 'High-hanging fruit' project (Dang & Voskuilen, n.d.) (Dang & Voskuilen, n.d.). The project aims to explore sustainable and local heating methods for the monumental buildings in the inner city of Amsterdam. The goal of the 'High-hanging fruit' project is to develop a standardized approach for energy retrofitting using local sustainable heating.

The methodology developed from this research will enable the clustering of buildings and the integration of ATES, resulting in compact clusters with an optimized demand fulfillment. This method will be used to assess the performance of a potential 5GDHC network and to explore various configurations of 5GDHC networks and ATES installations. In combination with the standardized approach for energy retrofitting from the 'High-hanging fruit' project, this research aims to contribute towards creating a gas-free heating solution for the center of Amsterdam.

Overview design choices

This chapter provides an overview of the current state of fifth-generation district heating and cooling technology, as well as aquifer thermal energy storage. It explains the design choices available and discusses their advantages and disadvantages.

3.1. Fifth generation heating and cooling

A fifth-generation district heating and cooling network is an emerging technology, with only one existing network currently operational in the Netherlands (NLPW, 2022). The existing case is the Mijnwater district heating and cooling system in Heerlen, which uses a flooded coal mine as geothermal energy storage and integrates multiple decentralized heat sources (Verhoeven et al., 2014). The network supplies a large number of buildings with a size of more than 200,000 m² of building floor area (Boesten et al., 2019). The concept is illustrated in figure 3.1, where clusters of different building types are connected by cluster connections to the backbone. This backbone is connected to the warm and cold wells of the ATES, which supplies the clusters with heating and cooling. However, while the Mijnwater project is one of the most technologically advanced 5GDHC systems, alternative design decisions can also be considered (Buffa et al., 2019). Still, this concept has the potential to be successfully implemented in numerous other locations across the Netherlands (CE Delft, 2018).

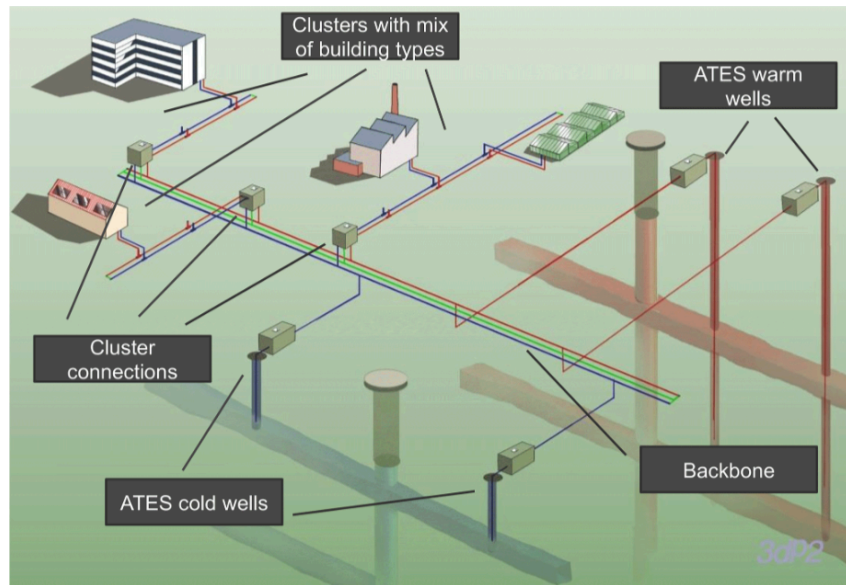


Figure 3.1: The concept of the Mijnwater project in Heerlen (Boesten, 2019)

3.1.1. Temperature

Based on the temperature of the water, district heating systems can be divided into 4 different categories, which can be seen in table 3.1. The numbers seen in the table are not the exact numbers, but an approximation.

Table 3.1: Temperature levels of different categories of district heating networks

Category	Temperature high	Temperature low
High temperature	90 °C	70 °C
Medium temperature	70 °C	40 °C
Low temperature	40 °C	20 °C
Ultra low temperature	20 °C	-

For a 5GDHC network, high temperature (HT) is infeasible. While it is technically possible to upgrade sources from 10 to 40 degrees Celsius to higher temperatures, this process requires a significant amount of electricity. In addition, the low temperature returns are insufficient for direct cooling (Ruijs, 2019). Medium temperature (MT) is still relatively high, as the supply would need to be upgraded again. At low temperature (LT), this problem is mitigated because the temperature of the potential supply is closer to the temperature of the network.

The temperature difference between the ATES system and the network is minimal. However, to use the heat for domestic heating water, an upgrade is still required. On the other hand, the return flow of heating can be directly used for cooling. This setup is well-suited for a 4-pipe network, but also works for a 2-pipe system. For ultra-low temperature (ULT), which is well-suited for a 2-pipe network, an upgrade is required for both heating and domestic hot water use. The advantage of an ultra-low temperature coupled with a decentralized network like the 2-pipe system is that it offers increased opportunities to utilize renewable sources and recover excess heat efficiently (Gjoka et al., 2023).

3.1.2. Required electricity

Choosing a lower temperature for the network increases electricity costs. For HT and MT, these costs primarily involve pumping. However, for LT there is an additional cost for upgrading the water temperature to the temperature level required for domestic hot water use. ULT systems also require the upgrading of the water temperature to the level used for heating. These upgrades all require electricity, contributing to higher operational costs (Ruijs, 2019).

3.1.3. Temperature fluctuations

Even though a temperature level can be selected, the temperature in the pipes is not fixed and can fluctuate depending on different conditions; How much energy is used during cooling or heating, the temperature outside and the temperature in the subsurface. These fluctuations can be absorbed by installing a heat pump at each customer, which is able to upgrade the temperature if necessary (Roossien, 2020). This is a way to limit heat losses, by bringing it to the right temperature as close to the customer as possible (NLPW, 2022).

3.1.4. Insulation

While it is crucial for the network to supply sufficient heat, it is equally important for the customer to have well-insulated buildings to effectively utilize the heat received (NLPW, 2022). If this is not the case, a 5GDHC network is not economically attractive and the network may not be able to supply enough heat to bring the building to the desired temperature (T. Sommer et al., 2020). 74% of the housing stock in Amsterdam does not yet meet the required insulation levels, leading the municipality to consider these buildings as insufficiently insulated (Bos, 2023). Insulating all these buildings to the required levels is a huge task, for which no solution has yet been found.

3.1.5. Pipe configurations

Arguably, one of the most critical decisions in designing a 5GDHC network is determining the number of pipes to incorporate into the system. There are several configurations to choose from, ranging from a two-pipe to a four-pipe system (Buffa et al., 2019).

3.1.5.1. Two-pipe system

In conventional district heating networks, a two-pipe system comprises a supply and a return pipe. Water is delivered to the heat pumps and chillers through the supply pipe, and then it returns via the return pipe. The temperature of the supply pipe is higher than that of the return pipe when there is a greater demand for heating, and vice versa when there is a higher demand for cooling. For a 5GDHC network, a two-pipe system consists of two pipes: one dedicated to cooling and the other to heating. After being used for cooling, the water is released into the heating pipe, and vice versa.

Figure 3.2, sourced from a paper by Blom et al.(2024), illustrates the operation of a two-pipe system within a 5GDHC network. This paper looked at the possibility of using a vertical farm as a local heat source in a low temperature district heating network.

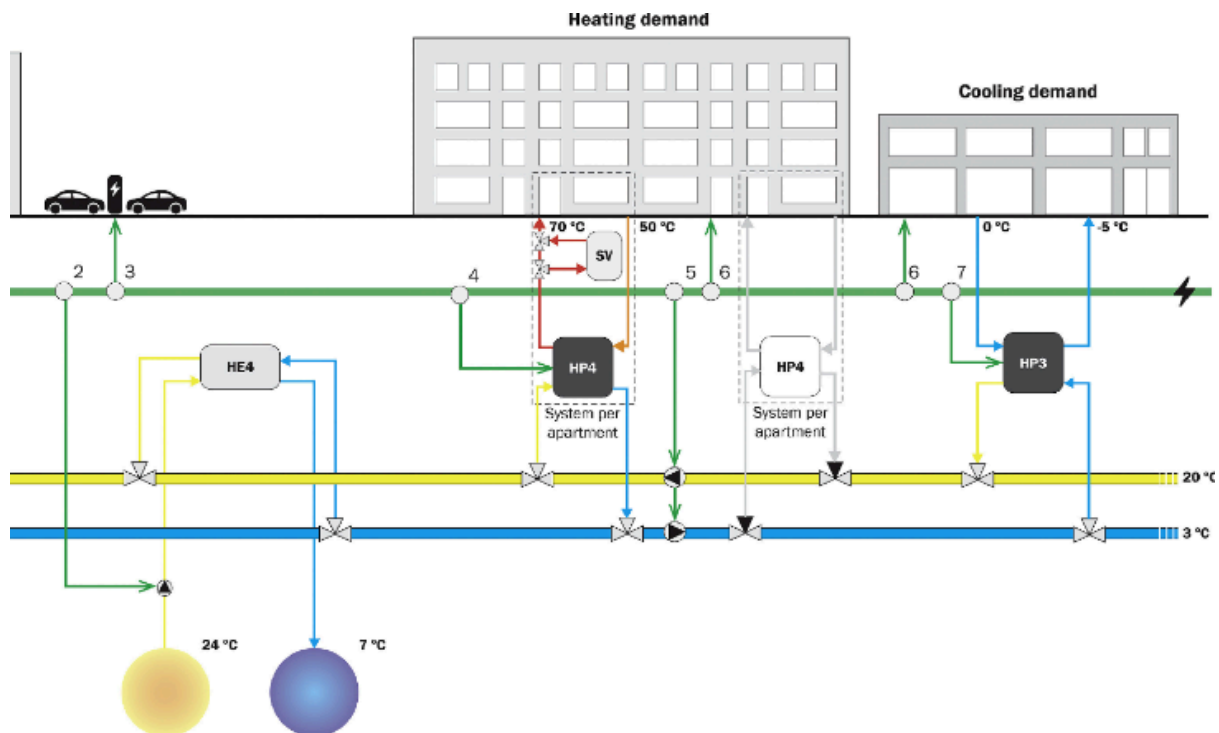


Figure 3.2: The concept of a decentralized 2 pipe system (Blom et al., 2024)

Figure 3.2 shows a 2 pipe system, which is a decentralized system. This means that the temperature of the heat is only increased or decreased where it is needed. Each apartment or building is equipped with its own heat pump, capable of adjusting temperatures to desired levels for both cooling and heating. For district heating water, an additional booster unit is required. If the demand for cooling can no longer be met locally, heat is extracted from the ATEs. For heating, water is pumped from the warm well and its energy is extracted via a heat exchanger. Subsequently, it is reinjected into the cold well. Contrary, during excess cooling demand, this process is reversed.

3.1.5.2. Three-pipe system

Conventional district heating networks with a 3-pipe system contain an extra pipe that serves for either direct heating or cooling, depending on the system's primary requirement. Once used, it flows into the pipe leading to the heat pumps or chillers. The Mijnwater project was initially developed as a 5GDHC network with three pipes (Verhoeven et al., 2014). The concept involved a supply pipe for both hot and cold water, alongside a third pipe designated for combined discharge purposes. But in line with the principles of a 5GDHC network, the first two pipes have become bidirectional, making the return pipe redundant. A three-pipe system is not a practical design choice for a 5GDHC network since the third pipe is redundant.

3.1.5.4. Pipe configuration conclusion

The only practical design options for a 5GDHC network are the two-pipe and four-pipe systems, as the three-pipe system essentially functions as a 2-pipe system due to its redundant third pipe. Both the two-pipe and four-pipe systems offer distinct advantages over each other. The two-pipe system requires half the number of pipes, which reduces underground space requirements. Moreover, it experiences lower thermal losses because the temperature remains closer to that of the subsurface. On the other hand, the four-pipe system requires less space within buildings since heating and cooling are changed centrally. This requires only a heat exchanger within buildings instead of individual heat pumps, saving space. Additionally, no booster unit is needed, saving even more space.

3.2. Aquifer thermal energy storage

In the Netherlands, there are around 2,000 ATES systems in operation, supporting approximately 0.2% of the country's buildings (Bloemendal et al., 2018).

Approximately 600 of these systems are located in Amsterdam, where the subsurface conditions are highly favorable for their operation (Ruijs, 2019). Amsterdam has an aquifer that is 150 meters thick, capable of storing a significant amount of heat. This is considerably more than in a city like Utrecht, where the aquifer is only about 20 meters thick (Bloemendal, 2018). Of these 150 meters, approximately 100 meters can be utilized by the ATES, which is still substantial (Bbl, 2023). Since the ATES will be used to supply a 5GDHC network, it will be classified as a low-temperature ATES. This means the well temperatures will be below 30 degrees Celsius. In contrast, medium-temperature ATES operates with well temperatures between 30 and 50 degrees Celsius, while high-temperature ATES features well temperatures above 50 degrees Celsius (Lee, 2013).

3.2.1. Exclusion of BTES as an Alternative

Although the decision was made to implement ATES, borehole thermal energy storage (BTES) could also be considered as an alternative. BTES uses boreholes to circulate water through pipes that exchange heat with the ground (Rad & Fung, 2016). Unlike ATES, which uses water to store heat in an aquifer, BTES stores heat directly in the ground. While the amount of energy stored depends on the subsurface structure, ATES consistently stores more heat (GeoERA, n.d.). Therefore, if an aquifer is available, ATES is the preferable choice over BTES.

3.2.2. Regeneration

ATES systems need to be regenerated to maintain their effectiveness and capacity over time. Regeneration entails that the thermal balance must be maintained within one year, by re-injecting as much energy as was extracted during the year. Not applying regeneration results in efficiency losses and degradation of the aquifer. The first potential source to regenerate the ATES are solar thermal panels. These panels can be placed on the roof of buildings and use the irradiation of the sun to heat up water (Mekhilef et al., 2011). This heated water can then be used to regenerate the heat well of the ATES. The disadvantage is that this technique is not effective at regenerating the cold well. However, this is less critical since the cooling demand is lower than the heating demand.

Another potential source for the regeneration of ATES systems is the surface water from Amsterdam's canals. The thermal energy potential of this surface water is estimated to be sufficient to regenerate 40-60 percent of the heat demand and 100 percent of the cold demand (Ruijs, 2019). Surface water cannot be used for heating and cooling directly because of its temperature, which varies with the season. The temperature often doesn't align with the desired form of heat extraction. In the summer, when the cooling demand is high, using surface water for cooling is preferable. However, this can degrade water quality and promote algae growth. Although using it for heating would benefit water quality, the heating demand is much lower in summer than in winter. Therefore, it is beneficial to connect this with a form of seasonal storage, such as ATES, to extract energy at optimal times and store it for periods of high demand (Fremouw & Dobbelsteen, 2020).

3.2.3. Monowell or doublet

An ATEs system consists of two wells. A well is a part of the aquifer that can be accessed after drilling to it. The aquifer is a water-bearing layer in the subsurface. This means that this layer can contain water and that water can flow through it. An ATEs system consists of two such wells, a cold well and a warm well. The position relative to each other determines the type of system. In a monowell configuration, the two wells are positioned one below the other in the same location within the aquifer. In contrast, in a doublet configuration, the two wells are placed next to each other within the aquifer (figure 3.4).

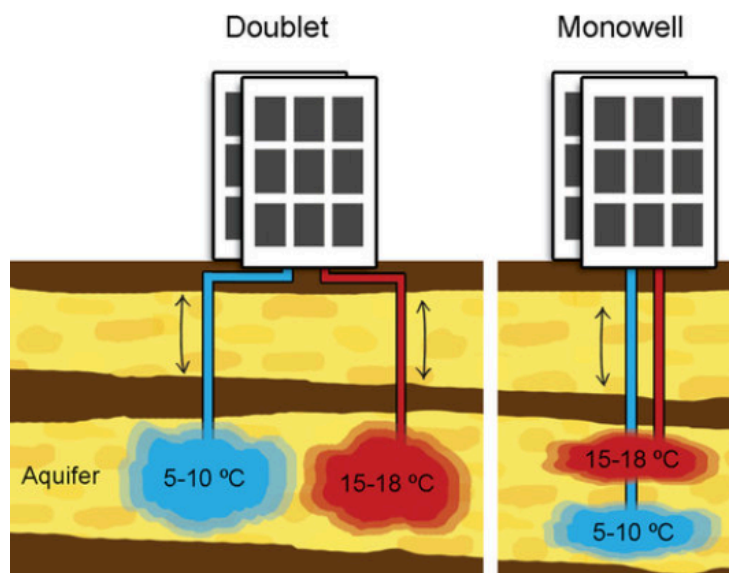


Figure 3.4: The placement of the wells in a doublet and monowell configuration (Bloemendal & Olsthoorn, 2018)

When deciding to implement an ATEs system for buildings, it is crucial to consider the thermal radius (R_{th}). The thermal radius is the distance from the well in which groundwater temperature is affected by the extraction or injection of water from the ATEs system. The thermal energy from this water affects the groundwater temperature if it differs from the temperature of the aquifer. If wells with different temperatures are situated too closely to each other, thermal interference may occur. Thermal interference means that the two wells will exchange thermal energy, which will flow from the high to the low temperature. When there are both warm and cold wells in close proximity, the temperature of the warm well tends to decrease while the temperature of the cold well increases. This situation negatively impacts the efficiency of the system. However, when wells of the same type are placed nearby, this effect can result in a reinforcing thermal exchange, resulting in reduced losses to the environment.

To prevent negative influence, there must be a certain distance between wells. This distance is equal to a multiple of the thermal distance, depending on the well types. To optimize the use of subsurface space, the distance between wells of different types is set at $2.5 R_{th}$, whereas the distance between wells of the same type is set at $1 R_{th}$ (Bloemendal, 2018). If the two wells have different thermal radii, the average of the two is calculated and used to determine the required distance between the wells.

When deploying doublets, the placement of wells becomes crucial. It is essential to consider the proximity of wells from neighboring systems. Placing a cold or warm well adjacent to the corresponding well of a neighboring system reduces the required distance between systems compared to placing opposite types of wells next to each other. Considering this factor allows for a more efficient utilization of the subsurface.

With monowells, this consideration is less significant since a distance of 2.5 times the thermal radius must always be maintained. In monowell configurations, a neighboring system will always have wells of the opposite type, because a monowell inherently combines both cold and warm wells in one borehole. Additionally, there must be a distance between the warm and cold wells of the monowell, equivalent to the length of the well screen. For instance, a monowell with a 10-meter well screen will occupy a total depth of 30 meters, consisting of 10 meters of cold well screen, followed by 10 meters of empty space, and ending with 10 meters of warm well screen..This means that monowells generally make less efficient use of the subsurface.

In areas with high demand for thermal storage, a doublet system is thus preferred because it maximizes the utilization of limited available space (Bloemendal, 2018). However, the advantage of monowells is cost-efficiency, as drilling is required only once compared to the two drillings needed for a doublet system.

It is clear that using both monowells and doublets is not ideal, as significant space must be maintained between a monowell and a doublet. The design choices that can still be made during the large-scale implementation of ATEs are explained below.

3.2.3.1. Design with doublets only

The first potential design only implements doublets. This indicates that significant spacing is still necessary between different cold and warm wells, but this can be minimized by strategically clustering cold and warm wells as closely together as possible. Achieving maximum utilization of the aquifer's thickness will result in enormous systems. Every system has a capacity, which denotes the amount of water removed from the system per second. The larger the system, the higher its capacity will be. Larger systems can be more challenging to control because there is a minimum capacity threshold that must be maintained during extraction and injection. For instance, if this threshold is set at 10% of the capacity, it may exceed the requirements of the heating network at that time. Thus, in terms of controllability, larger systems present greater challenges.

3.2.3.2. Design with equal well screen monowells only

The second potential design only implements monowells. The drawback of monowells is that there always needs to be empty space between the warm and cold wells within a monowell. Additionally, there must be a distance of 2.5 times the thermal radius between different monowells when they do not have the same length of well screen. If monowell A has a well screen of 10 meters and monowell B has a well screen of 30 meters, thermal interference occurs between the two monowells. Monowell A reaches a total depth of 30 meters (3 times 10 meters), placing both its warm and cold wells at the same depth as the first 30 meter well of monowell B. This necessitates maintaining a distance of 2.5 times the thermal radius. This issue is mitigated if monowells with identical lengths of well screens are selected. Each system will then have identical well depths, for instance, with all warm wells positioned above and all cold wells below. Consequently, there would be no need to maintain a distance of 2.5 times the thermal radius between them, since all thermal interference would be positive. Monowells thus maximize the use of the aquifer's width, whereas doublets maximize the use of the aquifer's depth.

3.2.4. Thermal capacity

The amount of energy that can be stored in the volume of the ATES depends on the temperature difference between the warm and cold well. This amount is determined by the thermal heat capacity, which is the amount of heat needed to raise the temperature of a substance by one degree Celsius. This also corresponds to the amount of heat released when lowering the temperature by one degree Celsius. When energy is extracted from the warm well of the ATES, a heat exchanger reduces the water temperature until it matches that of the cold well. Conversely, when water comes from the cold well, heat is added until it reaches the temperature of the warm well. The greater the temperature difference between the wells, the more energy can be stored. The temperature of the cold well typically ranges from 5 to 12 degrees Celsius, while the temperature of the warm well generally varies between 14 and 30 degrees Celsius (W. Sommer et al., 2015). The temperature difference between the warm and cold well is generally equal to 4 °C (Bloemendal, 2018).

In addition to the temperature difference, the total volume that can be stored in the ATES system depends on factors such as the length of the well screen and the thermal radius, as illustrated in figure 3.5. The well can be displayed as a cylinder because its screen is positioned vertically. Since water spreads uniformly in all directions from this point, it shapes itself into a cylindrical form. The volume of the well can be determined using the thermal radius and the length of the well screen. If 2 values of the volume, the well screen length and the thermal radius are known, the third can be determined. The way to do this is explained in chapter 5. The volumes of both wells must be equal because the water extracted from one well is subsequently injected into the other. If one well has a smaller volume than the other, it means that the larger well cannot utilize its full capacity.

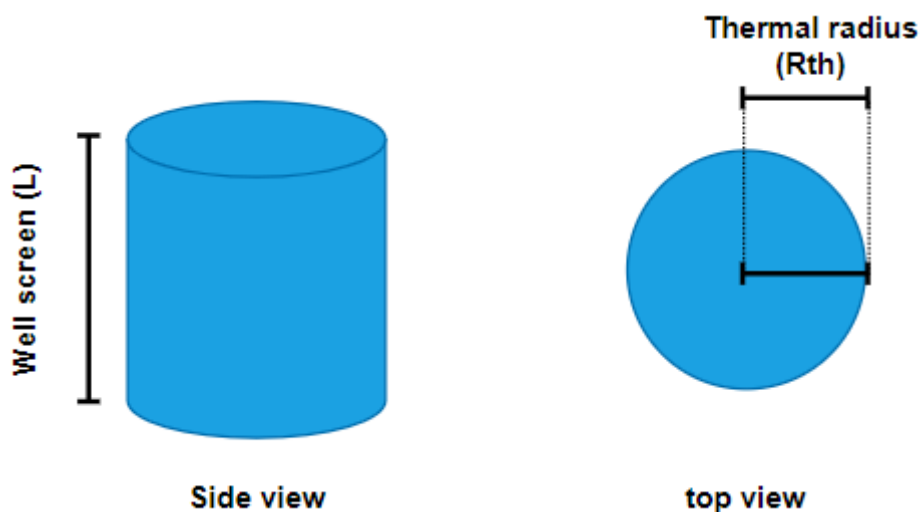


Figure 3.5: Simplified representation of the volume of an ATES well

3.2.5. Planning

The area required for an ATEs is determined based on the thermal footprint. This is the area that is created when a circle is made with the thermal radius with the ATEs system as the center. However, there is currently no system behind planning ATEs locations. All buildings that want to implement an ATEs system can apply for a permit and choose the dimensions and location that suits them best. Currently, well screens are made as short as possible to save on drilling costs. This approach does not optimize subsurface utilization, as it results in a larger thermal radius and leaves the lower portion of the aquifer unused (Doughty et al., 1982).

Considering thermal interference and efficient use of the subsurface, this is not an effective method. Since drilling costs constitute a significant portion of the total expenses, many projects opt not to drill deeply. If the aquifer is 100 meters thick but only 20 meters are drilled to save costs, this results in ineffective use of the subsurface. While another system could theoretically be installed deeper at the same location, this is not economically viable and thus rarely occurs (M. Bloemendal, personal communication, 3 May 2024).

3.2.6. Restrictions

ATEs systems cannot be installed everywhere due to various restrictions and limitations. To begin with, the entire area of Amsterdam's center is considered an 'area of attention for archaeology.' This does not prohibit the installation of ATEs systems, but it does require additional arrangements and considerations to proceed with the installation. Additionally, no drilling is allowed above metro tunnels, and no subsurface work is allowed in the entire area of the Dam and Damrak (Fremouw & Dobbelsteen, 2020). Finally, existing ATEs systems must be considered to prevent thermal interference.

Besides the fact that ATEs systems are not allowed everywhere underground, there must also be sufficient space above ground. This space is needed to accommodate the installation process, which requires an area of either 6 by 15 meters or 3.5 by 30 meters for drilling (Noome, 2013).

3.3 Summary design choices

When considering network temperature, LT and ULT are the best options. LT is advantageous because the water can be directly used for cooling, while ULT allows for greater utilization of renewable energy sources and more efficient recovery of excess heat. However, the temperature level is not relevant for this study, as the network itself is not directly analyzed. In terms of pipe configuration, both two-pipe and four-pipe systems are viable options. The two-pipe system is preferable because it requires half the number of pipes, reducing the need for underground space and experiencing lower thermal losses, as the temperature remains closer to that of the subsurface. The four-pipe system, on the other hand, requires less space within buildings since heating and cooling are managed centrally. Given the advantages of reduced thermal losses and minimized underground space requirements, the two-pipe configuration was selected.

For ATEs systems, a choice must be made between doublets and monowells. A doublet makes better use of the entire thickness of the aquifer as the two wells aren't above each other and therefore there is no empty space in between. In contrast, a monowell system maximizes the use of the aquifer's width, allowing for consistent placement of wells at a distance of 1 Rth, compared to the doublet system's requirement of 2.5 Rth opposing for well types. Given the significant thickness of the aquifer, prioritizing efficiency in the utilization of the width over efficiency in the utilization of the thickness leads to the decision to implement a monowell system.

4

Actor analysis

This chapter presents an analysis of the key actors involved in a district heating and cooling system, which will lead to the development of key performance indicators (KPIs). By identifying each actor's objectives, this analysis will guide design decisions and ensure that the new system meets the needs of all stakeholders.

4.1. Key actors

The key actors play an important role and have distinct objectives that the new system must address. Understanding these actors and their objectives is essential for successful implementation and the development of KPIs.

4.1.1. Heat and cooling users

A switch to a district heating network is not feasible if users are not in favor of it (Stichting Warmtenetwerk, 2021). It is crucial that they can participate in the decision-making process, as this can significantly increase the acceptance of an implementation. District heating networks are currently implemented primarily through a top-down approach, whereas users prefer a bottom-up approach (Stichting Warmtenetwerk, 2021). In addition, reliability is an important factor for the users of a district heating network. Users still perceive uncertainty due to potential electricity grid congestion; If a user were to lose power due to congestion, the heat pump would become inoperative and unable to provide heating or cooling. Additionally, users experience uncertainty due to fluctuating gas prices; potential declines in gas prices may extend the payback time, leading them to worry that using gas could be more cost-effective (Voermans, 2024).

4.1.2. Energy suppliers

Energy suppliers are essential because they will be responsible for supplying the heat to the users. Energy suppliers all share the goal of reducing their emissions. This typically involves striving for climate neutrality, assisting customers in adopting more sustainable practices and producing more sustainable energy (Eneco, 2024; Liander, 2024; Vattenfall, 2024). Additionally, they naturally aim to generate profit from the project, requiring a viable business case.

4.1.3. Housing corporations

For housing associations, it is crucial to provide well-functioning homes that satisfy their customers. This entails ensuring that the supplied heat is not only affordable but also reliable. Even though they do not bear the cost of heat themselves, having affordable and reliable heating in the buildings they offer is appealing to housing corporations, as it makes the properties more attractive to potential customers. Therefore, it is beneficial for housing corporations to have access to such a heat source, providing customers with more heating options.

4.1.4. Operators electricity grid

Electricity grid operators are crucial because a 5GDHC network consumes a significant amount of electricity, particularly for powering the heat pumps. As each building will have its own heat pump, the demand for electricity will increase. However, this increase will be smaller if the heating and cooling demands are (approximately) of equal size, as less external energy is needed for generation, resulting in lower electricity usage. The electricity grid operator must ensure that the electricity grid can accommodate this demand. Their objective is to maintain a reliable electricity grid that is free from congestion or outages. To alleviate the increasing congestion on the grid, grid expansions may be necessary. On top of that, they aim to stimulate a sustainable energy future (TenneT, 2024).

4.1.5. Municipality of Amsterdam

The municipality of Amsterdam aims to reduce CO₂ emissions and wants to be climate neutral with zero CO₂ emissions by 2050 (Gemeente Amsterdam, 2024). Additionally, they plan to provide alternatives to natural gas for all neighborhoods and be entirely natural gas-free by 2040. The implementation of a 5GDHC network aligns with these goals since it's a natural gas-free alternative for the heating of buildings, which will reduce CO₂ emissions. Furthermore, it is also crucial for the municipality of Amsterdam that the subsurface is utilized efficiently (Gemeente Amsterdam, 2019).

Table 4.1: The system objectives of the key actors

Actor	System objectives
Users	<ul style="list-style-type: none"> ● Bottom-up implementation ● Reliable heat supply ● Low costs for heating
Energy suppliers	<ul style="list-style-type: none"> ● Reduce CO₂ emissions ● Viable business case ● Produce sustainable heat
Housing corporations	<ul style="list-style-type: none"> ● Reliable heat supply ● Low costs for heating
Grid operators	<ul style="list-style-type: none"> ● Maintain the reliability of the electricity grid
Municipality of Amsterdam	<ul style="list-style-type: none"> ● Reduce CO₂ emissions ● The phasing out of gas ● Efficient subsurface utilization

4.2. Main objectives

All system objectives of the key actors can be found in table 4.1. A 5GDHC network inherently contributes to phasing out gas by eliminating its use for heating buildings. Achieving a good heat balance minimizes the requirement for external energy (KoWaNet, 2021). Minimizing the requirement for external energy will significantly reduce CO₂ emissions. This also contributes to a viable business case by lowering the costs, which translates to lower heating costs for customers. The use of renewable energy sources in the system ensures that it produces sustainable heat. All the objectives above can be met by having a maximized demand fulfillment in the system. This entails that the goal is to have 100% of the demand fulfilled by energy balancing within the clusters and the use of thermal energy storage. A balancing potential occurs

when there is cooling and heating demand at the same moment in time. The residual heat from cooling can be used for heating, and vice versa; Using the balancing potential and the thermal energy storage is beneficial, since it lowers the need for external energy. Although the goal is to achieve 100% demand fulfillment in every cluster, this is not always realistic. There may be insufficient balancing potential or inadequate space for thermal energy storage to meet the full 100%. Therefore, the objective is to maximize demand fulfillment to achieve the highest possible percentage.

A bottom-up approach with clusters provides grid operators sufficient time to assess the capacity of the electricity grid, determine the necessity for expansions, and implement them as needed. Improving the readiness of the electricity grid to meet the increasing demand reduces the risk of outages and congestion, making the 5GDHC network more reliable. Compact clusters also result in a reduction in the total pipe length needed to connect buildings, thereby reducing network costs and utilizing the subsurface more efficiently. All the objectives above can be met by implementing compact clusters. Compact clusters entail that the buildings within each cluster are close to one another. When buildings are situated closer together, the length of pipe required to connect them all is reduced.

The goal is to create balanced clusters, meaning that differences in demand fulfillment and cluster compactness are minimized across clusters. This balance is essential to meeting stakeholders' goals; if demand fulfillment is high in most clusters but extremely low in one, that cluster will require significantly more external energy, potentially leading to higher heating and cooling costs for that cluster. While the overall results may appear satisfactory, stakeholders in the underperforming cluster will be dissatisfied. Since 5GDHC networks can be implemented per cluster, it is important to evaluate each cluster individually for demand fulfillment and compactness. This evaluation helps identify which clusters, and therefore areas, have the highest potential for a successful 5GDHC network. Conversely, it also highlights clusters with less potential, where alternative methods for heating and cooling should be considered.

The main objectives can thus be summarized by:

1. The network must have a maximized demand fulfillment
2. The clusters of the network must be compact
3. The demand fulfillment and compactness must be balanced across all clusters

5

Methodology

This chapter outlines the methodology and its development process. First, the chapter examines the choices that were necessary to develop this methodology. This includes the identification of the key performance indicators (KPIs), which are based on the objectives established in the actor analysis. Consequently, the following methodology is elaborated upon and illustrated with a small example.

5.1. Key performance indicators

To test how well the model is able to meet the stated objectives, KPIs are identified. These must be able to measure the extent to which the method achieves the previously stated objectives and enable comparison between multiple results. The two system objectives from the actor analysis are stated below:

- The network must have a maximized demand fulfillment
- The clusters of the network must be compact
- The demand fulfillment and compactness must be balanced across all clusters

5.1.2. Demand fulfillment

To evaluate the demand fulfillment of clusters, a new metric has been devised, inspired by the demand overlap coefficient (DOC), first introduced by (Wirtz et al., 2020b).

The DOC describes which share of heating and cooling demands can be fulfilled within the cluster. This is assessed based on the overlappings of demands to determine the balancing potential, as illustrated in figure 5.1.

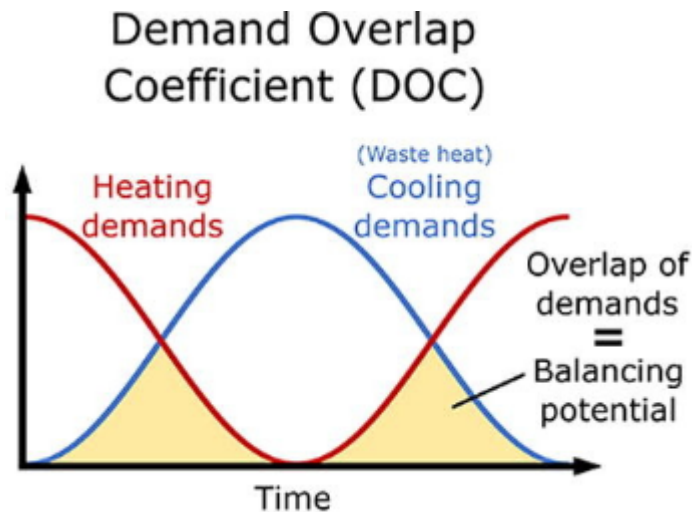


Figure 5.1: The overlapping in demands which determines the DOC (Wirtz et al., 2020b)

An example of how the DOC is calculated is shown in figure 5.2. The chart in this figure plots the heating and cooling demand over time, highlighting two instances where the demands overlap. For this scenario, the DOC is calculated to be 0.2, indicating that 20% of the heating and cooling demand can be fulfilled either within the building itself or between buildings. Consequently, 20% less energy needs to be generated.

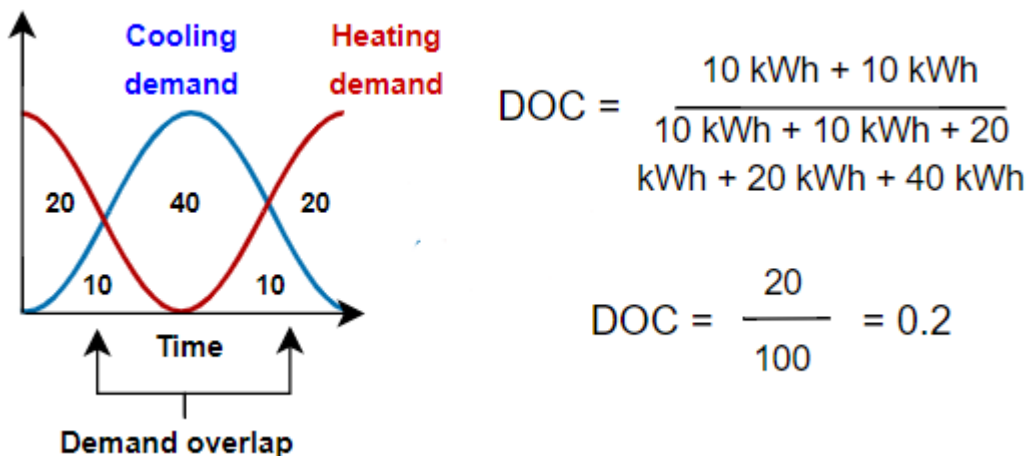


Figure 5.2: Example calculation of the DOC

The balancing potential can be within the building itself or between buildings. However, in a situation where ATES is implemented, it is not only about the part of the demand that the houses themselves can fulfill between each other, but also about the amount of demand that can be supplied by the ATES systems. Therefore, a new metric has been devised called the demand fulfillment coefficient (DFC). This metric indicates the share of heating and cooling demand that can be met within the network, including contributions from external sources like ATES. The DFC can be used to evaluate the efficiency of the 5GDHC network.

5.1.2. Cluster compactness

Compact clusters mean that the buildings within each cluster are close to one another. To evaluate the compactness of the created clusters, the within-cluster sum of squares (WCSS) will be used, by applying formula 1 and 2. This metric measures the sum of squared distances between each point and the center of its cluster (Sankalana, 2023).

$$W_k = \sum_{j \in C_k} \left\| x_j - \mu_k \right\|^2 \quad (1)$$

- W_k = The within cluster variation of cluster k (m^2), where $k \in \{1,2,\dots,K\}$
- K = The total number of clusters
- C_k = The center of cluster k , where $k \in \{1,2,\dots,K\}$
- x_j = The location of building j (m), where $j \in \{1,2,\dots,J\}$
- J = The total number of buildings
- μ_k = The location of the cluster center of cluster k (m), where $k \in \{1,2,\dots,K\}$

$$WCSS = \sum_{k=1}^K W_k \quad (2)$$

- WCSS = The within cluster sum of squares (m^2)

The more compact the clusters are, the shorter the distance between the buildings and the cluster center, resulting in a lower WCSS value; A lower value of the WCSS indicates a more compact cluster.

5.1.3. Balance across clusters

The spread of the demand fulfillment is used to evaluate the balance across the clusters. The values for compactness and demand fulfillment are plotted for all clusters, and the distribution of these values is analyzed. This analysis includes calculating the minimum, maximum, and standard deviation. This allows for an examination of the performance of the first two KPIs in each cluster.

5.2. Order of the methodology

Addressing the sub-questions involves two key tasks: clustering the buildings and integrating the ATES installations. Since there is no predetermined sequence for these two tasks, the order must be determined. The methodology starts with clustering, since it then becomes feasible to determine the necessary storage capacity based on the resultant clusters. This approach simplifies the integration of ATES systems into the clusters, as it can then be determined per cluster how many ATES systems are needed. Determining the optimal locations for ATES systems first is inconvenient because it's challenging to estimate the required number and placement of systems without prior knowledge of building clusters and their required storage capacity. If ATES systems are installed before clustering, each system must subsequently be grouped into clusters to avoid having too many individual clusters. Buildings would then need to be linked to these ATES clusters, provided there is sufficient storage capacity. This process results in less compact clusters, which is undesirable. The only scenario where it makes sense to choose ATES locations before clustering buildings is when aquifer space is very limited but there is ample surface space. In such cases, optimizing the use of the aquifer takes precedence over achieving compact clusters.

5.3. Clustering

To group the buildings into clusters, different clustering algorithms and heuristics can be applied, focusing on their spatial locations. Various methods have been identified in the literature and are described below. Considering the strengths and weaknesses of these methods alongside the data characteristics, the most suitable method is selected. The chosen clustering method will be applied to the data of the inner city of Amsterdam. This must be taken into account, since Amsterdam is a large city with a large quantity of buildings, resulting in a large data set. Computational efficiency is therefore very important, as otherwise the method will take too long to execute.

5.3.1.K-means

K-means clustering is an iterative algorithm used to divide a dataset into clusters based on the locations of the points. The number k must be chosen beforehand and is an input for the algorithm (Rodriguez et al., 2019). The clustering process starts with the placement of ' k ' centers. Each point is then assigned to the center closest to their location. The locations of the centers are then recalculated, by positioning them at the location that minimizes the total distance from the center to all points in the cluster. This process repeats, where points are assigned to the closest center and the location of the center is changed. This continues until no substantial changes in the center positions are observed (figure 5.3).

A limitation of the algorithm is the sensitivity of the initial center locations, where varying initial conditions can lead to different outcomes (Jain et al., 1999). Another limitation is the necessity to select the number of clusters ' k ' beforehand, as this information is not always available in advance (MacQueen, 1967). Nevertheless, k-means is a useful algorithm due to its speed and scalability (Coates & Ng, 2012).

Another option is to use k-median instead of k-means. In this approach, the median of the data points in each cluster is used to determine the center, rather than the mean. K-median is particularly advantageous in situations with significant density variations and numerous outliers (Wittek, 2014). However, when applying the clustering method to the data from the center of Amsterdam, where the entire area is densely populated and has a high concentration of buildings, it is expected that the density will remain relatively uniform throughout. Therefore, k-means is deemed more suitable than k-median in this context.

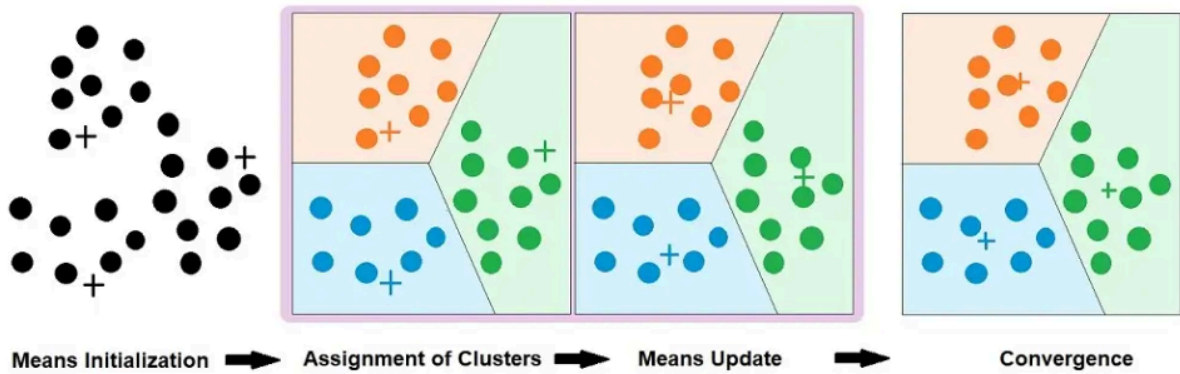


Figure 5.3: An example of implementing the *k*-means algorithm (Arya, 2022)

5.3.2. DBSCAN

DBSCAN (Density-Based Spatial Clustering of Applications with Noise) is a clustering algorithm utilized to identify clusters in spatial datasets based on density (figure 5.4). Points that are closely packed together form clusters, while remote points are labeled as outliers or noise. This is determined by the parameters minimum points (MinPts) and ϵ . MinPts is the smallest number of points required to form a cluster, and ϵ is the maximum distance between two points for them to be considered neighbors. Each point in a cluster has to contain at least MinPts points in a radius of ϵ , to be part of a cluster (Ester et al., 1996).

Finding the appropriate values for ϵ and MinPts can be challenging, and the algorithm is very sensitive towards these values. The algorithm is also sensitive to variations in density, which can result in clusters of significantly varying sizes (Campello et al., 2013).



Figure 5.4: The performance of DBSCAN on various point sets (Andrewngai, 2020)

5.3.3. Single linkage clustering

Single linkage begins with each point as its own cluster. All the distances between the different points are calculated. Then an iterative process starts where the clusters closest to each other are merged, forming a new cluster and replacing the old clusters (Maulik & Bandyopadhyay, 2002). The distances are recalculated and the process repeats. This can continue until a predetermined number of clusters remains (see Figure 5.5). Additionally, methods such as the dendrogram and the elbow method can be used to determine the optimal number of clusters based on the results.

A limitation of this method is the possibility of the chaining effect (Jarman, 2020). The dense areas are joined together first, since the closest clusters are merged first, while the outliers remain as separate clusters. This can result in large and elongated clusters, which can be undesirable. Additionally, the method usually fails to identify clusters if a dataset contains outliers (Klutchnikoff et al., 2021). Lastly, single linkage clustering has a high convergence time, making it unsuitable to use in combination with large datasets (Banerjee et al., 2021).

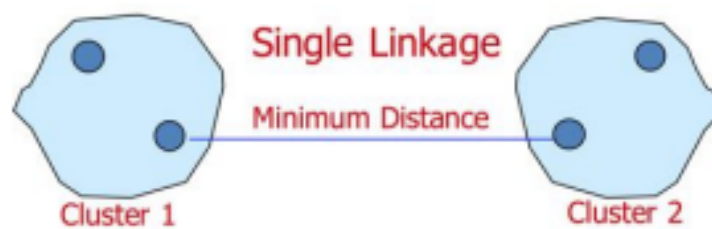


Figure 5.5: An example result of the single linkage algorithm (Dozmorov, 2016)

5.3.4. K-minimum spanning tree

The last heuristic is the k-minimum spanning tree, which has already been successfully applied to find the clusters in a topology of a district cooling network (Neri et al., 2022). In this heuristic, all the points are first connected to each other, where the distance towards the other nodes is assigned as a weight on the edges. Then the minimum spanning tree is determined, which is a subset of edges in a graph which forms a tree and connects all vertices with the lowest possible edge weight. The number of desired clusters needs to be determined and is equal to 'k'. For the next step the k-1 longest edges are removed from the minimum spanning tree, resulting in 'k' clusters (figure 5.6).

The difference between K-minimum spanning tree and single linkage clustering is that single linkage clustering looks at the minimum distance between clusters, while k-minimum spanning tree examines the overall structure of the minimum spanning tree across all points. This results in a lower likelihood of forming elongated clusters, leading the k-minimum spanning tree to produce more compact clusters.

The k-minimum spanning tree is sensitive to longer distance edges, which can lead to the formation of large, dense clusters if there are significant density differences in the graph. This heuristic also becomes computationally more expensive as the dataset grows larger (Raidl, 2000).

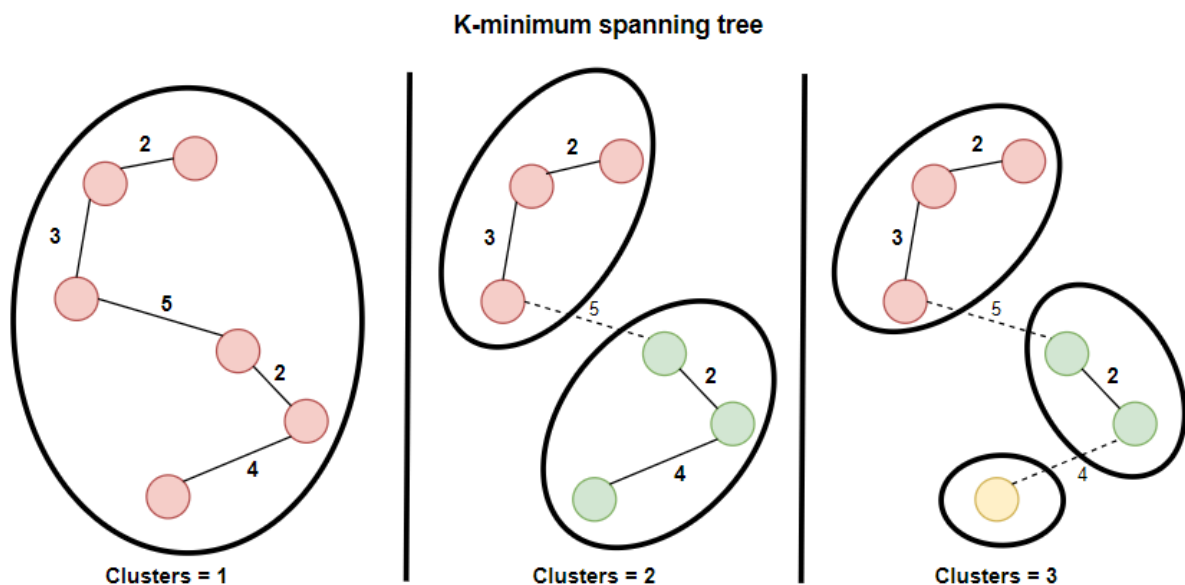


Figure 5.6: The results of the k-minimum spanning tree algorithm with varying numbers of clusters

5.3.5. Clustering method selection

Every clustering method found has its strengths and weaknesses. The chosen clustering method will be applied to the data of the inner city of Amsterdam which has a large quantity of buildings, resulting in a large data set. Both single linkage clustering and the k-minimum spanning tree are unsuitable, since the methods are computationally expensive.

K-means is preferred over DBSCAN due to its superior computational speed. Furthermore, DBSCAN requires the selection of two parameters— ϵ and MinPts—while k-means only requires one: the number of clusters k . This dual parameter selection can be more challenging, as the impact of one parameter is influenced by the other.

The chosen method of k-means has no limitations that conflict with the properties of the data. However, it is sensitive to the initial center locations and requires the number of clusters to be specified beforehand. The sensitivity to the initial center locations can be mitigated by doing several iterations of the method and selecting the best result. Furthermore, the need to select the number of clusters beforehand can be mitigated by running the method multiple times with a different number of clusters and selecting the number of clusters with the best outcome. This could involve achieving a desired level of compactness or ensuring a specific average, minimum, or maximum number of buildings in each cluster. Consequently, k-means is a suitable clustering method because its limitations can be effectively managed, and it can efficiently handle large datasets due to its computational speed.

Another advantageous feature of k-means is its potential extension known as equal size k-means (Elki project, n.d.). This method begins with a standard k-means process, followed by node exchanges between clusters to achieve clusters containing an equal number of nodes. While standard k-means already minimizes WCSS, exchanging nodes between clusters reduces compactness but might enhance the implementation feasibility of ATEs systems. The rationale behind this approach is that by equalizing the number of buildings in each cluster, the variation in required storage capacity per cluster is reduced, allowing for a more balanced distribution of the necessary ATEs systems across the area. However, this approach is not guaranteed to be effective, as the demand can vary significantly from building to building.

5.4. Method Selection and Explanation

The method will now be explained based on the choices made. The approach involves clustering the buildings and implementing ATEs installations within these clusters. The goal is to create compact clusters that can meet the heating and cooling demands to the fullest extent.

The method consists of four steps shown below:

1. Clustering of the buildings
2. Determining the required storage capacity for the clusters
3. Implementing ATEs installations
4. Evaluating KPI performance

5.4.1. Clustering of the buildings

Before clustering, the buildings are represented as a point positioned at its respective location. An example of how buildings are positioned is shown on the left in figure 5.7, which is an example area used to demonstrate how the method works. With the locations of the buildings established, the k-means algorithm explained in Chapter 5.3.1. can be applied. The results are shown on the right side of figure 5.7, where buildings of the same color belong to the same cluster. The centers are the points for which the total distance to all other buildings in the cluster is minimized. These points are marked by the red crosses located within the clusters.

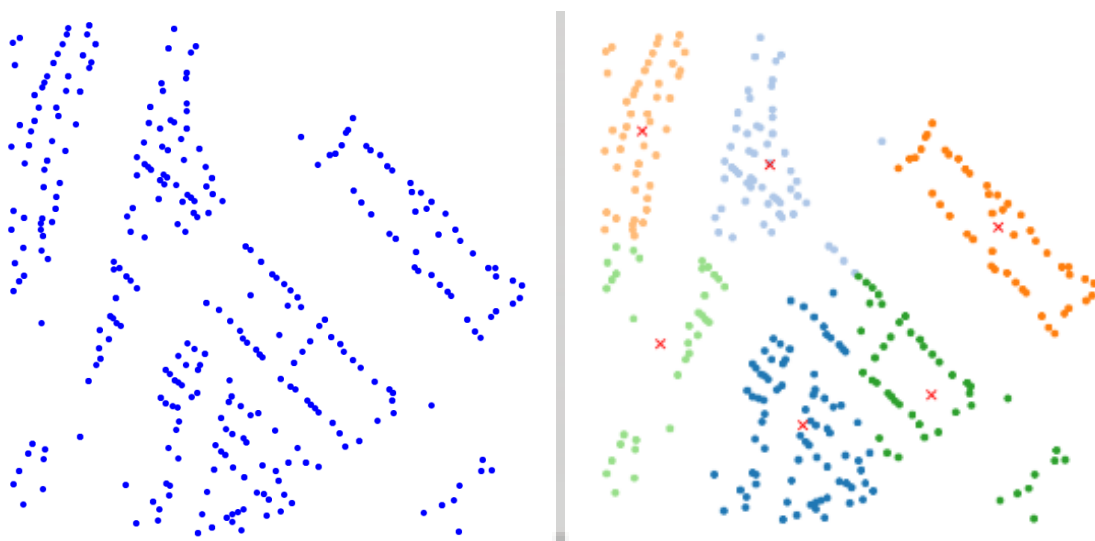


Figure 5.7: The result of applying k-means (right) on the small example area (left)

The k-means result is kept and also used as input for the equal-size k-means algorithm. This algorithm starts with the result of the normal k-means algorithm. This is seen on the left in figure 5.8, where points are grouped into clusters A, B, and C, each represented by a different color. In this example, the clusters are compact, but there are noticeable differences in the number of points within each cluster; cluster B contains significantly fewer points than cluster C. To address this, the equal-size k-means algorithm is applied, allowing points to be exchanged in order to achieve an equal number of points per cluster, as shown in the center of Figure 5.8.

Initially, the average number of points per cluster is calculated by dividing the total number of points by the number of clusters. If one cluster has fewer points than the average while another has more, points can be exchanged between them to bring both clusters closer to that average. Additionally, we consider whether points can be swapped between two clusters if each point is closer to the center of the other cluster than to its own. This process requires several iterations, as the cluster centers may shift after each improvement round. The final result is depicted on the right side of Figure 5.8, where all clusters contain an equal number of points.

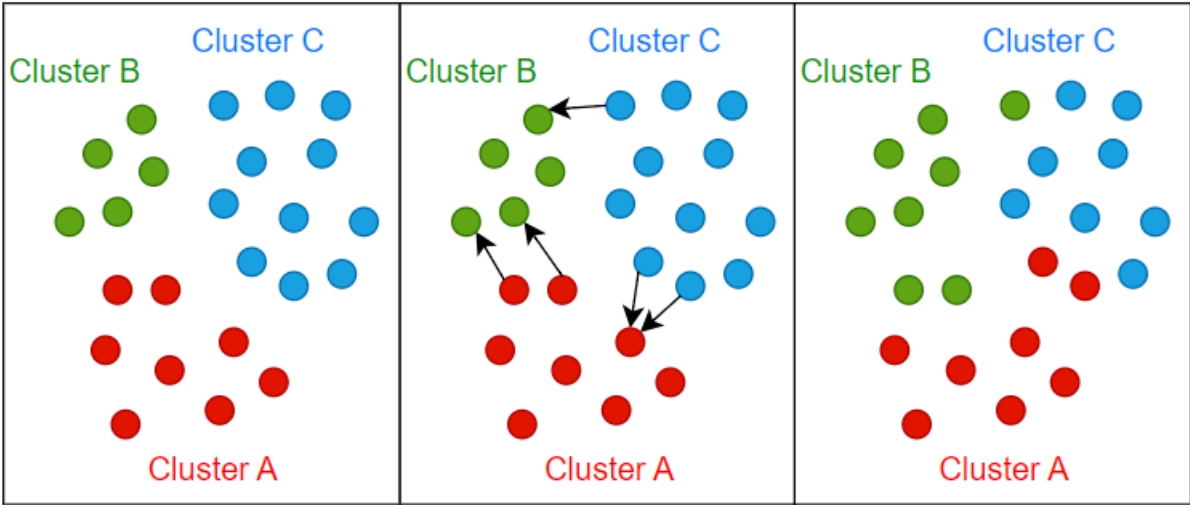


Figure 5.8: An example of applying the equal-size k-means algorithm

For larger datasets, a minimum number of improvements must be specified before the iteration rounds stop. Typically, the process continues until no further improvements are possible, but with larger datasets, the model may not converge. The required minimum depends on the specific dataset and must be determined based on experience in each situation. This method is implemented following a tutorial (Heijnen, 2023).

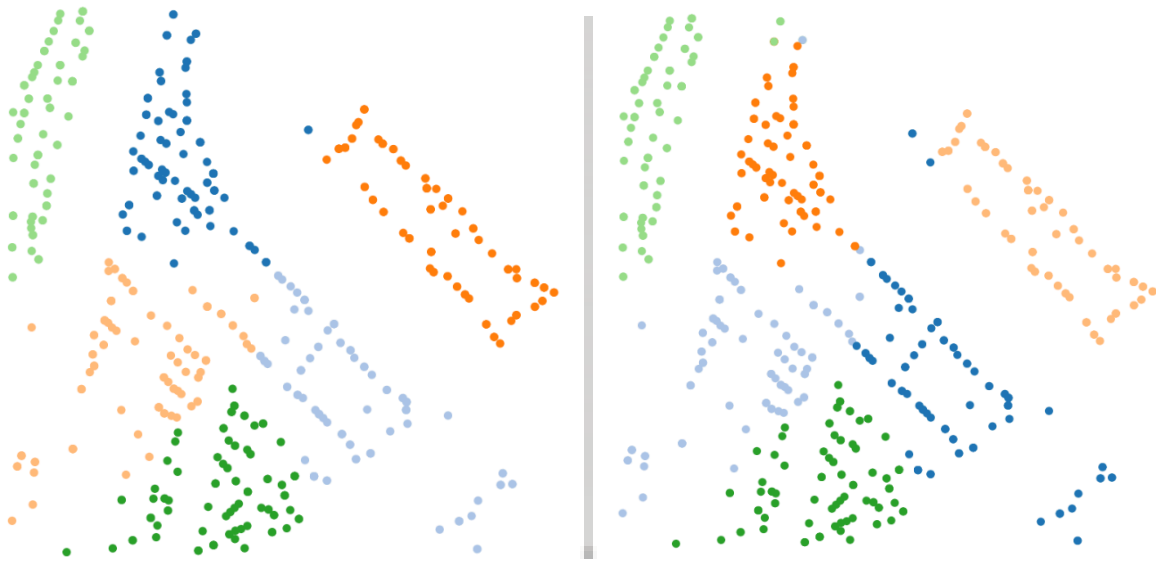


Figure 5.9: The results of *k*-means (left) and equal-sized *k*-means (right) to the example area

In figure 5.9, the comparison between the results of *k*-means (left) and equal-sized *k*-means (right) reveals small differences. In the equal-sized *k*-means clustering, certain outliers can be observed—buildings that are significantly distant from others buildings within their clusters. This phenomenon arises from the objective of achieving clusters with equal numbers of buildings and is recognized as a limitation of the method.

Both the resulting clusters of the *k*-means algorithm and the equal size *k*-means algorithm are carried forward to the next phase. They proceed through the steps of the method, allowing for a comparison of their outcomes, as shown in figure 5.10.

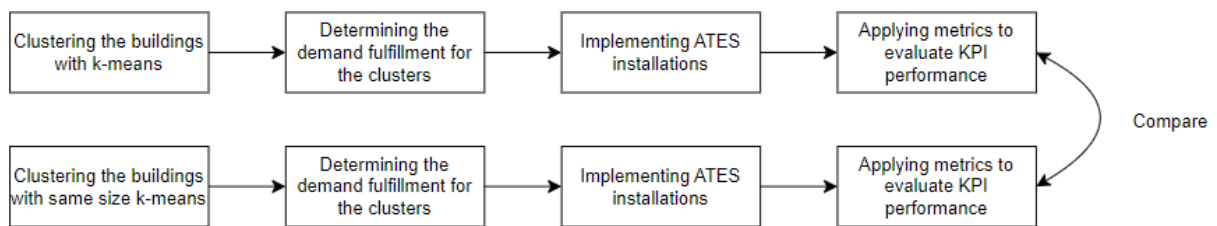


Figure 5.10: A representation of the method

5.4.2. Determining the required storage capacity for the clusters

To determine how much storage is needed per cluster, the annual demands of the buildings must first be determined. The total heating and cooling demands are assessed, along with the heating and cooling surplus. The surplus is defined as the amount of kWh by which the heating demand exceeds the cooling demand for a given hour, and vice versa. If the other type of demand is higher during that hour, the surplus is zero. This surplus will be used to calculate the demand overlap. Formulas 3 to 6 are used to calculate all these values, which are added up for all buildings in a cluster.

$$THD_j = \sum_{h=1}^G HD_{h,j} \quad (3)$$

- THD_j = The total heating demand of building j (kWh/year), where $j \in \{1,2,\dots,J\}$
- $HD_{h,j}$ = The heating demand for hour h of building j (kWh), where $h \in \{1,2,\dots,G\}$ and $j \in \{1,2,\dots,J\}$
- G = The total amount of hours in a year

$$TCD_j = \sum_{h=1}^G CD_{h,j} \quad (4)$$

- TCD_j = The total cooling demand of building j (kWh/year), where $j \in \{1,2,\dots,J\}$
- $CD_{h,j}$ = The cooling demand for hour h of building j (kWh), where $h \in \{1,2,\dots,G\}$ and $j \in \{1,2,\dots,J\}$

$$HS_j = \sum_{h=1}^G \max(HD_{h,j} - CD_{h,j}, 0) \quad (5)$$

- HS_j = The heating surplus of building j (kWh/year), where $j \in \{1,2,\dots,J\}$

$$CS_j = \sum_{h=1}^G \max(CD_{h,j} - HD_{h,j}, 0) \quad (6)$$

- CS_j = The cooling surplus of building j (kWh/year), where $j \in \{1,2,\dots,J\}$

Now that the clusters have been formed, it becomes possible to assess the demand fulfillment coefficient (DFC). Since no form of storage has been added yet, all demand must be met through exchange within and between buildings. Before the DFC can be determined, the demand overlap must first be calculated. The demand overlap is calculated by subtracting the demand surplus from the total demand of that type. This method utilizes the heating demand for this as shown in formula 6.

$$DO_k = TCHD_k - THS_k \quad (7)$$

- DO_k = The demand overlap between the heating and cooling demand for cluster k (kWh/year), where $k \in \{1,2,\dots,K\}$
- $TCHD_k$ = The total heating demand of cluster k (kWh/year), where $k \in \{1,2,\dots,K\}$
- THS_k = The total heating surplus of cluster k (kWh/year), where $k \in \{1,2,\dots,K\}$

The DFC is determined by dividing the demand overlap summed with the total storage capacity by the total demand of that type and is calculated per cluster, as shown in Formulas 8 and 9. Given that the heating demand is expected to be higher, Formula 8 is used in the method.

$$DFCH_k = \frac{DO_k + TC_k}{TCHD_k} \quad (8)$$

- $DFCH_k$ = The Demand Fulfillment Coefficient for heating of cluster k (-), where $k \in \{1,2,\dots,K\}$
- TC_k = The complete capacity of storage in the cluster k (kWh/year), where $k \in \{1,2,\dots,K\}$

$$DFCC_k = \frac{DO_k + TC_k}{TCCD_k} \quad (9)$$

- $DFCC_k$ = The Demand Fulfillment Coefficient for cooling of cluster k (-), where $k \in \{1,2,\dots,K\}$
- $TCCD_k$ = The total cooling demand of cluster k (kWh/year), where $k \in \{1,2,\dots,K\}$

Additionally, it is possible to determine the required amount of storage capacity needed to meet the total demand. This is determined by looking at the type of demand that remains the most unfulfilled. As stated in chapter 4.2.4., both the cold and warm wells must be of equal size. In most scenarios, heating demand exceeds cooling demand, requiring the application of formula 10. Conversely, if there is less fulfillment of cooling demand, formula 11 should be employed instead. This measures the total shortage in supply, which equals the surplus of that type of demand. Since energy is lost during transportation from the storage to the buildings, these must be accounted for in the required capacity.

$$RC_k = \frac{THS_k}{\eta} \quad (10)$$

- RC_k = Total storage capacity required to fulfill the total demand of the cluster k (kWh/year), where $k \in \{1,2,\dots,K\}$
- THS_k = The total heating surplus of cluster k (kWh/year), where $k \in \{1,2,\dots,K\}$
- η = The total efficiency of transporting energy from the wells to the buildings, expressed as a fraction (-)

$$RC_k = \frac{TCS_k}{\eta} \quad (11)$$

- TCS_k = The total cooling surplus of cluster k (kWh/year), where $k \in \{1,2,\dots,K\}$

This data is incorporated into the points of the cluster centers that will be utilized in the subsequent step.

5.4.3. Implementing ATEs installations

Before an ATEs system can be installed, its configuration and resulting capacity must first be determined. Since the method uses systems of equal size, this determination needs to be made only once. For the configuration, the thermal radius, storage volume and well screen length must be selected. If two out of the three parameters are selected, formula 12 can be used to determine the remaining parameter.

$$R_{th} = \sqrt{\frac{c_w V_{in}}{c_{aq} \pi L}} \quad (12)$$

- R_{th} = Thermal radius of the ATEs system (m)
- c_w = Volumetric heat capacity of water (J/m³/K)
- V_{in} = Groundwater storage volume per ATEs well (m³)
- c_{aq} = Volumetric heat capacity of the aquifer (J/m³/K)
- L = Well screen length (m)

The thermal radius is later used to determine the necessary distance between multiple monowells, to prevent thermal interference. The volume is utilized in formula 13 to calculate the storage capacity of a single well.

$$SC_{ates} = V_{in} * \Delta T * \frac{c_{aq}}{Z} \quad (13)$$

- SC_{ates} = The storage capacity of one ATEs well (kWh/year)
- ΔT = Temperature difference between the warm and the cold well (K)
- Z = Conversion factor used to convert joules to kWh (J/kWh)

A monowell consists of two wells: one warm and one cold well. Consequently, a single monowell has the determined capacity for both heating and cooling demand. Now that the capacity per monowell has been determined, the systems can be implemented within the clusters. To implement the ATES installations, the centers of the clusters are used to determine which locations of the free space are suitable to place an ATES installation. This process is shown in figure 5.11 and consists of 4 steps;

1. The center, indicated by the green circle with a C, checks which nodes from the free space, indicated by the open circles, are still available to place an ATES installation. Of all these nodes, the node closest to the center is chosen. Since the center is the point where the distance to all buildings is smallest, this gives the free space node the greatest chance to be in proximity to the buildings of that cluster.
2. An ATES system is placed at the location of the node found in step 1, indicated by the green circle. The total capacity of the ATES system is deducted from the demand that still needs to be fulfilled, as shown in formula 13.

$$NRC_k = \max \left[RC_k - n_k * SC_{ates}, 0 \right] \quad (14)$$

- NRC_k = Required capacity after the implementation of n monowells in cluster k (kWh/year), where $k \in \{1,2,\dots,K\}$
- n_k = The number of monowells placed in cluster k, where $n \in \{1,2,\dots,N\}$ and $k \in \{1,2,\dots,K\}$
- N = The maximum number of monowells that can be placed in the area

In addition, the area is marked in which thermal interference will occur if another ATES system is placed within it.

3. Since thermal interference must be prevented, all available nodes in the marked area are removed from the free space. This means that an ATES system can no longer be installed at those locations, which are indicated by the red circles.
4. The process stops if there is no more open space available or all demand from the cluster is fulfilled. If this is not the case, the process starts again from step 1.

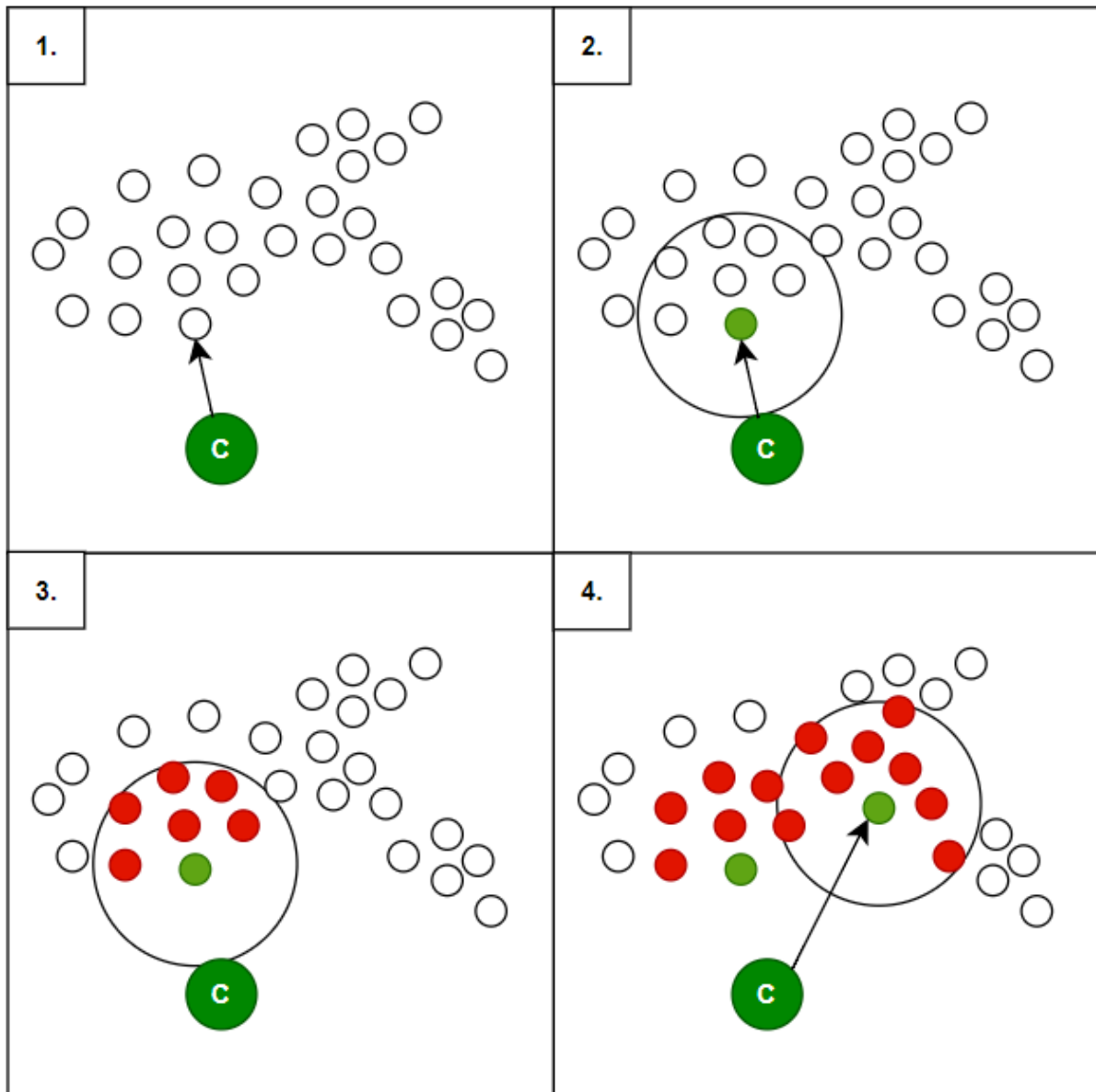


Figure 5.11: The process to determine suitable ATES locations

While the procedure for deploying ATES installations has been established, there may be insufficient available space to meet the demands of all clusters. Therefore, a prioritization reasoning must be selected for the sequence of ATES installations to be implemented. Furthermore, it is necessary to define a maximum distance from the center of each cluster within which available space can be utilized. This ensures that locations are chosen close to their respective clusters, maintaining computational efficiency. Increasing the maximum distance expands the pool of available free space points and extends computational processing times. Additionally, this ensures that the ATES installations are positioned close to the associated buildings within the cluster, minimizing the pipe length needed for connection.

The described process for each cluster persists until either the demand is fully met or no additional free space remains within the specified maximum distance. Below, the identified prioritization reasonings are outlined:

- Add one (Random): Each cluster is visited sequentially. Upon visiting a cluster, one ATES system is implemented using the process described above. The order in which the clusters are visited is random. After each cluster is visited, the process starts over.
- Add one (Highest first): Each cluster is visited sequentially. Upon visiting a cluster, one ATES system is implemented using the process described above. The sequence begins with the cluster needing the highest capacity and concludes with the cluster requiring the least capacity. After each cluster is visited, the process starts over.
- Add all (Random): Each cluster is visited sequentially. Upon visiting a cluster, ATES systems are implemented in this cluster until the demand is fulfilled or no available free space is left. The order in which the clusters are visited is random.
- Add all (Highest first): Each cluster is visited sequentially. Upon visiting a cluster, ATES systems are implemented in this cluster until the demand is fulfilled or no available free space is left. The sequence begins with the cluster needing the highest capacity and concludes with the cluster requiring the least capacity.
- Only closest: This prioritization reasoning differs from the previous four due to an additional constraint: each cluster can only utilize free space that is closer to itself than to any other cluster. Because of this constraint, the order of selection becomes irrelevant as each available space is allocated exclusively to the nearest cluster.

Prioritizing clusters based on their unfulfilled demand rather than using a random order is preferred because it promotes better balance across all clusters. Moreover, implementing ATES installations one by one is preferable to prevent significant variation in the demand fulfillment when space is limited. This approach ensures that ATES installations are placed sequentially, avoiding situations where a large amount of installations for one cluster are situated between buildings of another cluster. Finally, the Only closest prioritization reasoning may overly restrict areas with low demand. If a few ATES installations can fulfill the total cluster demand, it might prevent using remaining free space to fulfill the demand of neighboring clusters.

Based on this rationale, the decision was made to adopt the "Add one (Largest first)" prioritization reasoning into the methodology. With the selection process now defined, only the available free space remains to be determined. It's essential to identify all the available free space in the area, as the ATES installations will be placed there. The data for the available free space will be extracted from a shapefile. A shapefile contains polygons representing each area of free space. An example of such a polygon is depicted on the left in figure 5.12. Converting this free space data into data points is necessary for the methodology. In the methodology, sites within the available free space will be selected for installing ATES systems.

The total area is converted into a number of random points where ATES installations can potentially be placed. While placing more points has the benefit of more accurately representing the data, it significantly increases computational complexity. For each halving of the surface area per point, the runtime of the entire ATES installation implementation process, as described above, doubles. Therefore, it's crucial to strike a balance where the number of points is reasonable while ensuring the model runs efficiently, depending on how frequent the method is to be used. The number of points corresponds to how many times a certain area measurement fits into the total surface area of the space. For instance, in the example shown in figure 5.12, the area totals 1708 square meters. A point is allocated for every time the 10 m² fits into the total area of 1708 m², resulting in a total of 170 points, as illustrated on the right in figure 5.12.

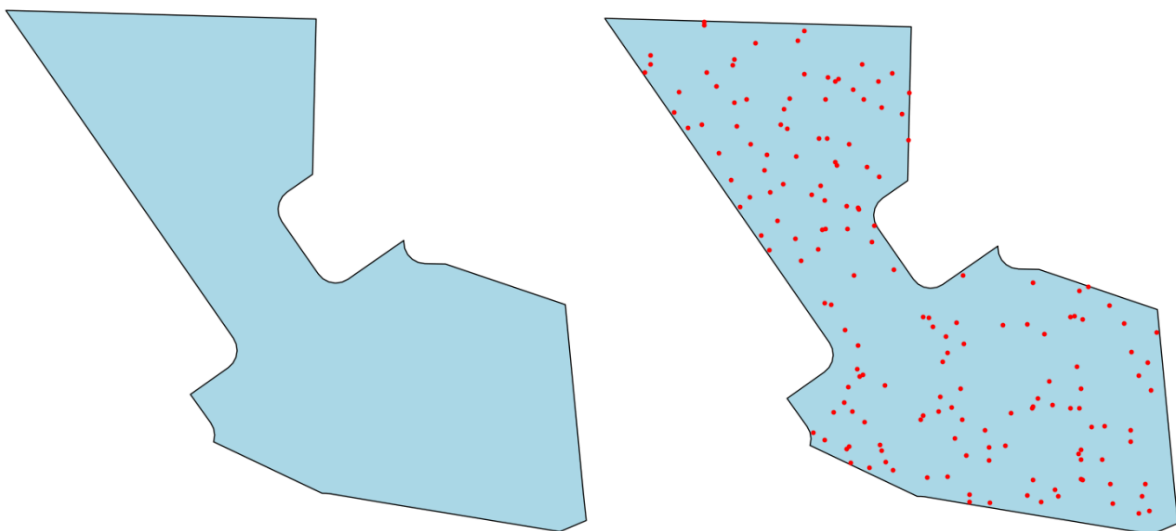


Figure 5.12: A polygon with the randomly placed points

Next, all points are added to one collection with their respective coordinates and the ATEs placement process is applied. It will be carried out until either no available free space is remaining or the total demand is fulfilled. Which nodes have been chosen from the free space can be seen in figure 5.13 for both k-means (left) and equal size k-means (right) of the small example area. This shows where the ATEs installations will ultimately be placed. Each colored circle represents an ATEs system, with all circles of the same color belonging to the same cluster. The gray points indicate the locations in the free space that were not selected.

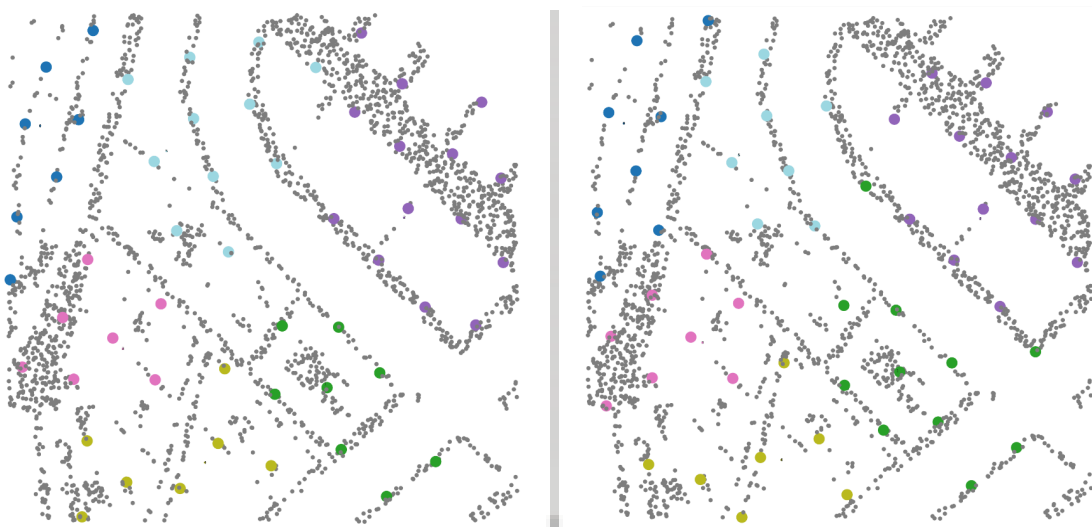


Figure 5.13: The chosen nodes from the free space for k-means (left) and equal size k-means (right) of the small example area

5.4.4. Evaluating KPI performance

With compact clusters established and ATEs installations implemented, we can now examine the KPIs of these results. This involves evaluating the compactness and Demand Fulfillment Coefficient. While the overall values for the entire area are crucial, it is also essential to assess the distribution of these values across different clusters to determine the balance of the results. To address this, the standard deviation, the minimum and maximum values for all the clusters are also determined. The within-cluster variation and the within-cluster sum of squares is calculated using Formula 1 and 2. The standard deviation, maximum, and minimum have been determined using the results of the application of these formulas.

Table 5.1: The properties of the compactness values for the 6 clusters in the example area, divided by 10^6

Compactness	Minimum	Total	Maximum	Standard deviation
K-means	0.28	2.59	0.57	0.125
Equal size k-means	0.23	2.79	0.74	0.174

Table 5.1 illustrates the discrepancy of the compactness between the final outcomes produced by the two methods. The compactness can be assessed using the within-cluster sum of squares (WCSS). Since WCSS is calculated solely for comparative purposes, the absolute values are not crucial. To better illustrate the differences between values, all WCSS values will be divided by 10^6 . It clearly demonstrates that the equal size k-means method sacrifices compactness in order to equalize the number of buildings across clusters. This is done in an attempt to reduce the variation in required storage capacity, allowing for a more balanced distribution of the necessary ATES systems across the area. Additionally, there is a greater spread, demonstrated by the increased maximum and decreased minimum values, along with a higher standard deviation.

To calculate the DFC after implementation, formula 8 and 9 are again used, which now yield different values because storage has been added. The results of applying this formula to the clusters are shown in table 5.2, which displays the DFC before and after the implementation of ATES. This is shown for the entire area, as well as the lowest and highest DFC values among the clusters.

Table 5.2: The properties of the DFC values for the 6 clusters in the example area before and after ATEs implementation

DFC		Minimum	Average	Maximum	Standard deviation
Before ATEs	k-means	0.007	0.011	0.015	0.003
	Equal size k-means	0.007	0.011	0.013	0.003
DFC		Minimum	Average	Maximum	Standard deviation
After ATEs	k-means	0.369	0.670	1.000	0.307
	Equal size k-means	0.235	0.657	1.000	0.310

The range of DFC values for the different clusters is illustrated in figure 5.14, where the DFC values are shown for both k-means (left) and equal size k-means (right). The color of the buildings corresponds to their DFC value: a building with a DFC of 0 appears dark red, while a building with a DFC of 1 appears dark green.

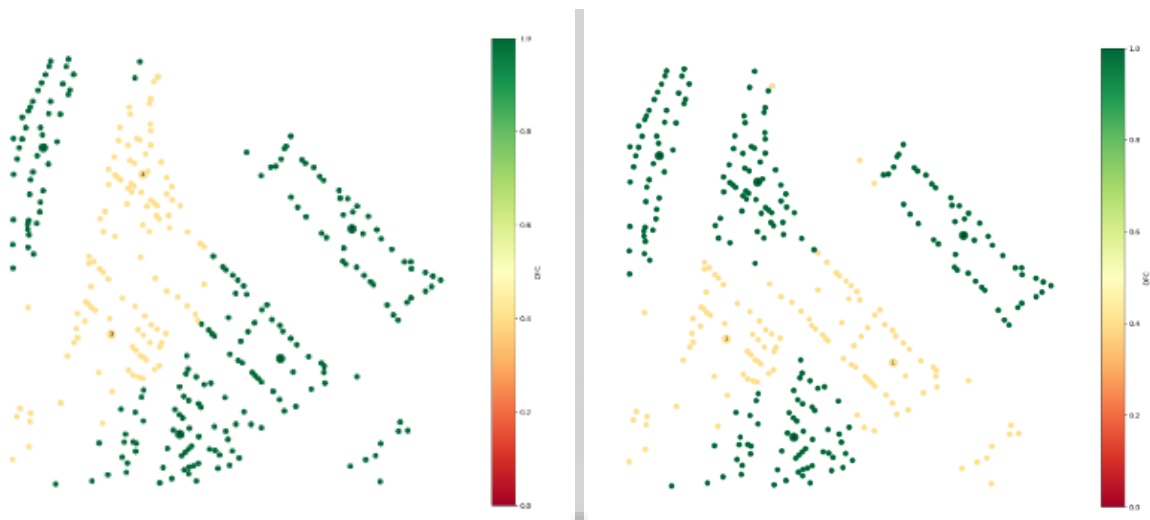


Figure 5.14: The DFC for the different clusters of k-means (left) and equal size k-means (right) after ATEs implementation

With all this information, it is possible to reflect on the compactness and demand fulfillment of the clusters of buildings with implemented ATEs installations. The assumptions underlying the method are detailed in Appendix A.

6

Model input

With the method developed in the previous chapter, the data and inputs will be determined, used to apply the method in the center of Amsterdam. This chapter explains the data and inputs, as well as the motivation behind the chosen input values.

6.1. Data

For clustering purposes, it is crucial to have the locations of the buildings in the center of Amsterdam. To incorporate ATES installations, the heating and cooling demand for each building must be known. Additionally, the potential sites for ATES installations need to be identified to determine where they can be placed. All the required data is provided by the AMS institute.

6.1.1. Heating and cooling demand per building

This data for the buildings consists of two parts: one part consists of different energy profiles, and the other part contains building information.

6.1.1.1. Energy profiles

The energy profiles contain the demand data for different building types. Each building type is its own archetype. The buildings are divided into 4 categories; Horeca, mixed-use, utilities and residential demand. Within each of these categories there are different profiles for a corner or a row building, while residential also has the profile of an apartment. Within a corner, row or apartment, a distinction is made based on the year of construction; built before 1976, built between 1976 and 1996 or built after 1996. Each archetype is therefore a combination of building function, building type and year of construction, resulting in a total of 27 archetypes.

An example; archetype 1 consists of the energy profile for residential buildings that are apartments built before 1976. Each profile includes the demand data for cooling, heating and domestic hot water for that specific archetype building, measured in kWh/m². Since domestic hot water is a form of heating demand, it will be merged with the heating demand. This data is provided for every hour of an entire year, based on the average temperature for each day over the past 10 years. Each archetype has three versions of the profiles: one for connection to low-temperature heating, one for medium-temperature heating, and one reflecting the current demands.

These three versions differ because, for medium-temperature heating, and even more so for low-temperature heating, it is assumed that each building is insulated to a certain level. Since low-temperature heating is characteristic of a 5GDHC network, the data from the low-temperature heating profiles is used. This should ideally be accompanied by a 2-pipe system, as it recovers excess heat more efficiently (Gjoka et al., 2023). However, the pipe configuration is outside the scope of the model, so this potential choice does not have any further influence. The profiles are aggregated to calculate the total heating and cooling demand for each month. The results of this aggregation can be observed in figure 6.1 for the heating demand across all archetypes and figure 6.2 for the cooling demand across all archetypes. These figures can also be found in Appendix B, where the legend has been included as well.

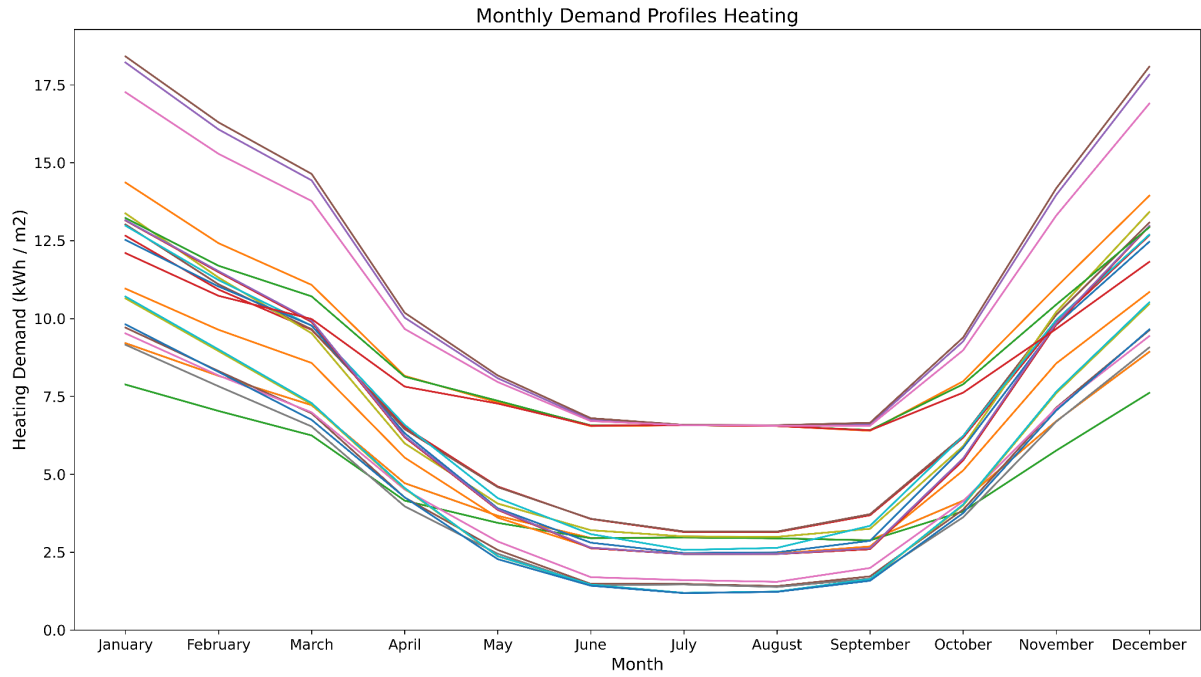


Figure 6.1: The monthly heating demand for all archetypes in kWh/m²

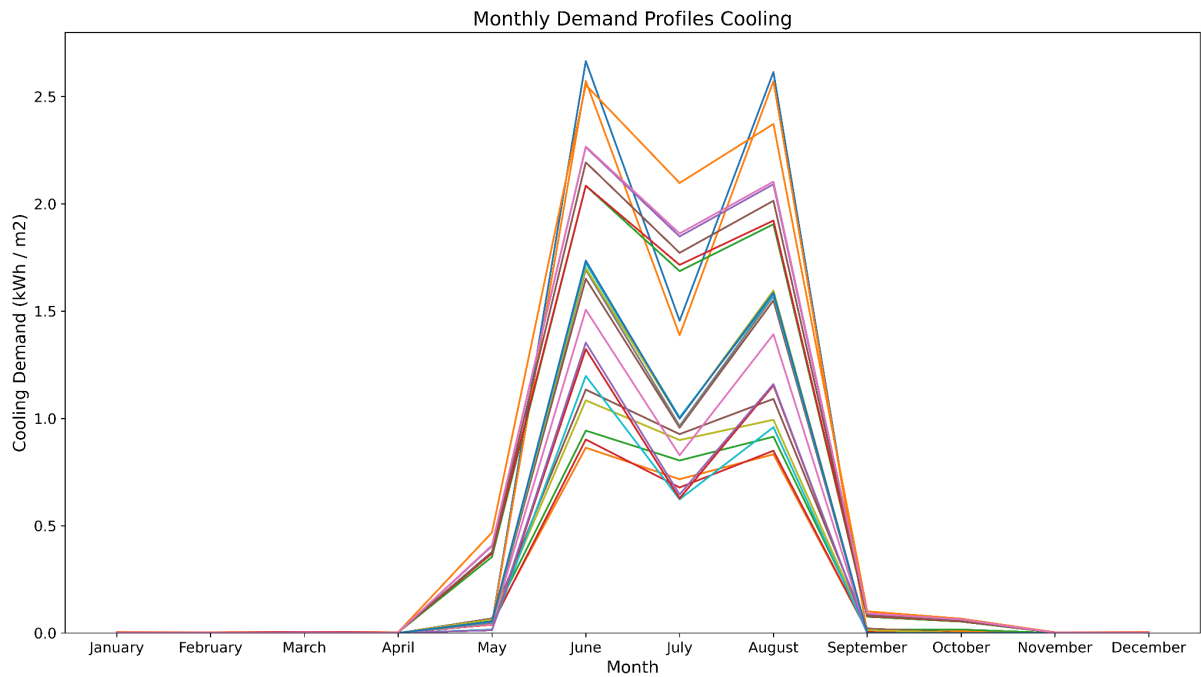


Figure 6.2: The monthly cooling demand for all archetypes in kWh/m²

Although the quantities of demand in kWh/m² per month vary among archetypes, there is a consistent trend that all archetypes follow for both heating and cooling. However, the scale of heating and cooling demands differs significantly; The highest value on the scale in figure 6.1 is 11.5 kWh/m², whereas the highest value on the scale in figure 6.2 is 2.5 kWh/m². The difference in scale illustrated for archetype 1 in figure 6.3.

Although the peaks of cooling demand coincide with the periods of lowest heating demand, cooling demand does not surpass heating demand. This trend is present in all 27 archetypes, where the total amount of heating demand is approximately 25 times greater than the total cooling demand.

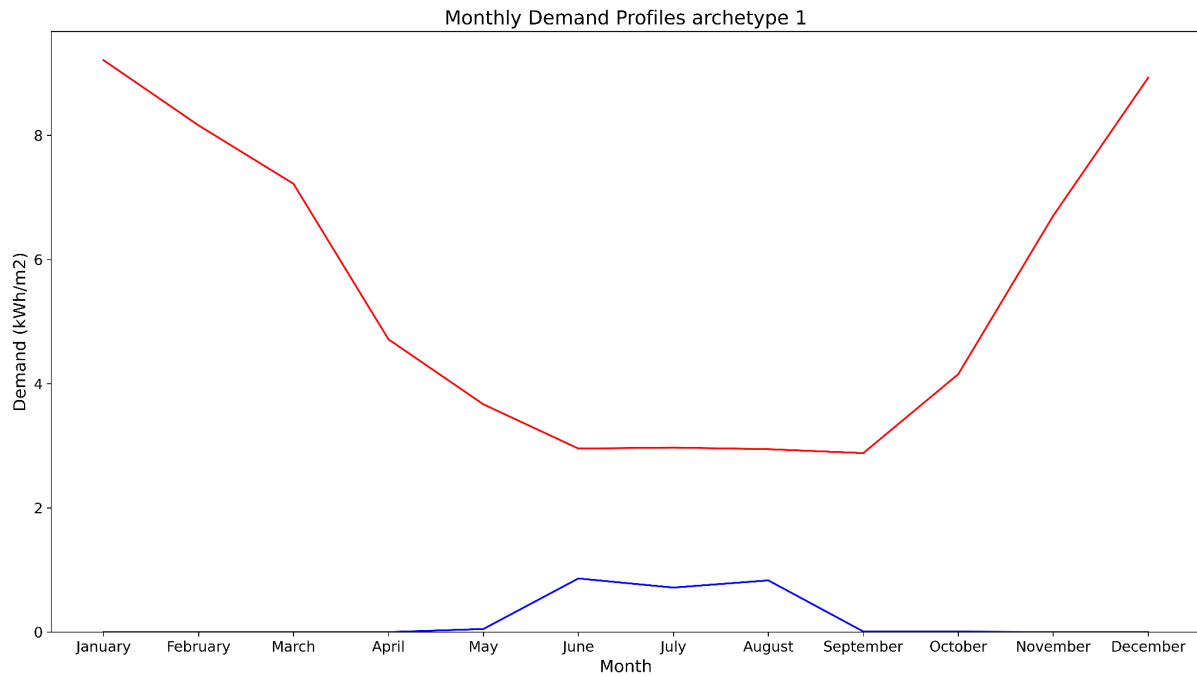


Figure 6.3: The heating and cooling demand for archetype 1 in kWh/m²

6.1.1.2. Building information

The second part of the building data comprises information about the buildings located in the center of Amsterdam. This data includes the location, the amount of square feet of surface area and the archetype for each building. In total, the data includes information from 16,455 buildings. However, some of these buildings are unheated. If a building has no heating or cooling demand, there is no justification for connecting it to a 5GDHC network. Therefore, these unheated buildings are not included in the model. A total of 14,693 buildings remain, and for these buildings, the total cooling and heating demand can be determined by multiplying the building's floor area in m^2 by the corresponding energy profile for the archetype of the building, given in kWh/m^2 . This method links all demand data to the buildings, whose locations can be visualized in figure 6.4.



Figure 6.4: The locations of all buildings from the dataset of the center of Amsterdam

6.1.2. Potential ATEs locations

To install an ATEs, adequate free space is required. Given that the center of Amsterdam is highly crowded, such space is limited. Data regarding available space is shown in figure 6.5. The data includes a total of 2.56 million square meters of free space available.



Figure 6.5: The available free space from the dataset of the center of Amsterdam

However, not every piece of free space is suitable for installing an ATEs installation. A minimum amount of space is required for the installation, as previously discussed in the method. Since Noome (2013) indicates that there must be at least 6 by 15 meters of free area, a minimum space requirement of 90 square meters has been assumed. Any free space smaller than 90 square meters will be excluded from the data. Consequently, the total amount of available free space decreases by 0.6%, amounting to 2.54 million square meters.

6.2. Input

The rationale behind the remaining input values is outlined below. A summary of the chosen input values can be found in the table at the end of this chapter.

6.2.1. ATES configuration

The ATES systems use a design with only monowells. However, determining the precise dimensions for the system is essential to achieve a realistic implementation.

The size of an ATES system is determined by the thermal radius (R_{th}) and the length of the well screen (L). The volume of the ATES is calculated based on these parameters, which determines the amount of energy that can be stored. However, not all the combinations of L and R_{th} values are practical. If R_{th} is significantly larger than L , the system forms a "pancake" shape, which is inefficient. Conversely, if L is much larger than R_{th} , the system requires very deep drilling, leading to excessively high costs. Therefore, a balanced approach between R_{th} and L is essential for an economically viable ATES system. For each volume of storage there is an optimal thermal radius ratio (L/R_{th}) for which losses to the environment are minimal. This is at a ratio of 2, since the length of the screen is then equal to the diameter of the cylindrical volume (Bloemendal, 2018). However, research by Doughty et al. (1982) shows that a ratio of 1.5 is more efficient if different thermodynamic properties of the aquifer are taken into account. However, in the work of Bloemendal (2018) a table can be found of average data from 109 ATES systems in Amsterdam, which is shown in figure 6.6.

Table 4.7: ATES-well properties in Amsterdam (rounded) [109], V =seasonal storage volume, L = screen length, z = depth of top of screen

	Monowells				Doublets		
	V [m^3]	L [m]	Z_{warm} [$m-sl$]	Z_{cold} [$m-sl$]	V [m^3]	L [m]	z [$m-sl$]
Perctile 0,1	40,000	10	60	90	75,000	15	70
Average	100,000	20	75	125	250,000	50	90
Percentile. 0,9	160,000	30	85	170	500,000	85	100

Figure 6.6: A table of ATES-well properties of Amsterdam (Bloemendal, 2018)

For the systems at Percentile 0.1, Average, and Percentile 0.9, the ratios between L and R_{th} have been calculated for both monowells and doublets. The calculation was carried out using formula 11 from chapter 5.4.3., while the results are shown in table 6.1.

Table 6.1: The L/R_{th} ratio determined based on different configurations

Type	Volume (m ³)	Well screen L (m)	Thermal radius R_{th} (m)	L/R_{th}
Monowell Percentile 0,1	40.000	10	43.37	0.23
Monowell Average	100.000	20	48.48	0.41
Monowell Percentile 0,9	160.000	30	50.07	0.60
Doublet Percentile 0,1	75.000	15	48.48	0.31
Doublet Average	250.000	50	48.48	1.03
Doublet Percentile 0,9	500.000	85	52.59	1.62

The thermal radius ratio varies significantly between these systems, and no fixed value can be determined. Since the logical relationship between L and R_{th} is unclear since the results contradict the literature, the monowell at Percentile 0.9 is implemented in the model. The goal is to efficiently use the aquifer's depth, which is achieved with a system featuring a 30-meter well screen. This system includes a 30-meter warm well screen, a 30-meter empty intermediate section, and a 30-meter cold well screen, totaling 90 meters. Given that there are 100 meters of usable aquifer depth, this setup is considered efficient, utilizing 90% of the entire aquifer, which consists of 60% ATES wells.

6.2.2. Remaining input values

Below, all other selected input values are defined, accompanied by explanations detailing why these specific values were chosen.

- The value of 90 square meters of free space required for installing an ATES installation has been chosen, as explained in chapter 4.2.6.
- In contrast to conventional district heating networks, which typically have distribution losses of 25%, fifth Generation District Heating and Cooling networks exhibit significantly lower losses. This is due to decentralized heat generation and lower network temperatures, resulting in only 5% distribution losses (Interreg North-West Europe, 2023).
- Apart from distribution losses, heat is also lost during storage. The efficiency with which stored energy can be reused is known as thermal recovery. W. Sommer (2015) analyzed the data from ATES systems in the Netherlands between 2005 and 2012, and came to the conclusion that the average thermal recovery for cold storage is equal to 82% and for heat storage is equal to 68%.
- For formula 11, the values for the volumetric heat capacity of both water and the aquifer are required. The assumed values for these parameters are $4.2 \cdot 10^6$ and $2.8 \cdot 10^6$ [J/m³/K], respectively (Bloemendal, 2018).
- The temperature difference between the wells is 4 K, as is common (Bloemendal, 2018).
- The distance required between 2 monowells is equal to 1 time the thermal radius (Bloemendal, 2018).
- The demand data for all houses is provided in kWh, while the volumetric heat capacities are in Joules/m³/K. To convert kWh to Joules, a conversion factor is required. This factor is 3.6 million, as there are 3.6 million joules in a kWh.
- The number of clusters (k) is set to 60, corresponding to the number of neighborhoods in the center of Amsterdam. This choice ensures that, on average, the number of buildings per cluster aligns with reality. This decision follows the proposal in the climate agreement to cluster buildings per neighborhood (Nijpels, 2018). This is done despite the fact that the clustering method in this context does not directly align with neighborhood boundaries.
- When using equal-size k -means, a minimum number of adjustments must be set before the model proceeds to the next round of improvements. If this number of adjustments is not met, the process terminates. Typically, improvement rounds continue until there are no further improvements, but due to the dataset's size, the process does not always converge. The lower this chosen value, the more compact the resulting clusters will be. For this dataset, a minimum of 10 changes was ultimately chosen, as the process failed to converge several times with lower values.

- The last two input parameters to be selected are surface area per point and maximum distance between the center and a potential ATES location, both discussed in Chapter 5.4.3. Surface area per point directly impacts the number of potential ATES locations. A lower value increases the number of potential locations, but excessively low values lead to many unusable locations due to the minimum distance requirement between ATES installations. Conversely, a too high value may not effectively utilize the available free space in the model. The maximum distance between a cluster center and an ATES location determines which potential locations are considered. It's crucial to set this value appropriately; if too low, viable ATES locations may be unjustly excluded. For data from the center of Amsterdam, a larger maximum distance does not negatively affect results due to limited available free space far from cluster centers; It's highly probable that this space has already been occupied by another cluster that is closer to it. Both parameters significantly impact model runtime. Hence, they should be chosen carefully to balance accuracy and runtime requirements. If frequent model runs are necessary, minimizing runtime by adjusting these parameters might be beneficial, albeit potentially reducing result accuracy slightly. In this model, the points per surface area is set to 20 m², and the maximum distance is 500 meters, resulting in an approximate runtime of one hour per run.

An overview of all input values can be found in table 6.2 on the following page.

Table 6.2: An overview of all input values

Input parameter	Value	Unit
Volume per well	160.000	[m ³]
Length well screen	30	[m]
Thermal radius (R_{th})	50.07	[m]
Free space required	90	[m ²]
Distribution losses	5	[%]
Thermal recovery cold storage	82	[%]
Thermal recovery heat storage	68	[%]
Volumetric heat capacity water (C_w)	$4.2 * 10^6$	[J/m ³ /K]
Volumetric heat capacity aquifer (C_{aq})	$2.8 * 10^6$	[J/m ³ /K]
Temperature difference between wells	4	[K]
Distance between monowells	$1 * R_{th}$	[m]
kWh to Joule conversion factor	3.600.000	[J/kWh]
Number of clusters	60	[-]
Minimum number of adjustments same size k-means	10	[-]
Surface area per point	20	[m ²]
Maximum distance between cluster center and ATES	500	[m]

7

Results

Now that the method has been defined in chapter 5, it will be applied to the center of Amsterdam. The data and input values used for the model are provided in Chapter 6. An overview of the input values is available in Table 6.2 at the end of the previous chapter. This chapter contains the results of the application of the defined method. After reviewing these results, a sensitivity analysis is conducted. Additional supporting figures can be found in Appendix B.

7.1. Model outcomes

After implementing the data, the buildings are grouped into clusters using k-means, as depicted in figure 7.1. These buildings were previously illustrated in figure 6.4 and are now differentiated by color to signify their respective clusters. Given the numerous clusters, some colors are used multiple times. Locally, buildings sharing the same color belong to the same cluster, whereas globally, buildings with the same color may not. Additionally, red crosses are placed among the buildings in the figure to indicate the cluster centers for each cluster. Equal size k-means clustering was also applied to the buildings, although these results are not shown due to the difficulty in distinguishing differences between the two clustering methods.



Figure 7.1: The buildings in the center of Amsterdam divided into 60 clusters by k-means

The distribution of the red crosses indicates that clusters are densely concentrated throughout most areas, with the exception of the eastern part where cluster centers are less frequent. This observation also highlights that there is notably more space between buildings in the eastern section compared to the rest of the center, making those clusters less compact .

Table 7.1: The properties of the DFC values for the different clusters in the center of Amsterdam before ATEs implementation

DFC	Minimum	Average	Maximum	Standard deviation
K-means	0.006	0.014	0.022	0.004
Equal size k-means	0.007	0,014	0.023	0.004

The values of the DFC are presented in table 7.1, which indicates the fraction of the demand that can be met within the clusters.. This reveals that across the entire Amsterdam center area, 1.4% of the heating demand can be fulfilled through an overlap with cooling demand. The cluster displaying the highest overlap reaches 2.2%, whereas the cluster with the lowest overlap achieves only 0.6%. The differences between the two methods are minimal.

Following this step, ATEs installations are allocated within the clusters using the "Add one (Highest first)" prioritization reasoning. The impact of this allocation on the DFC is reflected in table 7.2, which indicates which fraction of the demand can be met within the clusters and by utilizing storage. The difference between Tables 7.1 and 7.2 is that table 7.1 examines the situation before ATEs is implemented, while table 7.2 examines the situation after ATEs is implemented.

Table 7.2: The properties of the DFC values for the different clusters in the center of Amsterdam after ATEs implementation

DFC	Minimum	Average	Maximum	Standard deviation	ATEs placed
K-means	0.167	0.586	1.000	0.271	1885
Equal size k-means	0.134	0.582	1.000	0.272	1874

To achieve this DFC, 1885 ATEs installations were installed for the k-means method, while 1874 ATEs installations were installed for equal size k-means. It is evident that incorporating ATEs installations into the outcome of k-means clustering yields slightly better results compared to doing so with the outcome of equal size k-means. In both methods, just over 58% of the heating demand can be fulfilled. However, there is considerable variability within both methods: some clusters fulfill their entire demand, while others can fulfill as little as 13.4% in the worst-case scenario.

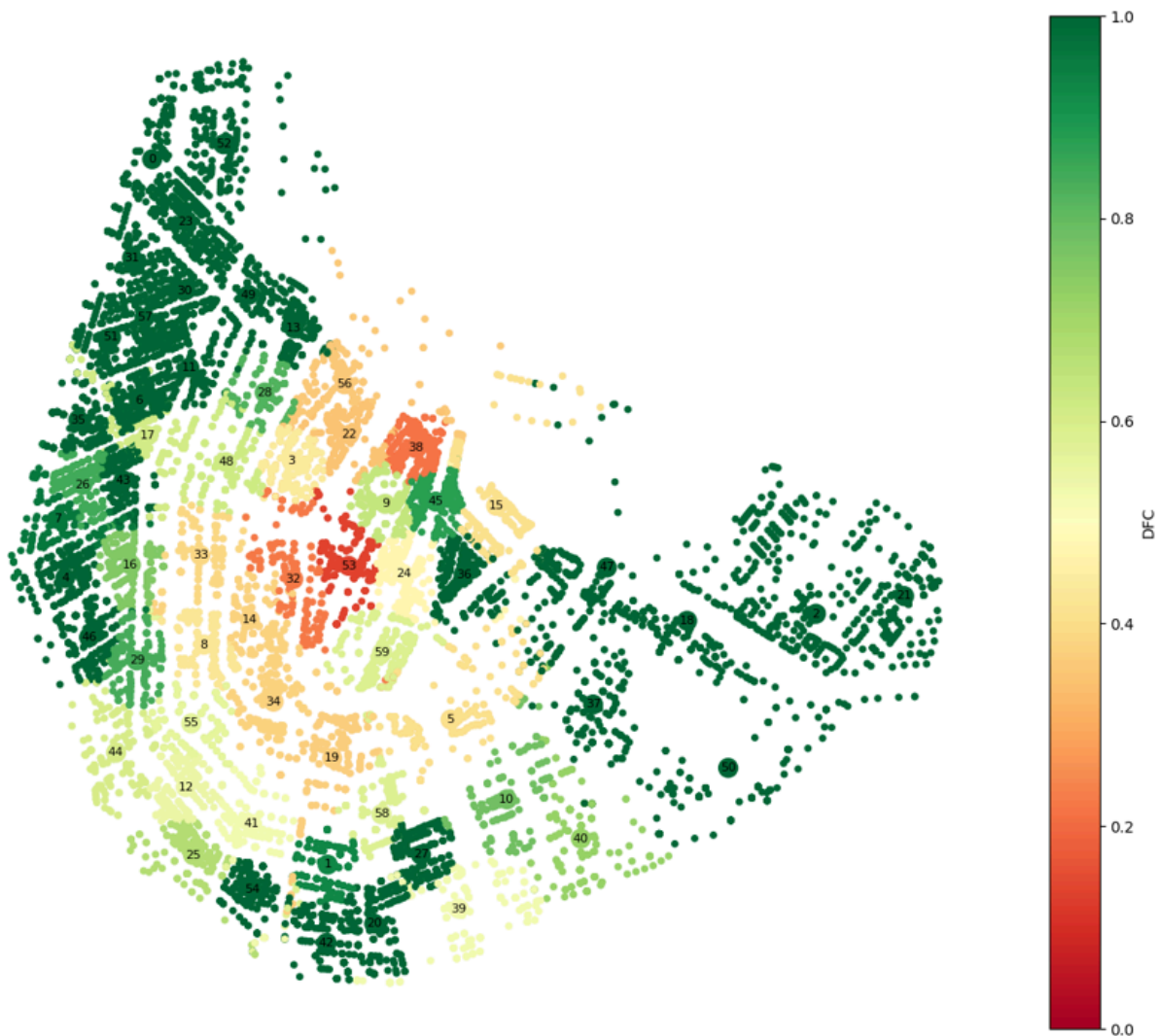


Figure 7.2: A visualization of the DFC values across the 60 clusters in the center of Amsterdam

The values for each cluster are shown in figure 7.2. Since these are largely the same for both clustering methods, only the k-means result is visualized. The figure displays all the buildings, with each building's color representing the extent to which its heating demand can be met. Clusters with lower DFC values are represented in red, while those with higher DFC values are shown in green. Notably, the central point of the center exhibits very low DFC values, attributed to high building density and limited available space for ATEs installations. Similar high-density conditions exist in other areas, but these are offset by more available space or lower overall heating demand.

For instance, the northwestern part of the center, despite multiple dense clusters, appears uniformly dark green, indicating full demand fulfillment. Another prominently dark green area is located to the east, where lower building density and therefore a reduced total heating demand contribute to better heat demand fulfillment. Additionally, abundant free space in this eastern area, as illustrated in Figure 6.5, alleviates pressure on the subsurface area for ATEs installation.

The differences in compactness between k-means and equal size k-means are visible in table 7.3. What becomes clear is that equal size k-means creates less compact clusters overall than k-means. The values for the compactness are higher in all categories, indicating lower compactness. Additionally, the standard deviation is much larger for equal size k-means, suggesting that the clusters are less proportional in compactness. Tables 7.2 and 7.3 thus make it clear that despite equal size k-means sacrificing compactness, this does not result in better demand fulfillment in these clusters. In fact, demand fulfillment is even getting worse.

Table 7.3: The properties of the compactness for the different clusters in the center of Amsterdam, divided by 10^6

Compactness	Minimum	Total	Maximum	Standard deviation
K-means	0.98	211.89	7.49	1.12
Equal size k-means	1.82	353.89	33.46	6.21

7.2. K-means sensitivity analysis

The method developed is largely deterministic, meaning that given a specific set of inputs, it consistently produces the same results due to its fixed steps and rules. However, there is a stochastic component in the method, introducing an element of randomness that can lead to differing outcomes. This stochastic element arises from the use of k-means clustering, where the initial placement of centers is random and can differ with each iteration. Consequently, this randomness can result in variations in the final outcomes. To assess the impact of this stochastic element, the method is repeated and the results are compared.

The findings are presented in table 7.4 for the Within clusters sum of squares (WCSS) and in table 7.5 for the DFC. First, the main results are reiterated, denoted by (1), followed by the results of the second iteration of the method (2).

Table 7.4: The properties of the compactness for the k-means sensitivity analysis, divided by 10⁶

Compactness	Minimum	Total	Maximum	Standard deviation
K-means (1)	0.98	211.89	7.49	1.12
Equal size k-means (1)	1.82	353.89	33.46	6.21
K-means (2)	1.16	209.70	5.89	0.976
Equal size k-means (2)	1.63	323.20	22.70	4.42

Table 7.4 indicates that the results for k-means are nearly identical across both iterations, with only minor dissimilarities. In contrast, there is a more pronounced difference between the two iterations of equal size k-means. This difference is influenced by the outcomes of normal k-means, as equal size k-means builds upon these results. It is evident that the WCSS values for the first iteration are notably higher, specifically the total, maximum, and standard deviation values. This difference is likely due to a significantly higher maximum value in equal size k-means compared to normal k-means. This difference can be attributed to the constraints of the equal size k-means method, which mandates an equal number of buildings per cluster. Consequently, some clusters may include buildings that are distant from their centers, resulting in elevated maximum WCSS values. These values, in turn, affect both the total and the standard deviation, and the higher maximum in the first iteration consequently accounts for the difference between the two.

table 7.5: The properties of the DFC values for the k-means sensitivity analysis

DFC	Minimum	Average	Maximum	Standard deviation
K-means (1)	0.167	0.586	1.000	0.271
Equal size k-means (1)	0.134	0.582	1.000	0.272
K-means (2)	0.138	0.587	1.000	0.273
Equal size k-means (2)	0.142	0.584	1.000	0.271

Table 7.5 clearly shows that the DFC is not sensitive to the results of the k-means algorithm. Only the cluster with the minimum DFC value shows a slight difference, but this does not have a significant impact and has no further consequences. All other values are so similar that it can be concluded there is no notable influence.

7.3. Number of clusters sensitivity analysis

To perform the k-means algorithm, the number of clusters must be chosen in advance. For the center of Amsterdam, 60 clusters were chosen, since this is how many neighborhoods there are in the area. This way, on average, there will be as many buildings in a cluster as in reality. However, this specific number is not mandatory, and a different number of clusters could have been chosen. To assess the robustness of the results with 60 clusters, a sensitivity analysis must be conducted on the number of clusters. This analysis evaluates how sensitive the method's outcomes are to changes in the number of clusters. It provides insight into the sensitivity of the compactness and demand fulfillment of the clusters relative to the amount of clusters. In this analysis, the results for 50 and 70 clusters will be examined. The findings are presented in table 7.6 for the compactness and in table 7.7 for the DFC. First, the main results are reiterated, followed by the outcomes of the sensitivity analysis.

Table 7.6: The properties of the compactness for the number of clusters sensitivity analysis, divided by 10^6

Compactness	Minimum	Total	Maximum	Standard deviation
K-means (60)	0.98	211.89	7.49	1.12
Equal size k-means (60)	1.82	353.89	33.46	6.21
K-means (70)	0.93	177.23	4.84	0.81
Equal size k-means (70)	1.12	262.76	11.47	2.80
K-means (50)	1.95	258.07	10.03	1.72
Equal size k-means (50)	2.24	446.76	76.77	11.39

The outcomes of this analysis revealed that the compactness of the clusters, as determined by the within-cluster sum of squares (WCSS), varied as anticipated. With k set to 50, both the WCSS and its standard deviation increased, indicating less compact clusters.

This is because fewer clusters mean that each cluster contains more buildings, resulting in higher variation within each cluster. On the contrary, with k set to 70, the WCSS and its standard deviation decreased, signifying more compact clusters. This occurs because more clusters allow for each cluster to contain fewer buildings, reducing the variation within each cluster. These results align with expectations, as increasing the number of clusters typically enhances compactness. This is because the distances between points and their respective centers are generally shorter with more centers present. However, decreasing the number of clusters increases the distance between points and their centers, thereby reducing compactness.

The ratios between k-means and equal size k-means remain consistent, even with different numbers of clusters. This demonstrates that the WCSS for equal size k-means is significantly higher than that for k-means. This difference is expected, as each cluster in equal size k-means is constrained to have an equal number of buildings. Consequently, some clusters must include buildings that are farther away due to the lack of closer options. This effect is particularly evident from the maximum value in table 7.6, which is substantially higher for equal size k-means compared to k-means.

Table 7.7: The properties of the DFC values for the number of clusters sensitivity analysis

DFC	Minimum	Average	Maximum	Standard deviation
K-means (60)	0.167	0.586	1.000	0.271
Equal size k-means (60)	0.134	0.582	1.000	0.272
K-means (70)	0.152	0.583	1.000	0.278
Equal size k-means (70)	0.140	0.579	1.000	0.280
K-means (50)	0.167	0.578	1.000	0.274
Equal size k-means (50)	0.194	0.580	1.000	0.272

Table 7.7 reveals that the number of clusters has no significant effect on the outcome of the DFC. While the lowest DFC values show slight fluctuations, these do not substantially impact the overall result. The standard deviations are also roughly the same across all scenarios. Regardless of the number of clusters, the DFC consistently hovers around 0.58. These fluctuations are likely not explained by the number of clusters but rather by the variability in k-means clustering outcomes, as similar variations are observed in Chapter 7.2. This indicates that the DFC is not sensitive to changes in the number of clusters.

7.4 Davies-Bouldin index

Another method used for evaluating the number of clusters in the Davies-Bouldin index. This index is used to determine both the compactness and separation of the clustering results (Davies & Bouldin, 1979).

A lower value of the Davies-Bouldin Index indicates better clustering quality. By calculating this index for various numbers of clusters, it is possible to identify which cluster count yields the best clustering results. This approach is particularly useful when applying K-means, as the number of clusters must be predetermined. The Davies-Bouldin Index has been evaluated for cluster counts ranging from 2 to 100, and the results are presented in figure 7.3.

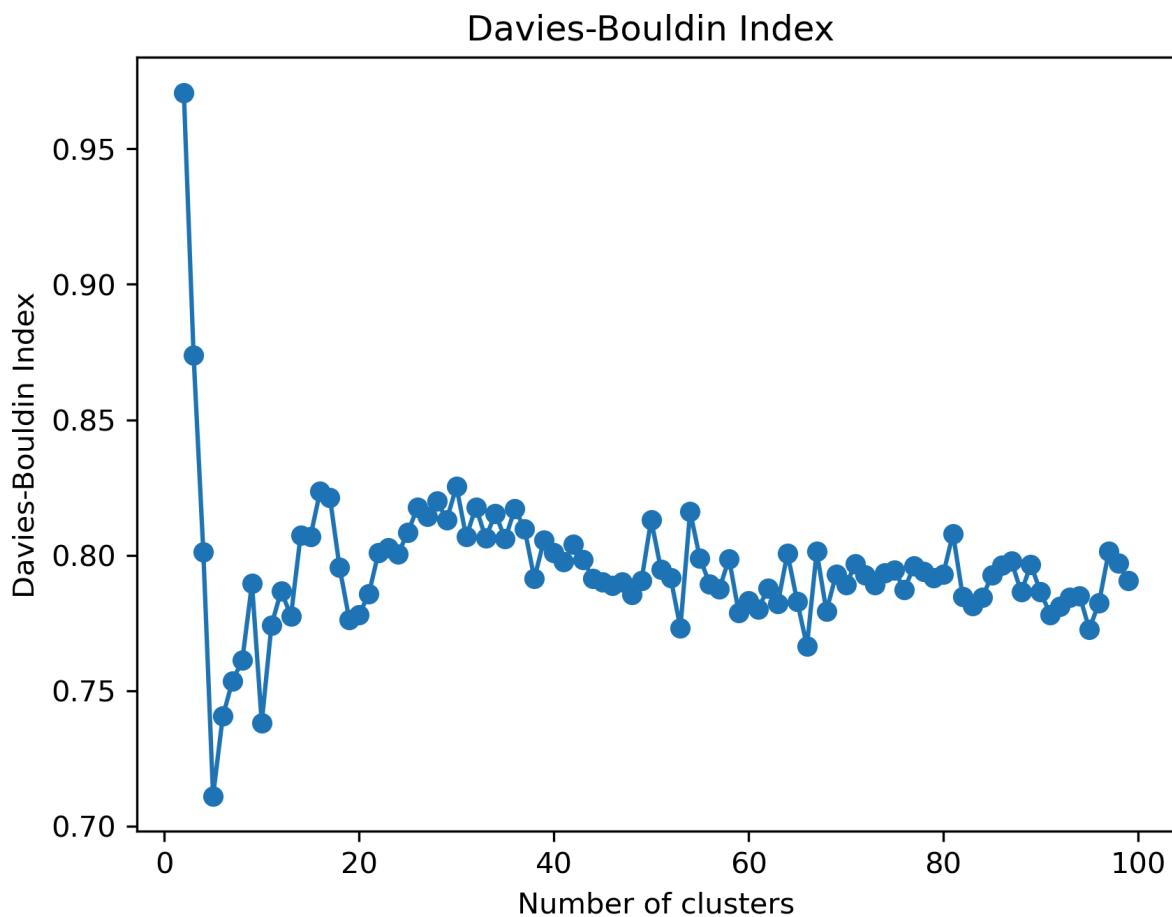


Figure 7.3: The Davies-Bouldin index for different number of clusters

Figure 7.3 indicates that the best clustering results for K-means occur with 5 clusters. However, this research also considers the size of the clusters, which should not be

excessively large or small. The current plan involves implementing heating networks on a district basis (Nijpels, 2018), resulting in 60 neighborhoods and therefore 60 clusters. While the Davies-Bouldin Index shows the best clustering outcome with 5 clusters, this is unrealistic since it would lead to clusters being 12 times larger than currently planned. For other cluster counts around the proposed 60 clusters, there are no significant differences, providing no compelling reason to deviate from the plan of using 60 clusters.

Discussion

In this chapter, the scientific and practical contributions of this research are presented. Additionally, the study's findings will be assessed by highlighting both its advantages and limitations. The aim is to present a balanced view of the research outcomes and the learning points for future research into fifth generation heating and cooling (5GDHC) and aquifer thermal energy storage (ATES).

8.1. Scientific and practical contribution

In conclusion, this research has made significant contributions to the fields of aquifer thermal energy storage and fifth generation district heating and cooling. By examining a larger area with a high density of buildings, this study has addressed critical gaps in existing literature. This study focused on large-scale implementation, which is scarcely addressed in the existing literature due to the relatively new nature of 5GDHC technology. Dividing buildings into clusters is essential for implementation, but the most effective methods for doing so are still unclear. This research applied a method that successfully accomplished this task. The integration of ATES installations into the design methodology for 5GDHC networks represents a new approach not previously researched, paving the way for future research and practical applications in sustainable urban heating and cooling.

Practically, the developed methodology, aimed at clustering buildings and optimizing demand fulfillment through ATES integration, holds promise for supporting the Amsterdam Institute for Advanced Metropolitan Solutions (AMS) in their 'High-hanging fruit' project. Overall, this research contributes valuable insights on fifth generation district heating and cooling and aquifer thermal energy storage, by demonstrating that applying ATES in the created clusters ensures that a large part of the demand can already be met with storage. However, this does differ per area, where areas that are very dense, such as the central part of the center, can meet less demand than areas that are less dense and where more free space is available, such as especially the east and northwest of the center.

8.2 Advantages

The identified method is robust and minimally affected by stochastic elements, as demonstrated by the sensitivity analyses in chapter 7. Moreover, it generates multiple figures that offer insights into potential characteristics of the final outcome and how these vary across different areas. Additionally, given the availability of necessary data, this method is adaptable for application in other geographical regions, regardless of the size or density of the area. However, this method is particularly useful in densely populated urban areas with limited space. In situations where there is high heat demand but little room to install ATEs systems, the method aims to meet the demand as effectively as possible. However, the method can also be applied in areas with more available space and lower heat demand, such as rural areas. In such cases, a more suitable approach may exist, as this method is designed for scenarios with minimal space and high heat demand. In rural areas, where there is ample space to accommodate lower heat demand, the method employed in this study imposes strict constraints on the placement of ATEs systems, requiring them to be positioned as close as possible to the center of the cluster. When numerous potential locations are available, a less rigid method that considers additional factors for selecting sites would be preferable.

8.3. Limitations

However, this research also has limitations; These have to do with the data used, but also with aspects that were not included in this research.

8.3.1. Demand data

The method developed in this research exhibits both advantages and limitations. One limitation of the research is the data utilized. The data consisted of demand profiles. These profiles predict the amount of heating and cooling demand for every hour of a year. The year being considered is an average temperature on that day over the past 10 years. The problem here is that the profile of each building is based on the same average, so the peaks in demand, although slightly different in size, are in the same places for all buildings, as shown in Figures 6.1 and 6.2. This means that less exchange is possible; there will never be a building that has a surplus of heating demand while another building has a surplus of cooling demand, so that exchange between buildings could take place. This only occurs in the data if both heating and cooling demand are present at the same time within the profile. These moments are very rare and only take place around the summer. That is the only time when there is cooling demand, and since there is heating demand in the form of domestic hot water throughout the year, there is an overlap. But even then, this does not have to be exchanged between different buildings, because it can be used in the building itself.

In addition, the profiles only look at the function and not at the type of building. The profiles are divided into Hospitality, mixed-use, utilities and residential demand. Figure 6.2 shows that no deeper distinction has been made between building types. There are building types, such as supermarkets and hospitals, that have cooling demand all year round. This has not been implemented in the model, as there are several months where the cooling demand is little to almost nothing.

Moreover, based on the average temperature of July, the cooling demand would be expected to be at its highest here. However, figure 6.2 shows a dip in July. This may be due to a flaw in the model from the AMS institute that created the data, but this is uncertain. It is clear that the cooling demand there is lower than it should be. It is noteworthy to mention that the AMS institute itself has indicated to have concerns regarding the quality and reliability of the cooling data.

Finally, the data looks at the past 10 years, but does not take the future into account. As a result, the cooling demand is estimated to be lower than it will likely be in the future, during a possible implementation of a 5GDHC network; This demand for cooling is expected to triple by 2050 without action (IEA, 2018).

It is precisely the balancing of heating demand with the product of cooling demand and vice versa that makes the concept of 5GDHC so attractive, and this is not reflected in the data because all buildings have profiles that have both peaks and dales on the same moments. In addition, only 1.4% of the heating demand can be covered by the cooling demand in the data. This is extremely low because buildings with a constant cooling demand such as supermarkets and hospitals are not represented in the data, the cooling demand is too low, which is visible from the July data, and because the data is based on the past and not on the future, where the cooling demand is expected to increase significantly. This means that the remainder of the heating demand must come from ATES, meaning that the number of ATES installations that will be required is higher than is realistic and a greater portion of the demand can actually be fulfilled.

8.3.2. Regeneration

Another limitation is that the regeneration of the ATES has not been addressed. There are ample possibilities for this, such as using the surface water from the canals and installing solar thermal panels on rooftops. Adequate regeneration is essential for an ATES, and this study has not considered whether it is feasible for the entire area or for individual systems. As a result, despite the many opportunities for regeneration in the center of Amsterdam, fewer ATES systems may be realistically implemented. This means that the actual demand met could be lower than the results indicate.

8.3.3. Subsurface limitations

A final limitation is the failure to consider existing subsurface limitations. Although the data for free space indicates potential locations for ATES systems above ground, it does not account for the potential lack of space underground. For instance, existing underground storage systems were not considered due to the unavailability of complete data. Additionally, underground restricted areas, such as those through which the metro passes, were not examined. Drilling is prohibited in these areas, making ATES installation impossible. This indicates that there are fewer options in the free space for installing ATES systems than assumed in this study, resulting in fewer ATES systems being implementable.

Conclusion

9.1. The outcome

The Dutch government aims to phase out gas usage by 2050, necessitating alternative heating solutions to replace current gas-based systems. This study explores the feasibility of implementing a fifth generation heating and cooling (5GDHC) network as a viable alternative. Focusing on Amsterdam, where the historic center's cooling demands are expected to rise, this research addresses significant gaps in the literature regarding large-scale 5GDHC implementation and the utilization of aquifer thermal energy storage (ATES). To bridge these gaps, the study clusters buildings and integrates ATES systems. The research question of this study is as follows:

How can buildings in a dense city center be clustered for a fifth generation district heating and cooling network (5GDHC) and integrated with Aquifer Thermal Energy Storage (ATES) to optimize the demand fulfillment, given the limited space?

Clustering the buildings allows a bottom-up approach, reducing both the investment risks and the overload risk. For the actors of the future system, it is important that the clusters are compact and have a high demand fulfillment. Compact clusters are crucial due to limited subsurface space and reduced piping requirements, which also lowers costs. A high demand fulfillment is achieved when the heating and cooling demands are met as much as possible by the products of heating and cooling demand, supplemented by storage in ATES. This demand fulfillment also reduces costs, as external sources are more expensive.

This study examines the implementation of ATES in the form of monowells. A method has been developed and implemented in a model to cluster buildings and integrate ATES systems, ensuring compact clusters and optimal demand fulfillment. The method uses the geographical location and demand of buildings, along with the open space for potential ATES locations. The buildings are clustered based on their geographical location using k-means and equal size k-means methods to ensure compactness. Each cluster's total heating and cooling demand is then assessed to determine the storage needed. After this, ATES systems are implemented in the clusters, which can only be placed in the available open space. These systems are placed as close as possible to the center of the cluster. However, there must be a minimum distance between the ATES systems to prevent thermal interference. Thermal interference means that the two systems are too close to each other and start to influence each other, resulting in decreased efficiency. This process continues until all demand is met or no free space remains. The compactness and demand fulfillment of each cluster and the entire area are then evaluated.

Data for the center of Amsterdam, including building demands and available free space, was provided by the AMS Institute. The model results indicate that implementing ATES systems can meet 58.6% of the center's total heating demand. This is on the condition that the buildings are insulated to an LT level. The demand fulfillment differs per cluster; some clusters achieve 100% fulfillment, particularly in the eastern and northwestern parts of the center, while others have lower fulfillment rates, with a minimum of 16.7%. The results show that very compact areas struggle more to meet heating demand. K-means outperforms equal size k-means in both compactness and demand fulfillment, making it the recommended method. The findings suggest that a 5GDHC network with ATES implementation has significant potential, with the most potential for clusters in the east and northwest. These areas have a lot of open space available for ATES placement so there is enough space to place storage and fulfill all demand. In other areas, particularly in the central part of the city center, it becomes evident that the combination of limited open space and high building density prevents the demand from being fulfilled.

9.2 Future research

There are numerous opportunities for future research. First, the impact of different design configurations for ATES can be explored, potentially providing insights for final implementation. A different configuration could be the implementation of doublets, where the location of the wells plays a more critical role. Unlike monowells, where wells are positioned vertically beneath each other, doublet wells are placed side by side, causing the thermal radius to vary based on their exact placement. To maximize space efficiency, it is advisable to cluster multiple wells of the same type together, a consideration not required for monowells and thus not included in the model. Another design configuration could use monowells, but with systems of varying sizes rather than uniform ones.

There are plenty of opportunities for future research for the AMS institute. A first option is to apply the ATES implementation method to the neighborhoods instead of using a clustering technique, to see whether the developed method produces better results than the already existing partition. Another option is to conduct research with more comprehensive data. Although this study highlights significant potential for a 5GDHC network with ATES, accurately estimating this potential with the current data is challenging. The demand data underestimates the potential since it does not account for heat exchange possibilities and the cooling demand was too small. Additionally, the data is based on the past 10 years, but it should account for future projections, as the cooling demand is expected to increase significantly. Conversely, the potential is somewhat overestimated because existing subsurface limitations, such as current underground systems and restriction areas, have not been factored in. Including these aspects into future research will clarify the potential more accurately.

Finally, research into the regeneration required for ATES systems remains valuable. While regeneration is not included in the current study, assessing potential regeneration for each area would be beneficial for a potential implementation of a 5GDHC network and ATES systems.

References

- AMS. (n.d.). *A map that shows where to 'find your cool' during heatwaves in Amsterdam*. AMS. Retrieved 13 February 2024, from <https://www.ams-institute.org/news/a-map-that-shows-where-to-keep-your-cool-during-heatwaves-in-amsterdam/>
- Andrewngai. (2020, June 9). *Understanding DBSCAN Algorithm and Implementation from Scratch*. Medium. <https://towardsdatascience.com/understanding-dbscan-algorithm-and-implementation-from-scratch-c256289479c5>
- Arya, N. (2022, April 10). K-Means Clustering for Unsupervised Machine Learning. *EJable*. <https://www.ejable.com/tech-corner/ai-machine-learning-and-deep-learning/k-means-clustering/>
- Averfalk, H., & Werner, S. (2020). Economic benefits of fourth generation district heating. *Energy*, *193*, 116727. <https://doi.org/10.1016/j.energy.2019.116727>
- Bakr, M., van Oostrom, N., & Sommer, W. (2013). Efficiency of and interference among multiple Aquifer Thermal Energy Storage systems; A Dutch case study. *Renewable Energy*, *60*, 53–62. <https://doi.org/10.1016/j.renene.2013.04.004>
- Banerjee, P., Chakrabarti, A., & Ballabh, T. K. (2021). Accelerated Single Linkage Algorithm using the farthest neighbour principle. *Sādhanā*, *46*(1), 45. <https://doi.org/10.1007/s12046-020-01544-6>
- Bbl (2023). *Well Design* [AMS_ATES_WellDesign].
- Bloemendal, M. (2018, May 16). *The hidden side of cities: Methods for governance, planning and design for optimal use of subsurface space with ATES*. Delft University of Technology. <https://repository.tudelft.nl/islandora/object/uuid%3A0c6bcdac-6bf7-46c3-a4d3-53119c1a8606>
- Bloemendal, M. (2024, May 3). *Personal communication* [Personal communication].
- Bloemendal, M., Jaxa-Rozen, M., & Olsthoorn, T. (2018). Methods for planning of ATES systems. *Applied Energy*, *216*, 534–557. <https://doi.org/10.1016/j.apenergy.2018.02.068>
- Bloemendal, M., & Olsthoorn, T. (2018). ATES systems in aquifers with high ambient groundwater flow velocity. *Geothermics*, *75*. <https://doi.org/10.1016/j.geothermics.2018.04.005>
- Blom, T. (Tess), Jenkins, A. (Andrew), & van den Dobbelssteen, A. A. J. F. (Andy). (2024). Synergetic urbanism: A theoretical exploration of a vertical farm as local heat source and flexible electricity user. *Sustainable Cities and Society*, *103*, 105267. <https://doi.org/10.1016/j.scs.2024.105267>

- Boesten, S., Ivens, W., Dekker, S. C., & Eijndems, H. (2019). 5th generation district heating and cooling systems as a solution for renewable urban thermal energy supply. *Advances in Geosciences*, *49*, 129–136. <https://doi.org/10.5194/adgeo-49-129-2019>
- Bos, J. (2023, January 30). *Isolatie opgave Amsterdam*. openresearch.amsterdam. <https://openresearch.amsterdam/nl/page/92346/isolatie-opgave-amsterdam>
- Buffa, S., Cozzini, M., D'Antoni, M., Baratieri, M., & Fedrizzi, R. (2019). 5th generation district heating and cooling systems: A review of existing cases in Europe. *Renewable and Sustainable Energy Reviews*, *104*, 504–522. <https://doi.org/10.1016/j.rser.2018.12.059>
- Bünning, F., Wetter, M., Fuchs, M., & Müller, D. (2018). Bidirectional low temperature district energy systems with agent-based control: Performance comparison and operation optimization. *Applied Energy*, *209*, 502–515. <https://doi.org/10.1016/j.apenergy.2017.10.072>
- Campello, R., Moulavi, D., & Sander, J. (2013). *Density-Based Clustering Based on Hierarchical Density Estimates*. *7819*, 160–172. https://doi.org/10.1007/978-3-642-37456-2_14
- CE Delft. (2018, May). *Weg van gas ; Kansen voor de nieuwe concepten LageTemperatuurAardwarmte en Mijnwater*. https://ce.nl/wp-content/uploads/2021/03/CE_Delft_3K61_Weg_van_gas_DEF.pdf
- Centraal Bureau voor de Statistiek. (2021, February 16). *92 procent woningen op aardgas begin 2019* [Webpagina]. Centraal Bureau voor de Statistiek. <https://www.cbs.nl/nl-nl/nieuws/2021/07/92-procent-woningen-op-aardgas-begin-2019>
- Coates, A., & Ng, A. Y. (2012). Learning Feature Representations with K-Means. In G. Montavon, G. B. Orr, & K.-R. Müller (Eds.), *Neural Networks: Tricks of the Trade* (Vol. 7700, pp. 561–580). Springer Berlin Heidelberg. https://doi.org/10.1007/978-3-642-35289-8_30
- Dang, M., & Voskuilen, P. (n.d.). *High-hanging fruit: Sustainable heating of Amsterdam's historic buildings*. AMS. Retrieved 19 June 2024, from <https://www.ams-institute.org/urban-challenges/urban-energy/sustainable-heating-solutions-for-amsterdams-historic-buildings/>
- Davies, D. L., & Bouldin, D. W. (1979). A Cluster Separation Measure. *IEEE Transactions on Pattern Analysis and Machine Intelligence*, *PAMI-1(2)*, 224–227. IEEE Transactions on Pattern Analysis and Machine Intelligence. <https://doi.org/10.1109/TPAMI.1979.4766909>
- Dickinson, J., Buik, N., Matthews, M., & Snijders, A. (2009). Aquifer thermal energy storage: Theoretical and operational analysis. *Géotechnique*, *59*, 249–260. <https://doi.org/10.1680/geot.2009.59.3.249>

- Dobbelsteen, A. van den. (2020, December). *WPI.3 – D1.2 Reuse report*. TU Delft/Climate KIC. <https://openresearch.amsterdam/nl/page/78651/reuse>
- Doughty, C., Hällstrom, G., Tsang, C. F., & Claesson, J. (1982, June). *A dimensionless parameter approach to the thermal behavior of an aquifer thermal energy storage system – Doughty – 1982 – Water Resources Research – Wiley Online Library*.
<https://agupubs.onlinelibrary.wiley.com/doi/abs/10.1029/WR018i003p00571>
- Dozmorov, M. (2016). *Hierarchical Clustering*.
https://mdozmorov.github.io/BIOS567/assets/presentation_Clustering/Clustering.pdf
- Elki project. (n.d.). *Same-Size K-Means*. Same-Size k-Means Variation. Retrieved 29 July 2024, from https://elki-project.github.io/tutorial/same-size_k_means
- Eneco. (2024). *Klimaat | Eneco*. <https://www.eneco.nl/over-ons/wat-we-doen/klimaat/>
- Ester, M., Kriegel, H.-P., & Xu, X. (1996). *A Density-Based Algorithm for Discovering Clusters in Large Spatial Databases with Noise*.
- Expertise Centrum Warmte. (n.d.). *Praktijktips – Hoe realiseer ik als gemeente een lokaal warmtenet?* Expertise Centrum Warmte. Retrieved 19 June 2024, from <https://www.expertisecentrumwarmte.nl/themas/marktordening+en+financiering/praktijktips+hoe+realiseer+ik+als+gemeente+een/default.aspx>
- Fremouw, M., & Dobbelsteen, A. van den. (2020, December 5). *WPI.4 – D1.2 Produce report*. TU Delft/Climate KIC.
https://openresearch.amsterdam/nl/pdf/viewer?file=%2Fimage%2F2021%2F12%2F14%2Fgld_d1_2_t1_4_produce_report_v1_3_210117_def.pdf
- Gemeente Amsterdam. (2019, February). *Het belang van een integrale benadering van de ondergrond* [Webpagina]. Amsterdam.nl; Gemeente Amsterdam.
<https://www.amsterdam.nl/wonen-leefomgeving/bodem/belang-integrale-benadering-ondergrond/>
- Gemeente Amsterdam. (2024). *Volg het beleid: Duurzaamheid* [Webpagina]. Amsterdam.nl; Gemeente Amsterdam.
<https://www.amsterdam.nl/bestuur-organisatie/volg-beleid/duurzaamheid/>
- GeoERA. (n.d.). *FACTSHEET6 Managing Urban Shallow Geothermal Energy AQUIFER THERMAL ENERGY STORAGE*.
https://geoera.eu/wp-content/uploads/2021/01/Task_2.4_FS_6.pdf
- Gjoka, K., Rismanchi, B., & Crawford, R. H. (2023). Fifth-generation district heating and cooling systems: A review of recent advancements and implementation barriers. *Renewable and Sustainable Energy Reviews*, 171, 112997.
<https://doi.org/10.1016/j.rser.2022.112997>
- Haiwen, S., Lin, D., Xiangli, L., & Yingxin, Z. (2010). Quasi-dynamic energy-saving judgment of electric-driven seawater source heat pump district heating system over boiler house district heating system. *Energy and Buildings*, 42(12), 2424–2430. <https://doi.org/10.1016/j.enbuild.2010.08.012>

- Heijnen, P. (2023). *SURFdrive—A service by SURF*. SURFdrive.
<https://surfdrive.surf.nl/files/index.php/s/NTSu7BhqZkh5fmH>
- Hoogenvorst, N. (2017, March 21). *Toekomstbeeld klimaatneutrale warmtenetten in Nederland | Planbureau voor de Leefomgeving*.
<https://www.pbl.nl/publicaties/toekomstbeeld-klimaatneutrale-warmtenetten-in-nederland>
- IEA. (2018). *The Future of Cooling – Analysis*. IEA.
<https://www.iea.org/reports/the-future-of-cooling>
- Interreg North-West Europe. (2023). *5GDHC in short | 5GDHC*.
<https://5gdhc.eu/5gdhc-in-short/>
- Jain, A. K., Murty, M. N., & Flynn, P. J. (1999). Data clustering: A review. *ACM Computing Surveys*, 31(3), 264–323. <https://doi.org/10.1145/331499.331504>
- Jarman, A. (2020). *Hierarchical Cluster Analysis: Comparison of Single linkage, Complete linkage, Average linkage and Centroid Linkage Method*.
<https://doi.org/10.13140/RG.2.2.11388.90240>
- Kadastralekaart.com. (n.d.). *Gemeente Amsterdam—KadastraleKaart.com*. Retrieved 19 June 2024, from <https://kadastralekaart.com/gemeenten/amsterdam-GM0363>
- Kiani, B., Hamamoto, Y., Akisawa, A., & Kashiwagi, T. (2004). CO2 mitigating effects by waste heat utilization from industry sector to metropolitan areas. *Energy*, 29(12-15 SPEC. ISS.), 2061–2075. <https://doi.org/10.1016/j.energy.2004.03.012>
- Klutchnikoff, N., Poterie, A., & Rouviere, L. (2021). *Statistical analysis of a hierarchical clustering algorithm with outliers*. <https://hal.science/hal-03153805>
- KNMI. (2024). *KNMI - Aardbevingen door gaswinning*.
<https://www.knmi.nl/kennis-en-datacentrum/uitleg/aardbevingen-door-gaswinning>
- KoWaNet. (2021, March). *Technisch Handboek Koele Warmtenetten*.
https://energygo.blob.core.windows.net/kowanet/D1.4%20Technisch%20handboek/KoWaNet%20Technisch%20Handboek%20Koele%20Warmtenetten_V1.1_mart%202021.pdf
- Lee, K. S. (2013). *Underground Thermal Energy Storage*. Springer.
<https://doi.org/10.1007/978-1-4471-4273-7>
- Liander. (2024). *MVO | Liander*. <https://www.liander.nl/over-ons/mvo>
- Liefting, R. (2022). *Feiten en cijfers over de aardgaswinning in Groningen—NRC*.
<https://www.nrc.nl/nieuws/2022/06/17/aardgaswinning-groningen-a4124922>
- Lund, H., Østergaard, P. A., Nielsen, T. B., Werner, S., Thorsen, J. E., Gudmundsson, O., Arabkoohsar, A., & Mathiesen, B. V. (2021). Perspectives on fourth and fifth generation district heating. *Energy*, 227, 120520.
<https://doi.org/10.1016/j.energy.2021.120520>

- Lund, H., Werner, S., Wiltshire, R., Svendsen, S., Thorsen, J. E., Hvelplund, F., & Mathiesen, B. V. (2014). 4th Generation District Heating (4GDH): Integrating smart thermal grids into future sustainable energy systems. *Energy*, *68*, 1–11. <https://doi.org/10.1016/j.energy.2014.02.089>
- MacQueen, J. (1967). Some methods for classification and analysis of multivariate observations. In *Proceedings of the Fifth Berkeley Symposium on Mathematical Statistics and Probability, Volume 1: Statistics: Vol. 5.1* (pp. 281–298). University of California Press. <https://projecteuclid.org/ebooks/berkeley-symposium-on-mathematical-statistics-and-probability/Proceedings-of-the-Fifth-Berkeley-Symposium-on-Mathematical-Statistics-and/chapter/Some-methods-for-classification-and-analysis-of-multivariate-observations/bsmsp/1200512992>
- Maulik, U., & Bandyopadhyay, S. (2002). Performance evaluation of some clustering algorithms and validity indices. *IEEE Transactions on Pattern Analysis and Machine Intelligence*, *24*(12), 1650–1654. *IEEE Transactions on Pattern Analysis and Machine Intelligence*. <https://doi.org/10.1109/TPAMI.2002.1114856>
- Mazhar, A. R., Liu, S., & Shukla, A. (2018). A state of art review on the district heating systems. *Renewable and Sustainable Energy Reviews*, *96*, 420–439. <https://doi.org/10.1016/j.rser.2018.08.005>
- Meesenburg, W., Ommen, T., Thorsen, J. E., & Elmegaard, B. (2020). Economic feasibility of ultra-low temperature district heating systems in newly built areas supplied by renewable energy. *Energy*, *191*, 116496. <https://doi.org/10.1016/j.energy.2019.116496>
- Mekhilef, S., Saidur, R., & Safari, A. (2011). A review on solar energy use in industries. *Renewable and Sustainable Energy Reviews*, *15*(4), 1777–1790. <https://doi.org/10.1016/j.rser.2010.12.018>
- Nationaal Programma Lokale Warmtetransitie. (2020). *Waterstof*. Nationaal Programma Lokale Warmtetransitie. <https://www.nplw.nl/technieken/warmtebronnen/waterstof/default.aspx>
- Nationaal Programma Lokale Warmtetransitie. (2021). *Groengas*. Nationaal Programma Lokale Warmtetransitie. <https://www.nplw.nl/technieken/warmtebronnen/groengas/default.aspx>
- Neri, M., Guelpa, E., & Verda, V. (2022). Design and connection optimization of a district cooling network: Mixed integer programming and heuristic approach. *Applied Energy*, *306*, 117994. <https://doi.org/10.1016/j.apenergy.2021.117994>
- Nijpels, E. (2018, December 21). *Ontwerp van het Klimaatakkoord—Publicatie—Klimaatakkoord* [Publicatie]. Ministerie van Economische Zaken en Klimaat. <https://www.klimaatakkoord.nl/documenten/publicaties/2018/12/21/ontwerp-klimaatakkoord>

- NLPW. (2022, August). *5e generatie warmte- en koudenetten*. Nationaal Programma Lokale Warmtetransitie.
<https://www.nplw.nl/technieken/warmtenet/5e+generatie+warmte+-en+koude+netten/default.aspx>
- Noome, W. (2013, May 22). *Masterplan open bodemenergiebronnen De Dam I*. IF Technology.
https://assets.amsterdam.nl/publish/pages/670670/6_masterplan_open_bodemenergiebronnen_de_dam_i.pdf
- Patz, J. A., Campbell-Lendrum, D., Holloway, T., & Foley, J. A. (2005). Impact of regional climate change on human health. *Nature*, *438*(7066), Article 7066.
<https://doi.org/10.1038/nature04188>
- Planbureau voor de leefomgeving. (2023). *Overzicht Transitievisies Warmte: Signalen, Obstakels & Potentieel*.
https://www.pbl.nl/sites/default/files/downloads/pbl-2023-overzicht-transitievisies-warmte-signalen-obstakels-potentieel_5051.pdf
- Rad, F. M., & Fung, A. S. (2016). Solar community heating and cooling system with borehole thermal energy storage – Review of systems. *Renewable and Sustainable Energy Reviews*, *60*, 1550–1561.
<https://doi.org/10.1016/j.rser.2016.03.025>
- Raidl, G. R. (2000). An efficient evolutionary algorithm for the degree-constrained minimum spanning tree problem. *Proceedings of the 2000 Congress on Evolutionary Computation. CEC00 (Cat. No.00TH8512)*, *1*, 104–111.
<https://doi.org/10.1109/CEC.2000.870282>
- Rijksoverheid voor ondernemend Nederland. (n.d.). *WKOtool*. Retrieved 3 July 2024, from <https://wkotool.nl/>
- Rodriguez, M. Z., Comin, C. H., Casanova, D., Bruno, O. M., Amancio, D. R., Costa, L. da F., & Rodrigues, F. A. (2019). Clustering algorithms: A comparative approach. *PLOS ONE*, *14*(1), e0210236. <https://doi.org/10.1371/journal.pone.0210236>
- Roossien, B. (Bart). (2020, July 1). *Technical design framework for cold heating and cooling networks*.
- Ruijs, T. (2019). *Het amsterdamse bronnenboek*. Gemeente Amsterdam.
https://openresearch.amsterdam/image/2024/6/6/het_amsterdamse_bronnenboek_online_versie_382748399.pdf
- Sankalana, N. (2023, September 20). K-means Clustering: Choosing Optimal K, Process, and Evaluation Methods. *Medium*.
<https://medium.com/@nirmalsankalana/k-means-clustering-choosing-optimal-k-process-and-evaluation-methods-2c69377a7ee4>
- Sanner, B., Karytsas, C., Mendrinou, D., & Rybach, L. (2003). Current status of ground source heat pumps and underground thermal energy storage in Europe. *Geothermics*, *32*(4), 579–588. [https://doi.org/10.1016/S0375-6505\(03\)00060-9](https://doi.org/10.1016/S0375-6505(03)00060-9)

- Sanner, B., Mutka, K., Papillon, P., Kalf, R., Stryi-Hipp, G., Weiss, W., Sanner, B., & Land, A. (2011). *2020-2030-2050, common vision for the renewable heating and cooling sector in Europe*. Publications Office of the European Union.
<https://data.europa.eu/doi/10.2788/20474>
- Sommer, T., Sulzer, M., Wetter, M., Sotnikov, A., Mennel, S., & Stettler, C. (2020). The reservoir network: A new network topology for district heating and cooling. *Energy*, 199. <https://doi.org/10.1016/j.energy.2020.117418>
- Sommer, W. (2015). *Modelling and monitoring of Aquifer Thermal Energy Storage: Impacts of soil heterogeneity, thermal interference and bioremediation*.
<https://research.wur.nl/en/publications/modelling-and-monitoring-of-aquifer-thermal-energy-storage-impact>
- Sommer, W., Valstar, J., Leusbrock, I., Grotenhuis, T., & Rijnaarts, H. (2015). Optimization and spatial pattern of large-scale aquifer thermal energy storage. *Applied Energy*, 137, 322–337. <https://doi.org/10.1016/j.apenergy.2014.10.019>
- Steinebach, E. (2013, August 19). *Aquifer Thermal Energy Storage*. WUR.
<https://www.wur.nl/en/show/aquifer-thermal-energy-storage.htm>
- Stemmler, R., Lee, H., Blum, P., & Menberg, K. (2024). City-scale heating and cooling with aquifer thermal energy storage (ATES). *Geothermal Energy*, 12(1).
<https://doi.org/10.1186/s40517-023-00279-x>
- Stichting Warmtenetwerk. (2021, October 19). *Participatie is de sleutel in de warmtetransitie*. Stichting Warmtenetwerk.
<https://warmtenetwerk.nl/nieuws/item/participatie-is-de-sleutel-in-de-warmte-transitie/>
- TenneT. (2024). *Doelstellingen voor mensen*. TenneT.
<https://www.tennet.eu/nl/doelstellingen-voor-mensen>
- UNFCCC. (2015). *Paris Agreement*.
https://unfccc.int/sites/default/files/english_paris_agreement.pdf
- van Burk, S. (2023). *Creating Clusters in a 5th Generation District Heating and Cooling Network: An alternative to a neighbourhood-based approach*.
<https://repository.tudelft.nl/islandora/object/uuid%3A059d58aa-9163-444a-94e2-a76e48626683>
- Vattenfall. (2024). *Onze klimaatambitie uitgelegd | Vattenfall Nederland*.
<https://www.vattenfall.nl/over-vattenfall/klimaatambitie/>
- Verhoeven, R., Willems, E., Harcouët-Menou, V., De Boever, E., Hiddes, L., Veld, P. O., & Demollin, E. (2014). Minewater 2.0 Project in Heerlen the Netherlands: Transformation of a Geothermal Mine Water Pilot Project into a Full Scale Hybrid Sustainable Energy Infrastructure for Heating and Cooling. *Energy Procedia*, 46, 58–67. <https://doi.org/10.1016/j.egypro.2014.01.158>

- Voermans, T. (2024, May 1). *Verkoop warmtepompen stort in, consumenten vertrouwen het niet meer | Binnenland | AD.nl*. AD.
<https://www.ad.nl/binnenland/verkoop-warmtepompen-stort-in-consumenten-vertrouwen-het-niet-meer~ab6ed652/>
- Volkova, A., Pakere, I., Murauskaite, L., Huang, P., Lepiksaar, K., & Zhang, X. (2022). 5th generation district heating and cooling (5GDHC) implementation potential in urban areas with existing district heating systems. *Energy Reports*, *8*, 10037–10047. <https://doi.org/10.1016/j.egy.2022.07.162>
- Wirtz, M., Kivilip, L., Remmen, P., & Müller, D. (2020a). 5th Generation District Heating: A novel design approach based on mathematical optimization. *Applied Energy*, *260*, 114158. <https://doi.org/10.1016/j.apenergy.2019.114158>
- Wirtz, M., Kivilip, L., Remmen, P., & Müller, D. (2020b). Quantifying Demand Balancing in Bidirectional Low Temperature Networks. *Energy and Buildings*, *224*, 110245. <https://doi.org/10.1016/j.enbuild.2020.110245>
- Wittek, P. (2014). 5—Unsupervised Learning. In P. Wittek (Ed.), *Quantum Machine Learning* (pp. 57–62). Academic Press.
<https://doi.org/10.1016/B978-0-12-800953-6.00005-0>

A

Assumptions

Appendix A contains the assumptions made to develop the method described in Chapter 5.4. These assumptions are outlined below.

- The decision was made to use the Euclidean distance when measuring the distance between two points, rather than the distance via the street network. While the street network distance better reflects the actual length of pipes required for the network, integrating it into the method poses challenges and adds computational complexity. To incorporate this distance into the model, it would need to be calculated individually for every pair of points. Clustering algorithms standardly use spatial coordinates, meaning they inherently use Euclidean distance to measure distance between buildings.
- This method focuses solely on determining the required ATES storage based on the clusters formed. It does not include the implementation of a 5GDHC network based on these clusters. Consequently, aspects such as pipe diameter, configuration, water flow, pressure losses and specific pipe locations are not addressed within the scope of this model.
- While Chapter 4.2.2. indicates multiple potential sources for regenerating ATES systems, this aspect is not incorporated into the model. Each ATES system is assumed to have adequate regeneration capacity available in its vicinity.
- All potential locations where ATES deployment is infeasible due to lack of subsurface space were nevertheless included. Despite the availability of a tool listing existing systems, it does not provide essential details required for implementation, such as thermal radius, volume, and well screen length (Rijksoverheid voor ondernemend Nederland, n.d.). As it is not possible to determine precisely how much space these existing systems occupy, this information has been excluded.

- The temperature level of the pipes in the 5GDHC network is outside of the scope of this model, as it does not affect the model's outcomes. The focus is exclusively on the amount of demand to be met and the degree to which ATES can fulfill it. Similarly, for the ATES wells, the specific temperatures are not considered; only the temperature difference between the hot and cold wells is taken into account, as this determines the ATES capacity.
- The losses in the 5GDHC network are estimated to be constant, with no variation across different months or cluster sizes.
- The losses during the storage in the ATES wells are estimated to be constant, with no variation based on the duration of storage.
- Although buildings occupy a larger area, this is not fully accounted for in the model. Each building is simplified to a single coordinate, specifically the center point of the building. This approach considers buildings rather than individual addresses, meaning all addresses within the same building are combined into a single point.
- No distinction has been made between different types of open space available for ATES installations; all space is considered equally suitable. In reality, some areas of free space are less desirable for these systems, while others are more intended for such use.
- Adding ATES systems to the method continues until all demand is fulfilled. Even if the most recently added ATES requires minimal storage, the system is still fully implemented.

B

Demand profiles

This appendix contains the monthly demand profiles for heating and cooling, which were discussed in chapter 6. The legend has also been added in this appendix, which is seen in figure B.3.

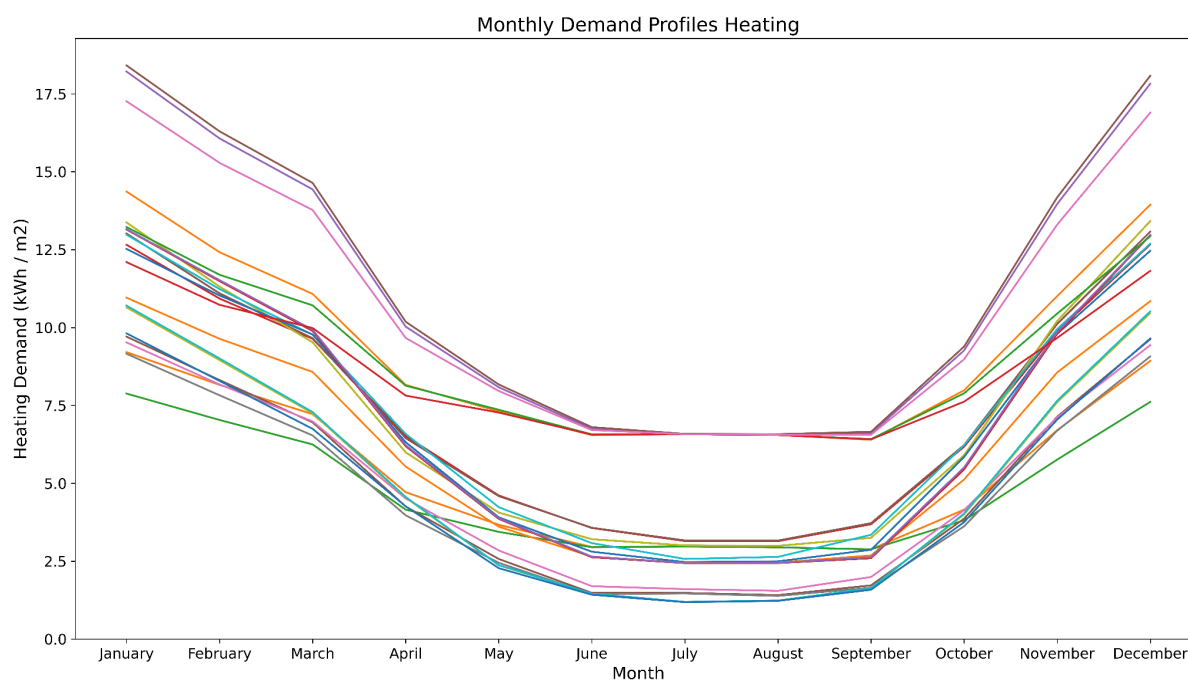


Figure B.1: The monthly heating demand for all archetypes in kWh/m²

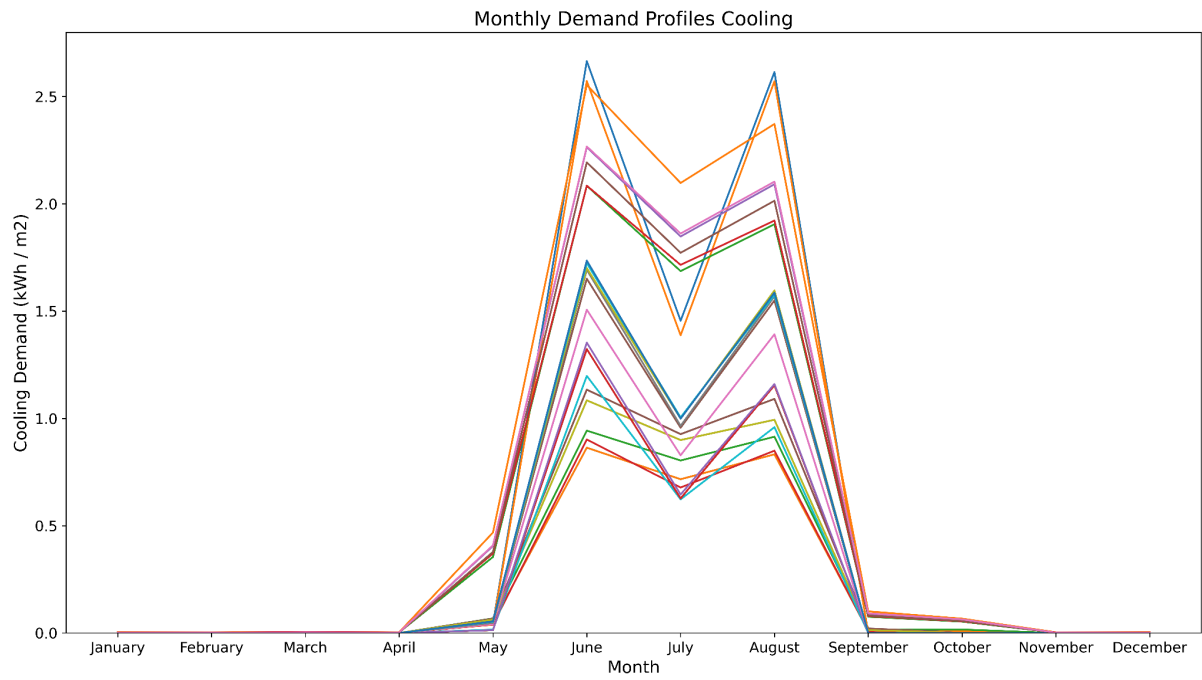


Figure B.2: The monthly cooling demand for all archetypes in kWh/m²

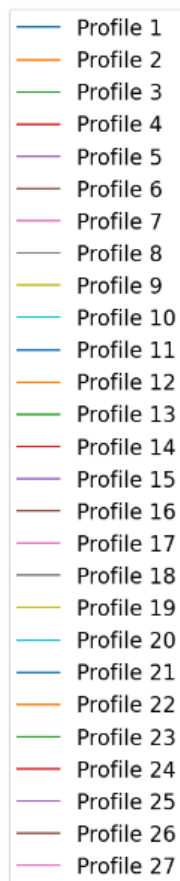


Figure B.3: The legend for both the heating and cooling demand profiles

C

Supporting figures results

This appendix contains additional supporting figures illustrating the model's outcomes. Figure C.1 depicts the locations of the ATEs installations by cluster. Each circle depicts one ATEs installation and the color of each circle represents the cluster it belongs to. The position indicates the placement of the ATEs installation in the free space. This concerns a total of 1885 ATEs systems. The figure clearly shows that a significant portion of the free space in the central area of the center of Amsterdam is occupied, leaving no room for additional installations. However, ample free space remains in the northwest and east regions. The clusters in these areas already fully meet the demand and thus do not fully utilize the available space.

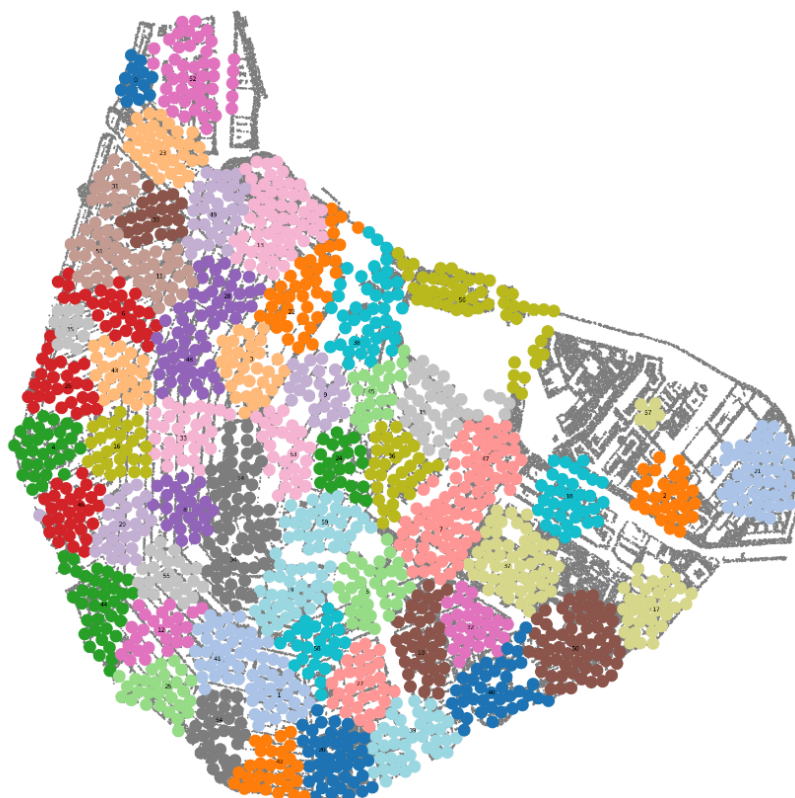


Figure C.1: The locations of placed ATEs systems in the center of Amsterdam

Figures C.2 and C.3 display the compactness per cluster for k-means and equal size k-means, respectively. Both figures illustrate the relative proportions of compactness within the results. The colors represent the within-cluster sums of squares (WCSS) values, with red indicating a high value and green indicating a low value. A lower WCSS value signifies a more compact cluster. These figures use different scales; the color ranges are determined by the minimum and maximum WCSS values within each result. Figure C.3 has a maximum value significantly higher than that of figure C.2. Consequently, figure C.3 appears more compact than figure C.2 due to more green areas, but this is misleading as the figures should be viewed independently. In figure C.2, the compactness distribution has a lower spread, with multiple occurrences of various colors from the spectrum. In contrast, figure C.3 predominantly shows extremes. Many clusters are green, but almost none are in the upper half of the color spectrum. The clusters in the upper half are extreme cases with exceptionally high WCSS values, marked by dark red.

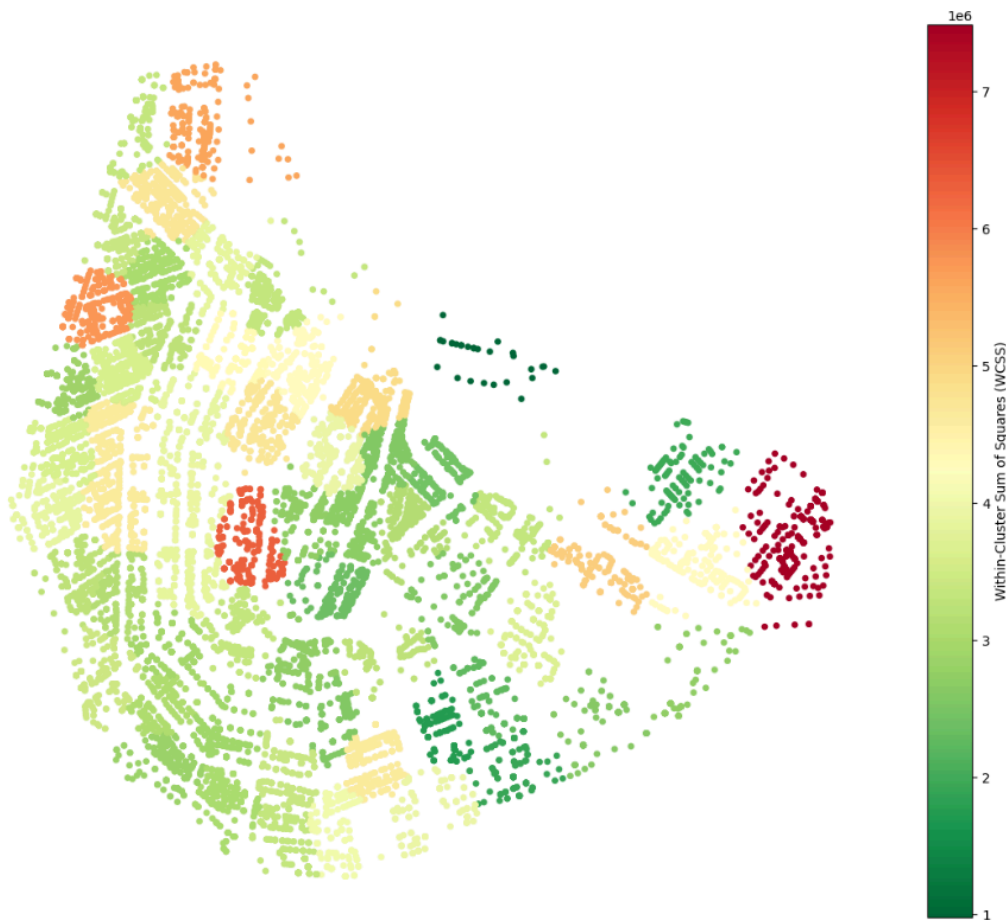


Figure C.2: The compactness per cluster for k-means with the shared scale

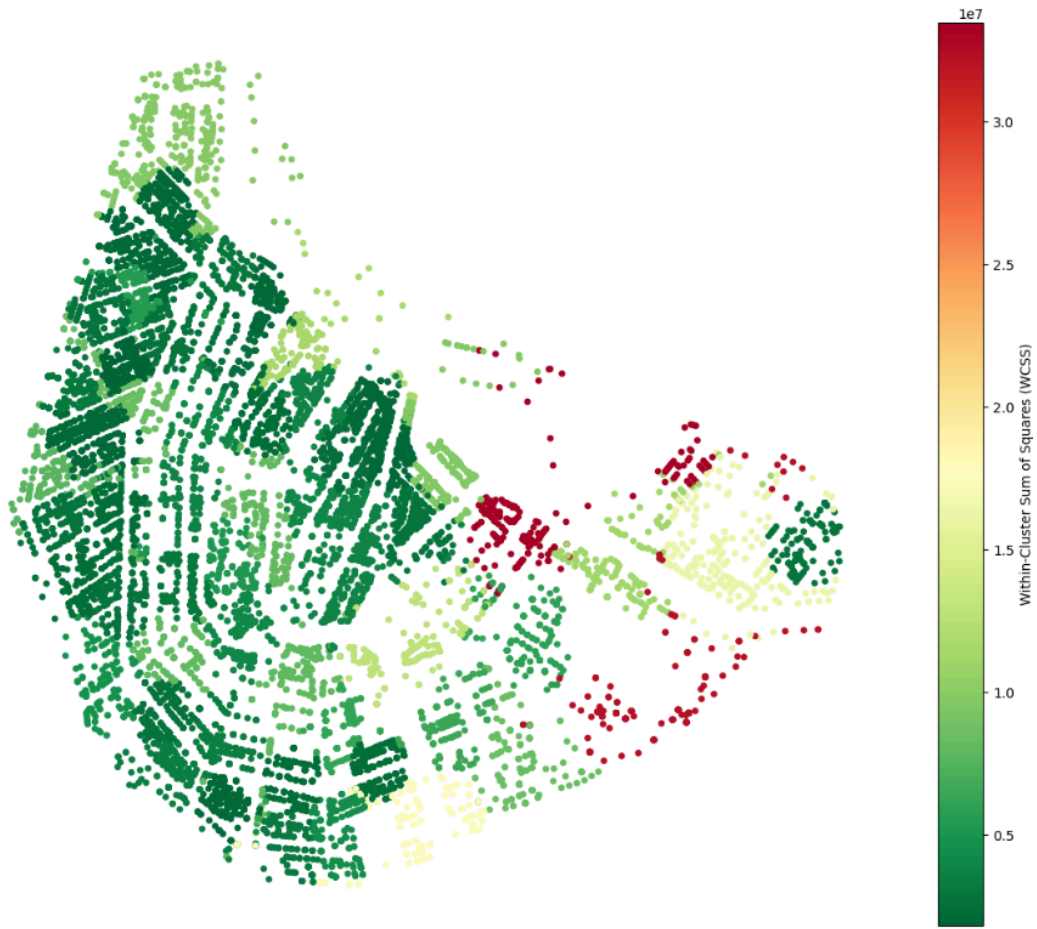


Figure C.3: The compactness per cluster for equal size k-means with the shared scale

Figures C.4 and C.5 present the WCSS results for k-means and equal size k-means, respectively, using the same scale. The extremes of the scale are determined by the combined minima and maxima of both results. In figure C.4, representing k-means, the clusters are much more balanced with lower dispersion, as indicated by their similar colors. In contrast, figure C.5, representing equal size k-means, highlights significant differences between some clusters. The few clusters with extremely high WCSS values are so much larger that there are almost no clusters with colors from the upper half of the spectrum.

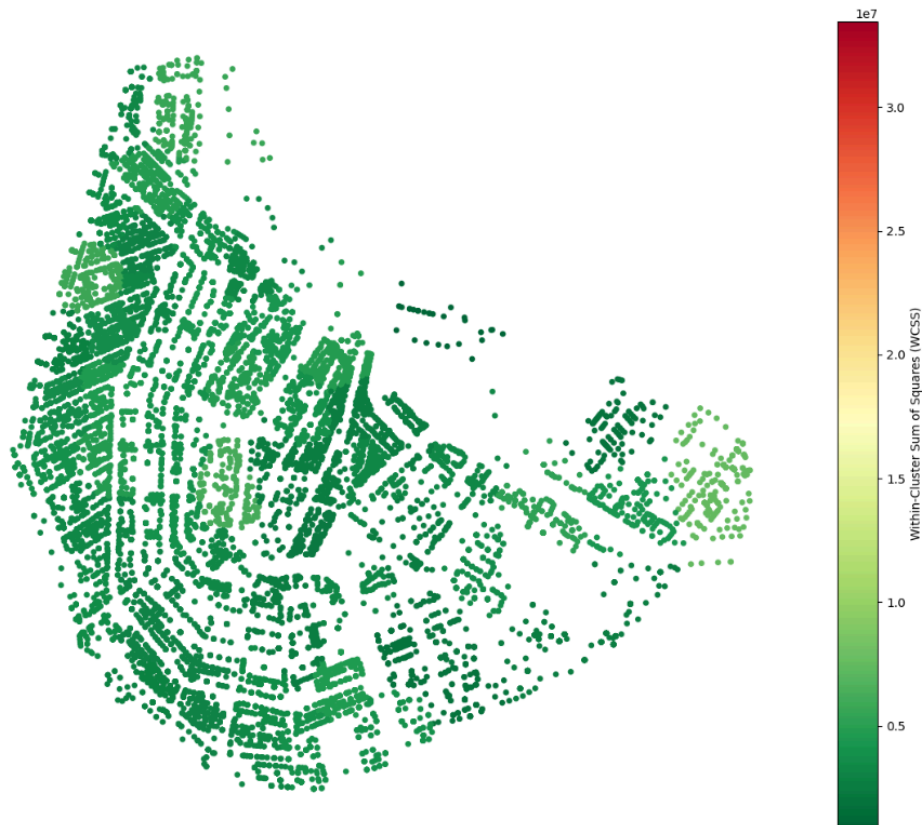


Figure C.4: The compactness per cluster for k -means with the individual scale

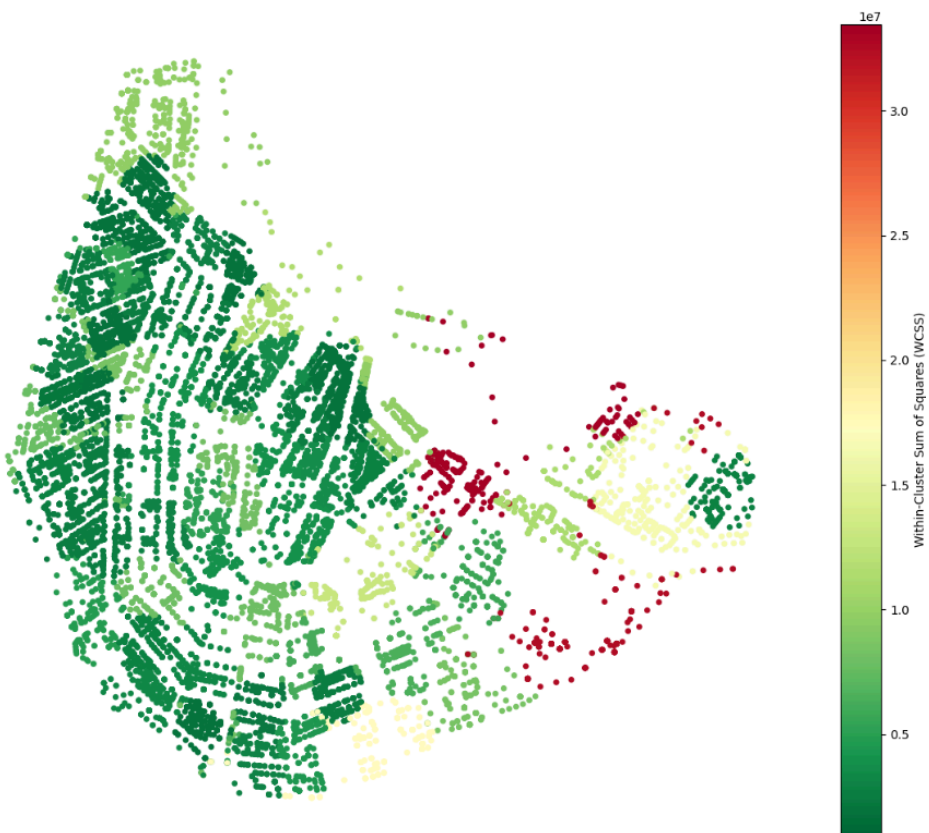


Figure C.5: The compactness per cluster for equal size k -means with the individual scale